Dissertation

submitted to the

Combined Faculties for Natural Sciences and for Mathematics

of the Ruperto-Carola University of Heidelberg, Germany

for the degree of

Doctor of Natural Sciences

presented by

M. Sc. Robert Reinhardt

born in Leisnig, Germany

oral examination:

March 13th, 2014

Cell intrinsic control of stem cell features in the retina

Referees:

Prof. Dr. Joachim Wittbrodt

Prof. Dr. Jan Lohmann

Table of Contents

Summary

Post-embryonic neurogenesis relies on the presence of neural stem cells, which are characterized by their multipotency and unique ability to self-renew. Despite their importance for the homeostasis and repair of the central nervous system, the transcriptional network governing stemness in adult neural stem cells is largely unknown.

We established the transcription factor Rx2 as proxy for retinal stem cells in the post-embryonic retina of the teleost medaka (*O. latipes*). By interrogating the regulatory input to the *Rx2 cis*-regulatory element, we identified four transcription factors (Sox2, Tlx, Gli3, Her9), which distinctly shape the stem cell domain and modulate stem cell features in the retina. First of all, we analyzed the gene expression and found that these genes have distinct spatio-temporal expression patterns in the retinal stem cell domain. Conditional mosaic analysis *in vivo* confirmed Sox2 and Tlx as activators of *Rx2*. The ectopic expression of *Sox2* or *Tlx* was sufficient to trigger de-differentiation of post-mitotic neurons and induced stem cell features therein. Conversely, sustained ectopic expression of *Gli3* or *Her9* repressed *Rx2*. Gain of *Gli3* or *Her9* in retinal stem cells arrested cell cycle progression and proliferation. Modification of conserved binding sites in the *Rx2 cis*-regulatory element revealed the importance of Sox and Gli transcription factors for the precise spatial *Rx2* expression in retinal stem cells. We propose that the combinatorial regulatory input of Sox2, Tlx, Gli3, Her9 confines *Rx2* expression and other features of retinal stem cells specifically to the periphery of the stem cell domain in the post-embryonic retina.

To elucidate the functional role of *Rx2* itself, mutants were established with the aid of targetable nucleases. Transcription activator-like effector nucleases were employed to induce double-strand breaks specifically in the *Rx2* coding sequence, which in the case of erroneous non-homologous end-joining created sequence alterations at the site of cleavage. The generation of stable, heritable mutations in the endogenous *Rx2* locus described here opens the opportunity for future genetic studies of *Rx2* in medaka.

Zusammenfassung

Postembryonale Neurogenese ist abhängig von der Präsenz von neuralen Stammzellen, die sich durch ihre Multipotenz und einzigartige Fähigkeit der Selbstteilung auszeichnen. Trotz deren Rolle für das Gleichgewicht und die Erneuerung des zentralen Nervensystems ist das transkriptionelle Netzwerk, welches Stammzellfähigkeiten von adulten neuralen Stammzellen reguliert, größtenteils unbekannt.

Wir etablierten den Transkriptionsfaktor *Rx2* als Marker für Stammzellen in der postembryonalen Netzhaut des Japanischen Reisfischs (*O. latipes*). Durch die Untersuchung des regulatorischen Elements von *Rx2* identifizierten wir vier Transkriptionsfaktoren (Sox2, Tlx, Gli3, Her9), die die Stammzelldomäne formen und Stammzelleigenschaften in der Netzhaut modulieren. Als erstes analysierten wir die Genexpression und fanden heraus, dass diese Gene individuelle zeitliche und räumliche Expressionsmuster in der Stammzelldomäne der Netzhaut besitzen. Konditionale mosaische Analyse *in vivo* bestätigte Sox2 und Tlx als Aktivatoren von *Rx2*. Die ektopische Expression von *Sox2* oder *Tlx* war ausreichend, um die Dedifferenzierung von Neuronen einzuleiten und in diesen Stammzelleigenschaften hervorzurufen. Umgekehrt reprimierte anhaltende ektopische Expression von *Gli3* oder *Her9 Rx2*. Gli3 oder Her9 in Stammzellen der Netzhaut hemmte den Fortschritt im Zellzyklus und Proliferation. Modifizierung von konservierten Bindestellen im *Rx2* regulatorischen Element enthüllte die Bedeutsamkeit von Sox- und Gli-Transkriptionsfaktoren für die präzise räumliche Expression von *Rx2* in Stammzellen der Netzhaut. Wir schlagen vor, dass der kombinierte regulatorische Einfluss von Sox2, Tlx, Gli3 und Her9 die Expression von *Rx2* und anderen Stammzelleigenschaften spezifisch in die Peripherie der Stammzelldomäne in der postembryonalen Netzhaut begrenzt.

Um die funktionelle Rolle von *Rx2* aufzuklären, wurden Mutanten mit der Hilfe von gezielten Nukleasen etabliert. Die spezifschen Nukleasen wurden benutzt, um Doppelstrangbrüche gezielt in der Sequenz von *Rx2* zu erzeugen, die im Falle von fehlerhaften DNA Reparaturmechanismen zu Sequenzveränderungen an der Schnittstelle führten. Die Erzeugung von stabilen, vererbbaren Mutationen im endogenen *Rx2* Genlocus, die hier beschrieben werden, eröffnet die Möglichkeit für zukünftige genetische Studien über *Rx2* im Japanischen Reisfisch.

INTRODUCTION

1 Introduction

1.1 The vertebrate eye

1.1.1 Architecture of the vertebrate retina

Of all tissues that constitute the CNS, the eye represents the most accessible part and a well-studied paradigm for the process of neurogenesis and cell determination.

The stereotypic spatial composition of the neural retina (NR), six types of neurons and one type of glia distributed in three nuclear layers interconnected by two synaptic layers, is conserved amongst vertebrates (Livesey and Cepko 2001). The ganglion cell layer (GCL) is located at the basal side of the retina and contains the cell bodies of displaced amacrine cells (ACs) and retinal ganglion cells (RGCs) (Figure 1). The axons of RGCs exit through an opening in the central retina, the so-called optic disc, and transmit visual stimuli through the optic nerve to their targets in the brain. ACs, bipolar cells (BPCs), horizontal cells (HCs) and Muller glia cells (MGCs), the only non-neural cell type in the retina, are found in the inner nuclear layer (INL). The processes of MGCs extend from the inner limiting membrane of the retina to the outer limiting membrane at base of the outer segments. The apical outer nuclear layer (ONL) is occupied by the cell bodies of cone and rod photoreceptors in radial arrangement. Neuronal processes occupy the space between each nuclear layer. Photoreceptor, bipolar and horizontal synapses are hosted in the outer plexiform layer (OPL), between the ONL and INL. The inner plexiform layer (IPL), which is located between the INL and the GCL, contains the synaptic connections of RGCs, BPCs and ACs. The NR is surrounded on its apical surface by the retinal pigmented epithelium (RPE), which serves as a shield, ensuring that light exclusively enters the eye through the lens (Figure 1B). When the light reaches the cone and rode photoreceptor outer segments below the RPE, a phototransduction cascade is triggered and information flows from the photoreceptors, to BPCs to RGCs, which send a response to the visual centers in the brain. The purpose of the RPE for the proper functionality of the NR extends beyond light and damage protection. Integrity of the RPE is required for normal development of photoreceptors and MGCs (Jablonski *et al.* 2000; Jablonski *et al.* 2001).

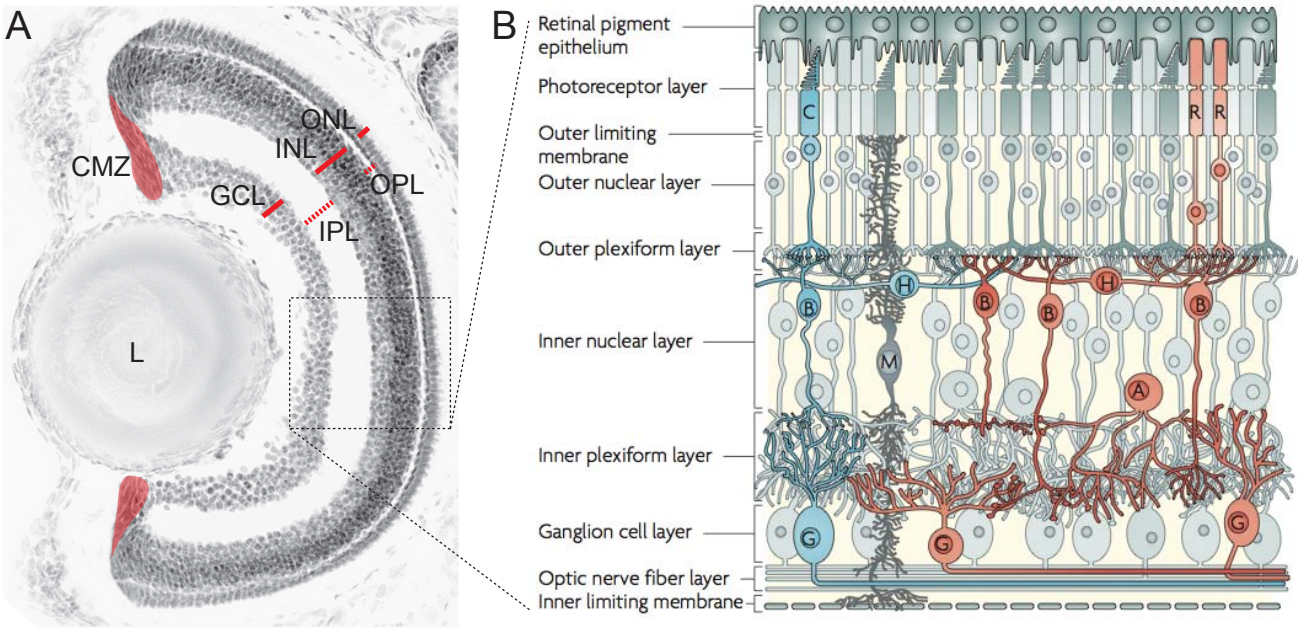

Figure 1. Shape and composition of the vertebrate retina.

(A) Cross-section through the adult fish retina. Nuclei were counter-stained with DAPI. Red lines indicate apico-basal axis of the nuclear layers. Dashed (red) lines indicate the apico-basal axis of the layers containing the cell bodies. The red areas at the margin represent the CMZ.

(B) Schematic representation of a magnified cross-section through the differentiated vertebrate retina. Apical side is up, basal side is down. Cone and rod photoreceptors are located in the ONL. They form synapses in the OPL with BPCs and HCs, which are located in the INL. Additionally, ACs are also found in the INL. RGC, positioned in the GCL, form synapses with ACs and BPCs in the IPL. MGCs span the entire apico-basal axis of the NR. Adapted from (Swaroop *et al.* 2010).

1.1.2 Retinal neurogenesis

The sequence of neurogenesis during embryonic development of the retina has been extensively studied in a variety of species. The temporal order of generated cell types is highly conserved across all vertebrates (Livesey and Cepko 2001). A common population of multipotent retinal progenitor cells (RPCs), arranged in a pseudostratified neuroepithelium, proliferates and gives rise to all different retinal cells types in a sequential yet overlapping order. The first cells to be generated are RGCs, followed by HCs, cone photoreceptors, ACs, rod photoreceptors, BCs and MGCs. The timing of RPC cell cycle exit is closely linked to cell fate the progeny adopt in retinal differentiation (Livesey and Cepko 2001; Marquardt and Gruss 2002; Cremisi *et al.* 2003). For instance, early cell cycle exit is associated with an over-production of early cell types at the expense of late cell types, while delayed cell cycle exit results in additional rounds of division and a reduction in early born cell types (Ohnuma *et al.* 2002; Dyer *et al.* 2003). During a process called interkinetic nuclear migration, the nuclei of retinal progenitors

move between the apical and basal surfaces of the neuroepithelium depending on the current phase of cell cycle. DNA synthesis (S-phase) takes place at the basal (vitreal) side, while mitotic nuclei (M-phase) are located apically (Del Bene 2011). It has been suggested that the plane of cell division relative to the apical surface of the neuroepithelium influences the outcome of cell divisions. During the genesis of RGCs in the developing zebrafish retina, circumferential divisions are more likely to produce asymmetric fates, such as one RGC and one non-RGC, while radial divisions generate symmetric fates with a higher frequency, both daughter cells committing to ganglion cell fate (Poggi *et al.* 2005).
An extensive number of cell lineage studies have proofed the mutipotency of retinal progenitors, (Turner and Cepko 1987; Holt *et al.* 1988; Wetts and Fraser 1988). The finding that RPC derived clones can vary greatly in size and composition, implicates a role for stochasticity in cell fate decisions controlling the balance between proliferation and differentiation (Wong and Rapaport 2009; He *et al.* 2012). Instead of different lineage-restricted progenitor cells producing different differentiated cells, it has been demonstrated that RPCs are restricted to make temporally appropriate cell types only. As shown in heterochronic transplantations, where RPCs from a particular time window are exposed to an younger or older environment, extrinsic cues from the environment are able to alter the relative proportions of each cell type generated at a particular time, but they cannot dictate the commitment towards a specific fate (Watanabe and Raff 1990; Austin *et al.* 1995; Belliveau and Cepko 1999; Belliveau *et al.* 2000). Progenitors pass progressively through a series of competence states, during each of which the progenitors are competent to produce a subset of retinal cell types (Livesey and Cepko 2001). This feature, that the sequence of cell birth is intrinsically determined in the progenitors cells, is similar to other lineages of the CNS, such as developing cerebral cortex (Qian *et al.* 2000). In addition to being multipotent, undifferentiated retinal precursors have been demonstrated to give rise to both NR and RPE in the retina of medaka (Centanin *et al.* 2011).

1.1.3 The ciliary marginal zone

Tissue growth and homeostasis during development and adulthood are fundamental features of all vertebrate species. In the CNS, both cell replacement and cell addition depend on newborn neurons being generated by neural stem cells (NSCs). NSCs have the ability to self-renew infinitely and contribute differentiated progeny to both neural and glial lineages, which will be integrated in the established circuitry.
Whereas the existence of adult NSCs in the mammalian brain has been confirmed in the subventricular zone of the lateral ventricles and the subgranular zone of the dentate gyrus in the hippocampus (Lois and Alvarez-Buylla 1993; Kuhn *et al.* 1996), the NR of mammals is considered to be a post-mitotic

tissue (Amato *et al.* 2004). In contrast, the non-mammalian retina contains a reservoir of mitotically active cells after conclusion of initial retinogenesis. This stem cell domain, the ciliary marginal zone (CMZ), is spatially separated from post-mitotic cells and situated at the periphery of the retina (Figure 1A). Birth dating studies in lower vertebrates (frog and fish) have implicated the CMZ as the source of post-embryonic neurogenesis, which provides new neurons and glia to accommodate the life-long growth of the NR (Hollyfield 1968; Straznicky and Gaze 1971; Johns 1977). It has been suggested that the spatial distribution of the CMZ, from peripheral to central, reflects the temporal progression of embryonic retinogenesis (Harris and Perron 1998; Perron and Harris 2000). Slowly dividing retinal stem cells (RSCs) reside in the peripheral-most part of the CMZ, which give rise to short-term rapidly dividing progenitors (Figure 2A). These transiently amplifying progenitors are located more centrally. Cells in the CMZ, which are found closest to differentiated neurons, do not divide and in terms of gene expression resemble committed RPCs. Interestingly, *in vitro* studies have demonstrated that cells derived from the pigmented ciliary margin of mice, which is a domain topographically comparable to the non-mammalian CMZ, proliferate and form neurosphere colonies in culture (Tropepe *et al.* 2000). Lineage tracing analysis has identified bona fide multipotent RSCs in the medaka CMZ (Centanin *et al.* 2011). Single-cell-derived clones consist of all seven cell types, which comprise the vertebrate NR. Moreover, in the life-long growing medaka retina, post-embryonic stem cells maintain the simultaneous expansion of NR and RPE (Figure 2B-C). In frog and fish, the compartmentalized proliferation and addition of new cells occurs in the marginal domain of the RPE, which covers the CMZ (Perron *et al.* 2003). Thus, the post-embryonic medaka retina constitutes an excellent model to investigate adult NSCs.

It is currently unknown when the stem cell domain is established during development. The extracellular and intracellular signals defining the ciliary margin in amphibians have been addressed through gene expression profiling and modulation of signaling cascades mostly at embryonic stages. A number of studies have suggested opposing roles for canonical *Wnt* and *Shh* signaling pathways in the regulation of undifferentiated retinal progenitors - *Shh* shortens the length of the cell cycle (Locker *et al.* 2006), while *Wnt* targets such as *Hes4* lengthen the phases of the cell cycle (El Yakoubi *et al.* 2012). Furthermore, both pathways have been demonstrated to inhibit each other through their downstream mediators in the margin of the retina (Borday *et al.* 2012).

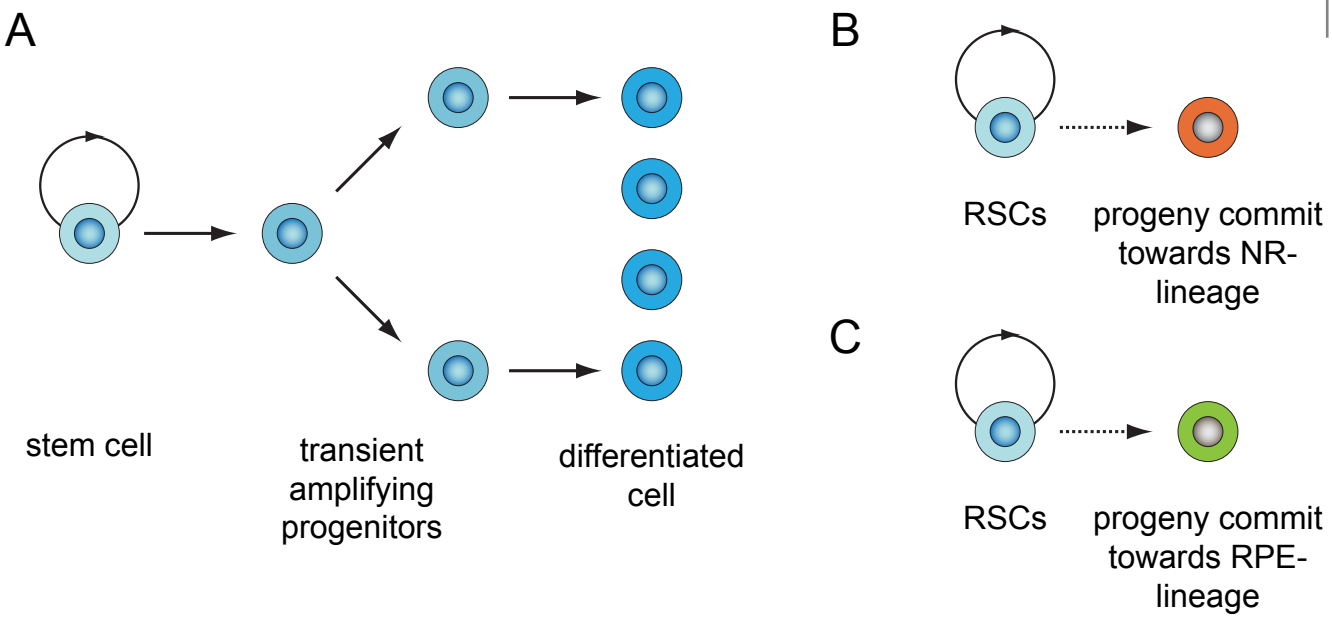

Figure 2. Model of self-renewal in the fish retina.

(A) Regarding the growth of the NR in fish and frog, it has been proposed that slowly-cycling stem cells self-renew and generate rapidly dividing transient amplifying cells, which in turn give rise to differentiated cells (Locker *et al.* 2006).

(B-C) During the lifelong growth of the medaka retina, two tissues, the NR and the RPE, are independently maintained by individual RSCs located in the CMZ. Multipotent RSCs generate all seven cell types of the NR (B) or post-mitotic cells of the RPE (C). Descendents of each dedicated stem cell are either committed towards the NR- or RPE-lineage (Centanin *et al.* 2011).

1.1.4 Optic vesicle formation

Eye development begins at the end of gastrulation with the determination of the eye field, an epithelial eye precursor in the anterior neuroectoderm, simultaneously with the patterning of the prospective forebrain. Eye field specification requires the downregulation of Bmp signals, known inhibitors of a neural fate (Gestri *et al.* 2005). Similarly, findings in fish have indicated that beta-catenin-dependent Wnt signaling has to be repressed for the patterning of the anterior neural plate. It has been shown that Wnt8b-mediated ectopic activation of the canonical Wnt signal cascade antagonizes the specification process (Cavodeassi *et al.* 2005), while loss of *wnt8* results in the reduction of posterior neuroectoderm and an expansion of forebrain structures and axial mesoderm (Lekven *et al.* 2001). The Zebrafish mutant *masterblind*, carrying a mutation in Axin1, lacks eyes and parts of the telencephalon, accompanied by an expansion of diencephalic tissue (Heisenberg *et al.* 2001; van de Water *et al.* 2001).

Experimental data from Xenopus and zebrafish indicate the importance of activation of IGF signaling for patterning of the retinal anlage. Blocking of the pathway through dominant-negative IGF receptors interferes with CNS development, particularly with the formation of anterior neural structures, leading to reduction or loss of head and eye (Pera *et al.* 2001; Eivers *et al.* 2004).

Following specification and patterning, the single retinal anlage is split into the two retinal primordia. Midline-derived signaling molecules, such as sonic hedgehog (Shh) and fibroblast growth factor (Fgf), are instructive for the split of the eye field and patterning of the laterally formed optic vesicles (Ekker *et al.* 1995; Macdonald *et al.* 1995; Chiang *et al.* 1996; Koster *et al.* 1997; Carl and Wittbrodt 1999).
The morphogenetic events occurring during optic vesicle evagination have been analyzed in detail through 4D microscopy at a single-cell level in medaka and zebrafish (Rembold *et al.* 2006; Keller *et al.* 2008). The evagination of optic vesicles is initiated during neural tube closure by individual cell migration towards the midline. Future RPCs converge slower in comparison to the surrounding future forebrain cells, resulting in the formation of a wider domain from which the vesicles will arise. Afterwards, outward-directed migration of RPCs leads to the splitting of the eye field. In the forming optic vesicle individual RPCs intercalate and promote formation of the vesicular epithelium.

1.2 Homeodomain transcription factors Pax6, Rx and Six3 play central roles in eye development

It has been suggested that Pax6, Rx and Six3 are part of a highly conserved genetic network, which directs the initiation of eye development, in particular the establishment of retinal identity in cells involved in morphogenesis of the optic vesicle (Halder *et al.* 1995; Oliver and Gruss 1997; Gehring and Ikeo 1999). Consistent with their proposed role in specification of retinal fate, ectopic expression of each of these factors during amphibian embryonic development results in mutual cross-activation and ectopic formation of retinal tissue (Mathers *et al.* 1997; Chow *et al.* 1999; Loosli *et al.* 1999; Zuber *et al.* 1999; Bernier *et al.* 2000).
Loss of Pax6 is accompanied by defective optic vesicle formation and lens development, resulting in absent eyes (Jordan *et al.* 1992; Grindley *et al.* 1995). In the presumptive lens ectoderm, Pax6 is required for the inhibition of canonical Wnt signaling (Machon *et al.* 2010). Results from conditional inactivation implicated Pax6 in the maintenance of RPCs in a pluripotent state (Marquardt *et al.* 2001). The expression of other early eye field specification markers *Rx* and *Six3* were unaffected in conditional mutants, suggesting that the specific function of Pax6 in RPC proliferation is downstream or independent of these homeobox genes. Despite evidence that loss of Pax6 affects progenitor cell division, the molecular connection to the cell cycle remains unknown (Warren *et al.* ; Estivill-Torrus *et al.*).
Similar to *Six3*, *Rx* expression starts in the anterior neuroectoderm and later continues in progenitor cells during optic cup development. Cross-species analysis has highlighted early *Rx* function as a

crucial influence on steps of optic vesicle morphogenesis, convergence and evagination. In Xenopus, fish and mouse, inactivation of *Rx* is accompanied by reduced eye size or complete absence of eyes (Mathers *et al.* 1997; Andreazzoli *et al.* 1999; Loosli *et al.* 2001; Loosli *et al.* 2003; Kennedy *et al.* 2004). This conservation is underscored by findings that *Rx* is mutated in humans with anopthalmia (Voronina *et al.* 2004).

The medaka and zebrafish genomes contain three *Rx* genes, of which *Rx3* is expressed the earliest in the early eye field (Loosli *et al.* 2001; Loosli *et al.* 2003).

The role of *Rx3* in eye morphogenesis was further elucidated by *in vivo* imaging analysis, which showed that mutant cells converge fully towards the midline but fail to migrate outwards to form the optic vesicles (Rembold *et al.* 2006). Analysis of the underlying molecular mechanism revealed that *Rx3* down-regulates expression of the Ig-domain protein Nlcam, which modulates the migration of progenitor cells during the initial phase of midline convergence (Brown *et al.* 2010).

The function of *Rx1* and *Rx2*, which are expressed following optic vesicle formation, is less clear. In zebrafish, morpholino oligonucleotide-mediated knockdowns failed to produce an early phenotype in the retina (Rojas-Muñoz *et al.* 2005). During later stages, expression of *Rx1* is required for the proliferation and survival of retinal progenitors, while both *Rx1* and *Rx2* are involved in regulating the expression of photoreceptor-specific genes (Nelson *et al.* 2009). In Xenopus, Rx, in combination with other TFs, is necessary for proper photoreceptor maintenance and function by direct regulation of genes such as rhodopsin and red cone opsin (Pan *et al.* 2010). Furthermore, *Rx* has been shown to be important for proliferation and migration of RPCs (Kenyon *et al.* 2001; Zaghloul and Moody 2007). Rx directly regulates Otx2 expression, which is required for photoreceptor cell fate determination, mainly in the final cell cycle prior to terminal differentiation of RPCs in the embryonic mouse retina (Muranishi *et al.* 2011). These results hint at a conserved *Rx* function in photoreceptor specification.

Rx transcription is upregulated as a response to injury in the retina of fish, while knockdown of *Rx* impairs wound healing in the frog retina (Raymond *et al.* 2006; Martinez-De Luna *et al.* 2011). In contrast to *Pax6* and *Six3*, *Rx* expression continues following embryogenesis RSCs and RPCs. *Rx1* and *Rx2* have been described as molecular markers for the post-embryonic CMZ in zebrafish and Xenopus (Locker *et al.* 2006; Raymond *et al.* 2006; Borday *et al.* 2012). Furthermore, *Rx* is expressed in the quiescent stem cells of the central NR, the MGCs, which have the ability to *trans*-differentiate upon injury (Bernardos *et al.* 2007). Notably, lineage-tracing experiments have highlighted *Rx2* as a marker for multipotent stem cells in the post-embryonic medaka retina (L. Centanin and J. Wittbrodt, unpublished). Clones derived from Rx2-postive cells through both traditional transplantation assays and conditional genetic labeling (inducible CreERT2 expressed under the medaka *Rx2* CRE) contained

all seven cell types of the NR. In addition, recombination triggered in Rx2-positve RSCs located in the CMZ, generated clones of epithelial cells in the RPE. Examination of the clone composition underscored that a pool of Rx2-positive stem cells maintains both tissues independently, since cell types of the RPE and NR have never been found in the same clone. However, the function of either paralog in the RSC domain remains unknown.

1.3 Transcriptional cues regulating *Rx* expression

The regulatory elements upstream of the Xenopus *Rx* genes have been isolated and shown to be capable of driving reporter expression in the developing eye and mature retina (Zhang 2003; Martinez-De Luna *et al.* 2010). Detailed examination of the regulatory organization highlighted the importance of upstream *trans*-acting factors Otx2 and Sox2 for direct activation of the Xenopus *Rx cis*-regulatory element (CRE) (Danno *et al.* 2008), and implied the involvement of other factors such as Pou and forkhead TFs in the transcriptional regulation of *Rx* (Martinez-De Luna *et al.* 2010). Although a number of factors have been implicated in the upstream regulation of *Rx*, the exact molecular nature of their interaction and how they function on the CRE *in vivo* remains unknown. The isolated medaka *Rx2* CRE has been shown to drive reporter expression in RPCs (Martinez-Morales *et al.* 2009), faithfully recapitulating endogenous *Rx2* expression during the optic cup development and later retinogenesis (Inoue and Wittbrodt 2011). The fact that *Rx2* labels *bona fide* RSCs *in vivo* and the availability of the relatively short (2400 base pairs) CRE makes the retina-specific TF Rx2 an interesting candidate to elucidate the regulatory framework governing stemness in the adult fish retina.

1.4 Following mitotic lineages

To understand the contribution of an individual progenitor or stem cell to tissue growth or maintenance, all descendents coming from this single cell have to be investigated. Lineage represents the result of each cell division in a temporal order. Diverse lineage-tracing techniques have been established to address a variety of questions, from exploring the embryonic origin of different tissues, over how certain progenitors contribute to a tissue, to finding the cellular origin of cancer. Ideally, the techniques allow labeling of individual cell and examining cellular fate dynamics by reconstruction of an entire lineage at single-cell resolution.

1.4.1 Label-retaining assays

Stem cells that divide slowly or infrequently will incorporate a marker during S-phase such as DNA analogs (e.g., BrdU) or fluorescent histone labels (e.g., H2B-EGFP) following pulse labeling, and upon repeated cell division pass them on to their progeny. The dilution of the label can be used to track the fate of their daughter cells, which provides knowledge about the properties of the initially labeled stem cell population (Cotsarelis *et al.* 1990; Tumbar *et al.* 2004).

In model amenable to direct visualization of cell movements in high spatio-temporal resolution by light microscopy, lineages can be followed *in vivo*. Data obtained from the tracking of cell movements via fluorescently labeled chromatin over time has shed light on the mitotic lineages within key developmental processes, e.g., migration of retinal progenitors in the medaka anterior neuroectoderm, early zebrafish morphogenesis and the gastrulation in the fruitfly (Rembold *et al.* 2006; Keller *et al.* 2008; McMahon *et al.* 2008). Reconstruction of an entire lineage, by means of tracking cells via *in vivo* imaging analysis or in fixed samples, relies on the ability to clonally label the cell population of interest.

1.4.2 Cell transplantation

Transplantation assays, including the generation of interspecies chimeras or genetic mosaics, have been used extensively in developmental embryology to study cell fate in a clonal manner. Permanently labeled cells (e.g., fluorescent protein) transplanted into an unlabeled host present elegant ways to increase our understanding of tissue homeostasis and development, such as within the lung and retina (Giangreco *et al.* 2009; Centanin *et al.* 2011). However, non-permanent labels are prone to diffusion into neighboring cells (e.g., vital dyes) and quick turnover after successive rounds of cell division (e.g., fluorescent proteins provided by mRNA injections).

1.4.3 Genetic Recombination

In general, systems used for genetic recombination to achieve clonal labeling consist of two components: a recombinase and a genetically encoded conditional reporter gene. The two systems most commonly deployed are Flp/*FRT* and Cre/*lox*, derived from *Saccharomyces cerevisiae* and bacteriophage P1, respectively (Branda and Dymecki 2004). Reporter constructs, typically under control of an ubiquitously active regulatory element, constitute of a “default” cassette (transcriptional roadblock or fluorescent marker) flanked by target sites (e.g., *lox2272*) followed by the coding sequence for the desired genetic marker (e.g., fluorescent proteins or beta-galactosidase). Expression of a recombinase (e.g., Cre) in a cell-specific manner triggers site-specific recombination and expression of a conditional reporter gene,

ideally initializing life-long genetic labeling of all progeny of the marked cells.

In the fruitfly *Drosophila melanogaster* cell lineage analysis is typically based on reporter constructs equipped with *FRT*-sites, which are recognized by the Flp enzyme (Harrison and Perrimon 1993). In mice the Cre/*lox* approach has become the most commonly employed recombination system. Constitutive, ubiquitous reporter expression is commonly achieved in mice by insertion into the *Rosa26* locus (Srinivas *et al.* 2001). Chimeric Cre, fused to the human estrogen receptor (ER), provide accurate spatio-temporal control over the recombination event (Metzger *et al.* 1995a; Metzger *et al.* 1995b). The ligand-dependent recombination, Cre translocation to the nucleus is only permitted in case of hormone binding, has been significantly improved in terms of efficiency and sensitivity with the advanced CreERT and CreERT2 recombinases (Feil *et al.* 1996; Feil *et al.* 1997). The system is modular by crossing different cell-specific drivers controlling the recombinase to the same transgenic reporter, in theory allowing temporal and spatial control over the recombination in any tissue. For monitoring specific events in signal cascades, the Cre activity can be coupled to post-translational specific modifications. For instance, when fused to extracellular domain of the Notch1 transmembrane receptor, Cre protein is free to enter the nucleus and mediate recombination strictly upon receptor proteolysis, specifically tracing descendents of cells exposed to Notch1 activation (Vooijs *et al.* 2007). In addition, the system is expandable by stacking differently colored fluorescent proteins between incompatible *lox* variants, resulting in stochastic recombination and uniquely labeled clones (Livet *et al.* 2007). The tamoxifen-inducible Cre enzyme has emerged as one of the most powerful tools in fate mapping, in particular for stem cell research concerning adult stem cells, since it allows visualizing the lineage potential of the (post-embryonically) induced cell population. Using the CreERT2, significant findings in the mice model have been made on cell fate dynamics in the interfollicular epidermis, germline, hair follicle, intestine and stomach (Barker *et al.* 2007; Clayton *et al.* 2007; Nakagawa *et al.* 2007; Barker *et al.* 2010; Snippert *et al.* 2010a). Concerning the CNS, an elegant study revealed nestin-positive radial glia-like precursors as self-renewing and multipotent NSCs in the adult mouse dentate gyrus (Bonaguidi *et al.* 2011). In medaka, the multipotency of Rx2-positive adult RSCs has been demonstrated with specific Cre expression under the *Rx2* CRE at post-embryonic stages (L. Centanin and J. Wittbrodt, unpublished).

Recently, inducible genetic labeling offered potential solutions to the longstanding debate regarding the cellular origin of cancer. Lineage-tracing analysis of squamous skin tumors presents the first experimental evidence for the existence of cancer stem cells during unperturbed tumor evolution, independent of transplantation assays (Driessens *et al.* 2012). In another report examining the contribution of individual cells to tumor formation and growth in the mouse intestine, researchers

identified Lgr5-positive cells as the multipotent stem cells of adenomas (Schepers *et al.* 2012). Notably, this study took advantage of a reporter construct with inverted components and *lox*-sites facing each other, continuing to switch colors after the initial induction as long as tamoxifen is provided, a process termed re-tracing.

Applied in zebrafish, fate-mapping through recombination of genetic markers shed light on different processes, such as the development of the cornea and plasticity of cardiac lineages during regeneration (Pan *et al.* 2013; Zhang *et al.* 2013). Moreover, lineage-tracing contributed greatly to our understanding of stem cell behavior in growing or renewing tissues, and whether asymmetry exists at the level of individual stem cells or an entire stem cell population. In the past numerous studies showed individual stem cells divide asymmetrically, giving strictly rise to one daughter cell that retains stem cell identity, therefore argued for a fate pattern of invariant asymmetry maintaining tissue homeostasis. More recently, quantitative analyses of long-term progression of labeled clones suggest that the prevalent strategy for homeostasis in cycling tissues is achieved by population asymmetry, for instance in the mammalian epidermis and the intestine (Clayton *et al.* 2007; Snippert *et al.* 2010b). Rather than maintaining balance by strictly dividing asymmetrically, clones in these tissues can be partially or entirely lost due to terminal differentiation or injury, while others expand through symmetric division to compensate for their absence, a pattern similar to what has been described in the germline (Morrison and Kimble 2006).

1.5 Reprogramming of terminally differentiated somatic cells

During the development of an entire organism, irreversible cellular identities are established and maintained in the embryo, all arising from undifferentiated pluripotent stem cells. It has been a long-standing challenge to reverse terminally differentiated cells back into a stem cell-state.

Reprogramming by somatic cell nuclear transfer was first demonstrated by the generation of tadpoles and adult frogs from unfertilized oocytes that had received a nucleus from the epithelial cells of the adult intestine (Gurdon 1962b; Gurdon 1962a). More than 30 years later, based on the same principle, the first mammals were successfully cloned from differentiated cells, which still hold all of the required genetic informations needed for the development of entire organisms, while unfertilized eggs contain factors that can reprogram the nuclei of somatic cells (Wilmut *et al.* 1997; Wakayama *et al.* 1998).

Embryonic stem cells (ESCs), derived from the inner cell mass of a blastocyst, are characterized by their ability to self-renew indefinitely and differentiate into any of the three germ layers. Fused with somatic cells, ESCs are capable of forming pluripotent hybrids (Tada *et al.* 2001). Nuclear reprogramming in

cell hybrids proofed the plasticity of differentiated mammalian cells; their differentiated state can be reversed when they are fused with embryonic germ cells or ESCs (Tada *et al.* 1997).

Induced cell fate changes include de-differentiation of somatic cells into a stem cell-state, as well as *trans*-differentiation into another cell type. The idea of lineage-defining factors, single TFs that determine and induce the fate of a given lineage, stems from mis-expression experiments resulting in *trans*-differentiation. In Drosophila, ectopic expression of homeotic genes, such as *Antennapedia* or *eyeless,* was shown to be sufficient to induce the transformation of one body part into another (Schneuwly *et al.* 1987; Gehring 1996). The direct conversion of mammalian fibroblasts into myoblasts was achieved by forced expression of single TF, MyoD (Davis *et al.* 1987).

Combining the observations from nuclear reprogramming through cell fusion and lineage-defining TFs led to the hypothesis that reprogramming of somatic cells back into the embryonic state is achieved by the presence of multiple factors in unfertilized oocytes or ESCs. Therefore, it was tested if the simultaneous expression of defined factors induces a de-differentiation of somatic cells. Yamanaka and colleagues identified the four TFs Oct4, Sox2, Klf4 and c-Myc as sufficient to reprogram mouse and human embryonic fibroblast cells back to a pluripotent state (Takahashi and Yamanaka 2006; Takahashi *et al.* 2007). Global expression analysis revealed that in these so-called induced pluripotent stem cells (IPSCs) large quantities of ESC-specific genes are reactivated and many epigenetic marks are removed.

Recently, the first cellular reprogramming *in vivo* in genetically engineered mouse lines expressing the reprogramming TFs in an inducible manner was reported (Abad *et al.* 2013). Upon expression of Oct4, Sox2, Klf4 and c-Myc the mice developed teratomas, disorganized tissues containing cells representative of all three germ layers, across multiple tissues. When reprogrammed, IPSCs isolated from the bloodstream of transgenic mice were cultured, they adopted characteristics of trophoblast stem cells, indicating totipotency.

The successful reprogramming of differentiated cells into IPSCs followed by directed differentiation into the desired cell type offers an attractive route to regenerate any damaged or missing tissue. An alternative approach is the direct reprogramming - switching from one somatic lineage to another - through the expression of a multiple lineage-specifying TFs. One of the first studies reporting successful direct reprogramming was the conversion of exocrine cells to endocrine cells in the mouse pancreas mediated by a combination of Ngn3, Pdx1 and Mafa (Zhou *et al.* 2008).

Combined expression of the TFs Brn2, Ascl1 and Myt1l was sufficient to directly reprogram mouse fibroblast cells and human IPS cells into fully functional neuronal cells (Vierbuchen *et al.* 2010; Pang *et al.* 2011). Recently, it was demonstrated that expression of a single TF, Sox2, is capable of inducing

NSC-characteristics in cultured mouse and human fibroblast cells (Ring *et al.* 2012). These induced NSCs resemble wild-type NSCs in their morphology, self-renewal, ability to form neurospheres, and gene expression profiles. Directly reprogrammed NSCs are self-renewing and multipotent, as they differentiate into several classes of mature neurons, as well as astrocytes and oligodendrocytes.

The freedom to generate patient-specific pluripotent stem cells provides new avenues for basic research and transplantation therapies with fully immunologically matched grafts for neurological and degenerative diseases. Moreover, cells could be manipulated for therapeutic purposes (e.g., cell replacement) towards a specific lineage, for instance a specific neuronal or glial cell type.

1.6 Gene knockdown and knockout in developmental genetics

1.6.1 Forward genetics

A common approach to interrogate the biological function of genes is the analysis of the loss-of-function phenotypes. In mutational analysis genes are functionally inactivated by disruptive mutations altering the protein-coding sequence, resulting in defective biological processes and the appearance of perceptible phenotypes. Alternatively, methods depleting mRNA transcript pool or interfering with translation or splicing allow functional characterization of genes without the necessity of introducing mutations into the genome. In addition, they allow studying the effect of knockdowns of multiple targets in one system, with the drawback that studies are limited to the early development.

Traditionally, most gene functions have been exposed in phenotype-based approaches, where arbitrary gene disruption is followed by identification of mutant phenotypes. Mutants are identified by their displayed phenotypes; as a consequence the altered allele is mapped within the genome and associated with the observed phenotypic changes. Forward genetic screens have been successfully carried out in model systems as diverse as flies, worms, fish and mice (Brenner 1974; Nüsslein-Volhard and Wieschaus 1980; Hitotsumachi *et al.* 1985; Kubota *et al.* 1995; Driever *et al.* 1996; Haffter *et al.* 1996; Loosli *et al.* 2000). Base modifications resulting in heritable codon changes can be induced through ionizing radiation or chemical agents such as ENU or EMS, while transposase-mediated random insertions of transposable DNA elements provide a different method to cause disruption of extant coding sequences (Cooley *et al.* 1988; Gossler *et al.* 1989).

1.6.2 Reverse genetics

Teleost species medaka and zebrafish have become increasingly popular in biological research, in particular as resources in vertebrate developmental genetics. They are perfectly suited for large-scale forward genetic screens due their small size, accessibility and transparency. A large number of human disease genes have orthologs in medaka (more than 65%) and zebrafish (more than 75%), making both species amenable to disease-related genetic studies (Kasahara *et al.* 2007; Howe *et al.* 2013). While the forward genetic screen is a powerful tool for uncovering unknown gene functions of great diversity, a reason why this approach is of interest for research in models where targeted mutagenesis is available (Anderson 2000), it imposes a number of limitations. The gene discovery is phenotype-driven and therefore relies on mutations that produce a visible phenotype. For instance, some mutations will lack an overt phenotype because of the existence of genes with redundant functions. Likewise, mutants can be missed during the screening process due to their subtle phenotype. Moreover, this approach is incapable of generating individual mutations at will for a specific gene of interest. This presents a general problem for model organisms such as fish and frogs, where the lack of reliable approaches mediating targeted mutagenesis has limited the functional analysis of genes.

1.6.2.1 Targeting induced local lesions in genomes

One application to bridge the gap between forward and reverse genetics in model organisms such as fish is targeting induced local lesions in genomes (TILLING). Pioneered in *Arabidopsis thaliana*, the initial steps of large-scale forward genetic screens based on random mutagenesis (e.g. chemically induced in sperm or spermatogonia) remain the same (McCallum *et al.* 2000; Colbert *et al.* 2001). However, instead of phenotypic selection, individual DNA samples are obtained for sequence-based selection beforehand. Prior knowledge of the genomic sequence is required for the gene-specific PCR amplification steps, which are followed by endonuclease treatment to uncover mismatches in complementary DNA strands. Once the existence of a mutation in the gene of interest is confirmed, phenotypic consequences can be analyzed in the corresponding mutant fish (Wienholds *et al.* 2002; Ishikawa *et al.* 2010). Reduced sequencing costs make whole genome sequencing comparison an attractive alternative approach to identify altered coding sequences. Recently, the combination of large-scale random mutagenesis and high-throughput sequencing identified mutations in more than 38% of the proteincoding zebrafish genes (Kettleborough *et al.* 2013). Large-scale genetic screens in fish remain relevant for the systematic identification of vertebrate gene function due to their ease and range; adding to their appeal is the possibility to pair them with rapid and cost-efficient sequencing

protocols in order to identify precisely the altered sequence in the genome.

1.6.2.2 Morpholino oligonucleotides

Exploring gene function in fish and frog based on reverse genetics has mainly relied on injection of antisense oligonucleotides into the yolk or cytoplasm of a fertilized oocyte. Morpholino oligonucleotides are DNA analogues modified to resist endogenous enzymatic degradation processes and are designed to be complementary to the 5'UTR of a specific gene to block translation (Summerton and Weller 1997). Antisense morpholino oligonucleotide-mediated knockdown has been shown to phenocopy known zebrafish mutants (Nasevicius and Ekker 2000). While this approach has been successfully adopted to study gene function in a variety of model systems, prevalent limitations include dilution of efficiency through cell divisions, non-specific side effects and false-positive phenotypes through off-target knockdowns (Heasman 2002).

1.6.2.3 Targeted genome editing

Elucidating gene function by altering the coding sequence of a specific gene first and investigating the resulting phenotype later depends on the availability of efficient and sequence-specific methods for targeted genome editing in the model system of choice. Genome editing comprises a variety of applications, such as base pair deletions to induce frame shifts, substitutions to alter the amino acid sequence and therefore the protein structure, or insertion of exogenous DNA fragments into the host genome.

Recombination between homologous sequences permits the introduction of any desired fragment from exogenous DNA plasmid into the target genome. HR provides an unmatched precision (e.g. single nucleotide modifications) in the field of genome engineering. First established in yeast, HR has become the conventional method for mouse geneticist, aided by the existence of mouse ESCs, to engineer the mouse genome (Hinnen *et al.* 1978; Orr-Weaver *et al.* 1981; Thomas *et al.* 1986; Thomas and Capecchi 1987), in particular to investigate the role of genes in development and disease. The dominant role of model organisms with experimentally manipulable genomes is reflected by the vast knowledge we obtained from reverse genetic applications about gene function fundamental biological process, which to contributed to the desire for the availably of genome editing methods as precise and efficient in other species.

Technologies developed for targeted mutagenesis such as zinc-finger nucleases (ZFNs), transcription activator-like effector nucleases (TALENs), and more recently RNA-guided systems can introduce chromosomal double-strand breaks (DSBs) to trigger endogenous repair pathways (Kim *et al.* 1996;

Lu *et al.* 2011; Tesson *et al.* 2011; Jiang *et al.* 2013; Wang *et al.* 2013). The error-prone repair of DNA DSBs by NHEJ can produce specific gene lesions but comes at the cost of unpredictable insertion and deletion mutations. Homology directed repair comes with the advantage of having complete control over the genomic modifications. By presenting donor DNA with homologous sequences to the desired locus, base pair deletions, insertions and substitutions of choice can be produced, extending the list of experimental applications beyond the generation of mutagenic lesions in coding sequences.

1.6.2.4 Zinc-finger nucleases

The ability to do reverse genetics - manipulate any desired locus in the genome followed by investigation for the phenotypic consequences - has been significantly enhanced by the emergence ZFNs. These hybrids comprised of zinc-finger arrays and *FokI* endonuclease offer precise genetic modification, in particular in living organisms that previously proofed too complicated or impossible to experimentally manipulate, for instance flies, fish or rats (Bibikova *et al.* 2002; Doyon *et al.* 2008; Meng *et al.* 2008; Geurts *et al.* 2009). The applications for ZFNs go beyond determining the biological role of arbitrary genes during development. ZFN-mediated disruption of HIV host co-receptor chemokine receptor 5 in T cells has been demonstrated to provide heritable protection against HIV-1 infection *in vivo*, highlighting the potential of ZFNs for therapeutic purposes (Perez *et al.* 2008). Similarly, the mutated alleles causing monogenic disorders could be specifically targeted and restored in their wild-type form. Cys2His2 zinc-fingers are DNA-binding domains that typically recognize three base pairs of DNA and are assembled in arrays of three to six fingers, therefore providing sequence specificity through binding to 18-36 base pairs of genomic DNA (Urnov *et al.* 2010). The zinc-finger arrays are fused to the non-specific proteolytic domain of the *FokI* (*Flavobacterium okeanokoites*) endonuclease. *FokI* nucleases catalyze DNA cleavage as dimers, thus the assembly of two customized ZFNs for one target locus is prerequisite for the generation of a DSB (Bitinaite *et al.* 1998). Development of obligate heterodimeric *FokI* nuclease domains has improved target specificity through reduced occurrence of unwanted homodimers (Miller *et al.* 2007). Following the generation of a ZFN-mediated site-specific DSB, NHEJ is triggered. Erroneous repair - insertion or deletion of base pairs - is likely to induce heritable frameshift mutations.

1.6.2.5 Transcription activator-like effector nuclease

Part of the desire for an alternative method stems from the difficult assembly process of individual zing-fingers, which has been reported as inefficient and laborious (Ramirez *et al.* 2008). TALENs are similar to ZFNs, as both are chimeras consisting of a customizable DNA-binding domain and a non-

specific *FokI* cleavage domain. The DNA-binding domain in TALENs is an array of highly conserved repeats, so-called TAL effectors, which were discovered in plant pathogenic bacteria. Upon entering the host plant cell, these transcriptional regulators are able to directly bind genomic DNA, therefore alter gene transcription in the nucleus during the course of pathogenesis (Boch and Bonas 2010). Binding specificity is achieved through tandem repeats in the central DNA-binding domain. Each repeat consists of two hyper-variable amino acid residues and allows binding to one base pair of genomic DNA (Boch *et al.* 2009; Moscou and Bogdanove 2009). The modularity of TAL effectors allows the construction of artificial effectors with novel binding specificities to target essentially any sequence of interest. As with ZFNs, the ability of TALENs to alter gene expression has been tested in a wide range of model organisms and cell types (Joung and Sander 2012). Studies reporting modification of the zebrafish genome were the first instances of gene disruptions created by TALENs in a vertebrate system (Huang *et al.* 2011; Sander *et al.* 2011). In addition, TALEN-mediated DSBs complemented with single-stranded DNA oligonucleotide donors yielded precise insertions into the zebrafish genome (Bedell *et al.* 2012). In this instance a *loxP*-site was inserted, offering the possibility to elucidate gene function in conditional mutants based on the Cre/*lox* or Flp/*FRT* recombination system (Branda and Dymecki 2004). In medaka, the successful generation of heritable lesions via TALENs has been reported; an exon of *DJ-1*, a gene implicated in the onset of early Parkinson's disease, has been targeted (Ansai *et al.* 2013). Both TALENs and ZFNs have been used to specifically activate gene expression, adding targeted transcriptional gene regulation to the list of applications. Instead of the *FokI* proteolytic fragment, a transcriptional activator domain was fused to the DNA-binding domain (Blancafort *et al.* 2004; Cermak *et al.* 2011; Miller *et al.* 2011), making them highly versatile tools to modify genes and gene expression.

1.6.2.6 RNA-guided genome modification

With more and more genomic resources available, there is an increasing demand for reliable reverse genetic approaches in fish. The rise of TALENs can be attributed to their easy design and rapid modular assembly; each TAL effector repeat recognizes one base pair in the target-binding site. A more recent class of engineered endonucleases employed for genome editing purposes achieves sequence specificity independent of a DNA-binding domain. RNA-guided nucleases are part of the adaptive immune system in bacteria and archea, which protects the organism against invading foreign DNA (Horvath and Barrangou 2010; Marraffini and Sontheimer 2010). Short fragments of nucleic acids from previous viral infections are integrated as clustered, regularly interspaced, short palindromic repeats (CRISPRs) into the host genome. Upon renewed infection, short CRISPR-derived RNAs (crRNAs) are

transcribed and guide the CRISPR-associated (Cas) protein, a non-sequence-specific nuclease, to the foreign genetic material, which will then be cleaved and inactivated. In type II CRISPR/Cas systems, another type RNA, *trans*-acting antisense RNA (tracrRNA), forms an RNA duplex together with pre-crRNA that is processed by RNase III (Deltcheva *et al.* 2011). The CRISPR/Cas system modified for genome editing purposes in eukaryotic cells features a single guide RNA (sgRNA), a hybrid between crRNA and tracrRNA, with 20 nucleotides of homology to the target. Immediately downstream follows the protospacer adjacent motif (PAM). The *Streptococcus pyogenes* Cas9 nuclease, which has been proposed to prefer the PAM sequence NGG, forms a ribonucleoprotein complex with the sgRNA and the homologous genomic target sequence. Choosing targets with deviations in the second or third nucleotide of the PAM sequence is detrimental to the cleavage efficiency, but does not entirely abolish cutting (Hsu *et al.* 2013; Jiang *et al.* 2013; Pattanayak *et al.* 2013). The binding specificity of the complex is determined by the sgRNA; therefore, the CRISPR/Cas approach requires generation of sgRNA matching the desired locus but is free of time-consuming engineering of specific DNA-binding fragments. The Cas nuclease and one specific guide RNA are the only components necessary and sufficient for induction of targeted DSBs. The efficacy of CRISPR/Cas system has been tested in human cells, zebrafish and mice (Chang *et al.* 2013; Cong *et al.* 2013; Hwang *et al.* 2013; Jao *et al.* 2013; Mali *et al.* 2013b; Shen *et al.* 2013). The applications in zebrafish include recapitulation of known phenotypes (Chang *et al.* 2013), germline transmission of the induced mutagenic lesions (Hwang *et al.* 2013; Jao *et al.* 2013), recessive null-like phenotypes induced by biallelic gene disruption (Jao *et al.* 2013), and knock-ins of experimenter-provided donor oligonucelotides (Chang *et al.* 2013; Hwang *et al.* 2013). Furthermore, a nuclease-inactivated version of the Cas9 protein has been fused to a transcriptional activator, allowing RNA-guided gene regulation (Mali *et al.* 2013a). Up to five genomic loci have been targeted simultaneously in ESCs and (Jao *et al.* 2013; Wang *et al.* 2013). The possibility of multiplex gene targeting will be beneficial in a number of applications, for instance the simultaneous introduction of multiple recombination sites to create conditional mutant alleles in a single step. Particularly research involving teleost fish, where multiple paralogs of one gene can exist as a result of whole genome duplication events, will profit from the multiplex feature of the CRISPR/Cas system. Paralogous genes can be targeted simultaneously with a single injection into fertilized eggs at one-cell stage, instead of performing tedious sequential single-knockouts.

So far, RNA-guided nucleases proofed to be at least as effective and versatile as ZFNs or TALENs in generating DSBs, which are the substrates for both mutagenic and homology directed repair. However, one constrain, when using the Cas9 protein, is presented by the required presence of the PAM site in the target sequence. Additionally, studies systematically testing the impact of mismatches in the

guide RNA found that single mismatches, particularly the ones near the PAM, reduced cleavage activity. Multiple mismatches rendered the targeted cleavage even less effective (Hsu *et al.* 2013). Furthermore, the system tolerated up to three mismatches, especially at PAM-distal positions of the sgRNA, highlighting the need for improved binding specificity in order to avoid off-target effects (Mali *et al.* 2013a).

1.7 Methodological approaches allowing the identification of upstream regulators of regulatory DNA elements

Chromatin immunoprecipitation offers the possibility to identify genomic DNA targets for a given TF *in vivo*. Interacting genomic DNA is identified by high-throughput sequencing following the co-immunoprecipitation with the protein of interest using an antibody against the protein (Collas and Dahl 2008). Likewise, prior knowledge of the binding site composition recognized by a TF allows bioinformatics-based search in non-coding promoter and enhancer regions. Computationally identified putative genomic targets need to be experimentally validated. Although chromatin immunoprecipitation is a very elegant method to show direct protein-DNA interactions *in vivo*, it is not suited to systematically search for transcriptional regulators of a given regulatory DNA. This would require the availability of specific antibodies against each protein or transgenic lines expressing epitope-tagged TFs.

Interactions between TFs and a defined promoter have been successfully tested in yeast-one-hybrid and luciferase reporter assays. In the yeast-one-hybrid system, the protein is fused to an artificial activation domain and upon binding to the regulatory DNA, reporter gene expression (e.g., histidine synthase) is activated (Li and Herskowitz 1993). Although this approach indicates physical protein-DNA interactions, it is unable to reveal the regulatory mechanisms and the strength of interactions.

The luciferase assay-based *trans*-regulation screen (TRS) has been shown to overcome those limitations. In this approach, cultured cells are co-transfected with the regulatory element upstream of a luciferase reporter (e.g., firefly luciferase), an expression vector encoding the candidate gene and a second reporter (e.g., *Renilla* luciferase). The obtained relative luminescence signals provide knowledge about the relative strength of activation or repression.

Since the approach is cell culture-based and requires no tedious modifications of cDNA clones, rapid screening of transcriptome-scale cDNA libraries is possible, as successfully demonstrated for the regulatory element of the *Atoh7* (also known as *Ath5*), a TF indispensable for ganglion cell specification (Souren *et al.* 2009).

1.8 Aim of this thesis

Over the last decades teleosts have become an increasingly popular model to study key developmental events and to dissect basic biological processes (Furutani-Seiki and Wittbrodt 2004). In particular the teleost eye, which is constantly growing from a compartmentalized stem cell domain, constitutes an excellent system to explore post-embryonic neurogenesis and the coordinated growth of several connected tissues. A recent study provided compelling evidence for the existence of multipotent NSCs in the post-embryonic medaka retina (Centanin *et al.* 2011). However, the molecular mechanism and the transcriptional framework underlying stemness in adult NSCs remain poorly understood.

This study aims to shed light on the gene regulatory framework orchestrating stem cell features in the retina by analyzing the regulatory cues controlling the expression of *Rx2*, a bona fide molecular marker for multipotent RSCs.

In addition, the study aims to establish the genetic tools to elucidate the role of *Rx2*. A plethora of studies in recent years described methods allowing the targeted modification of the genome (Gaj *et al.* 2013). These methods opened the opportunity to take advantage of reverse genetics with a precision previously available in a limited selection of model organisms. In both medaka and zebrafish, TALENs have been demonstrated to successfully introduce heritable mutations into the genomic sequences of choice (Sander *et al.* 2011; Ansai *et al.* 2013). Taking advantage of specific TALENs targeting endogenous *Rx2*, loss-of-function mutants are established, which will be analyzed in the future.

RESULTS

2 Results

2.1 Identification of regulators of retinal stem cell features

2.1.1 *Rx2* is specifically expressed in the eye

The embryonic expression of *Rx2* was first observed at the late neurula stage (stage 18) in retinal progenitors following the completion of optic vesicle evagination (Figure 3A). Later (stage 24) it was uniformly expressed in all RPCs throughout the proliferating mono-layered optic cup (Figure 3B). *Rx2* was centrally down-regulated concomitant with the onset of differentiation from the center, where the first progenitors exit the cell cycle and differentiate terminally into distinct neural retinal cell types. During the ongoing retinogenesis *Rx2* was progressively restricted to the margins of the expanding optic cup.

Figure 3. Eye-specific TF Rx2 is expressed throughout eye development.
(A-C) Brightfield images of whole-mount preparations at various developmental stages. *Rx2* transcripts are strongly detected in the optic vesicle (stage 18, A), the optic cup (stage 24, B) and the eye (stage 34, C).

2.1.2 *Rx2* is expressed in the peripheral-most part of the post-embryonic stem cell domain

Detailed analysis of the post-embryonic pattern of *Rx2* mRNA or protein and comparison with transgenic reporter animals expressing fluorescent proteins under the control of the *Rx2* CRE (Martinez-Morales *et al.* 2009; Inoue and Wittbrodt 2011) consistently revealed expression in stem cells in the most distal domain of the CMZ (stage 35) (Figure 4A'). The CMZ is populated by proliferating and undifferentiated cells, as indicated by the expression of the M-phase marker PHH3, the incorporation of the base analogue BrdU and the expression of the S-phase marker PCNA (Bravo *et al.* 1987; Negishi *et al.* 1991) (Figure 4B-D). Whereas PCNA protein co-localized with the majority of Rx2 protein and fluorescent reporter expression, PCNA staining was absent from the peripheral-most Rx2-positve cells (Figure 5F-J). Likewise, BrdU was incorporated only in the central-most Rx2-expressing cells after a short pulse (not shown). In contrast to the findings at post-embryonic stages, peripheral Rx2-positive

cells continuously expressed PCNA during optic cup stages (Figure 5A-E). Expression of *Rx2* and differentiation markers appeared mutually exclusive in the peripheral retina (Figure 4E). Rx2 protein was also detected in cells of the INL and photoreceptor cells in the ONL (Figure 4A''). Immunostaining against glutamine synthetase confirmed that Rx2 reporter and protein co-localize in MGCs throughout the INL (Figure 6). WISH analysis of *Rx2* expression was consistent with Rx2 immunostaining and reporter expression, confirming that the Rx2 reporter faithfully recapitulates *Rx2* expression in the post-embryonic retina (Figure 3C).

The expression analysis highlighted expression of *Rx2* as a specific marker for the peripheral-most region in the CMZ and underscores the precise spatial reporter expression of the *Rx2* CRE.

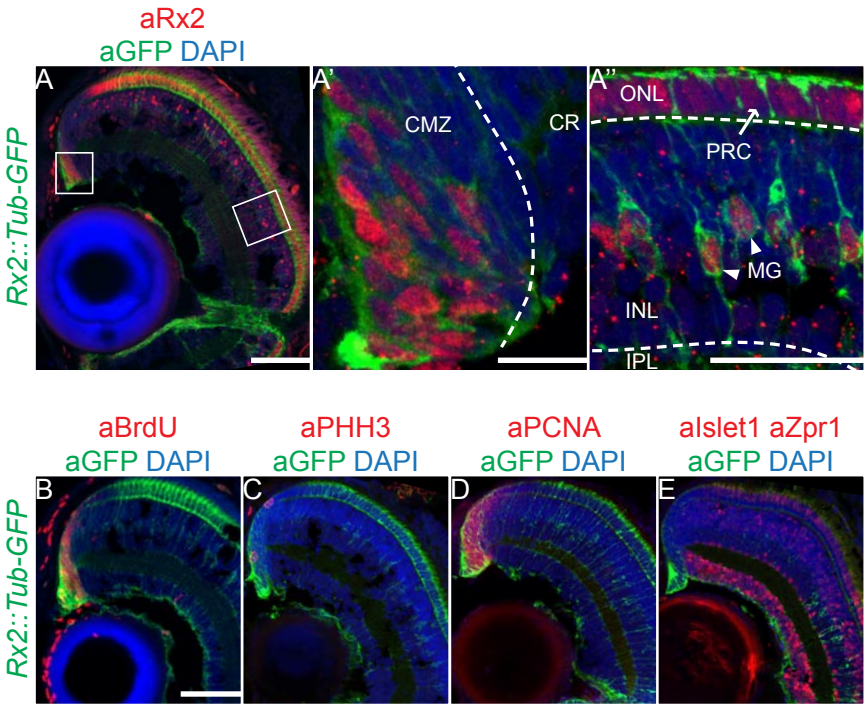

Figure 4. Rx2 reporter and protein expression co-localizes in the post-embryonic retina.
(A-E) Confocal stacks of frontal sections on the retina of transgenic Rx2 reporter (*Rx2::Tub-GFP*) embryo at stage 34. Transgenic reporter expression driven by *Rx2* CRE (A, green) and Rx2 protein (A, red) closely overlap (A). Higher magnifications of boxed regions in (A) highlight overlapping expression in the peripheral CMZ (A') and MGCs (white arrowheads) and photoreceptor cells (white arrow) of the central NR (A''). Dashed lines demarcate border between CMZ and differentiated retina (A') or between layers of the retina (A''). *Rx2* reporter expression in the periphery of the NR overlaps with mitotic markers BrdU (B, red), PCNA (C, red) and pHH3 (D, red). Markers of differentiated neurons Zpr1 (E, red) and Islet1 (E, red) are absent from the juvenile CMZ. Scale bars: 50 µm in A and B; 25 µm in A' and A''.

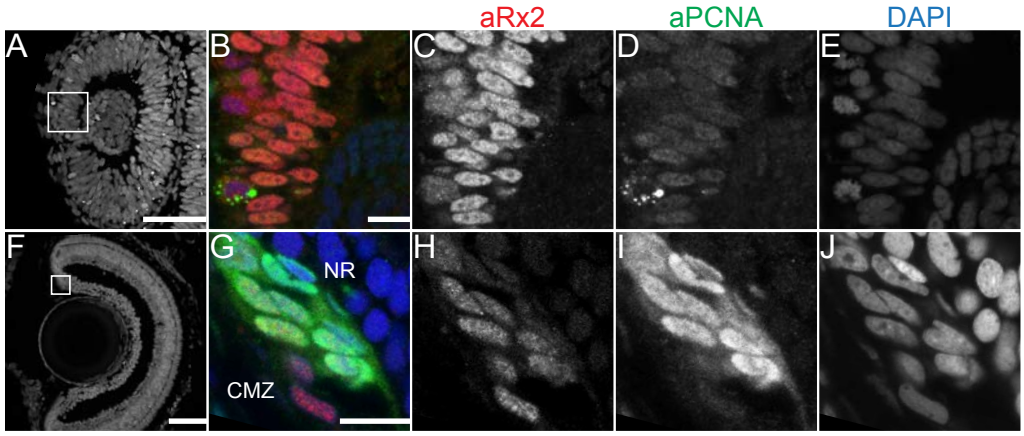

Figure 5. Rx2 and PCNA proteins are co-expressed at embryonic and post-embryonic stages.
(A-E) Confocal stacks of transversal sections show co-expression of Rx2 and PCNA in the optic cup (stage 24). (F-J) Confocal stacks of transversal sections show expression of Rx2 and PCNA in the post-embryonic retina (stage 37). Higher magnification pictures of boxed regions (A and F) are shown in (B-E and G-J). Scale bars: 50 µm in A and F; 10 µm in B and G.

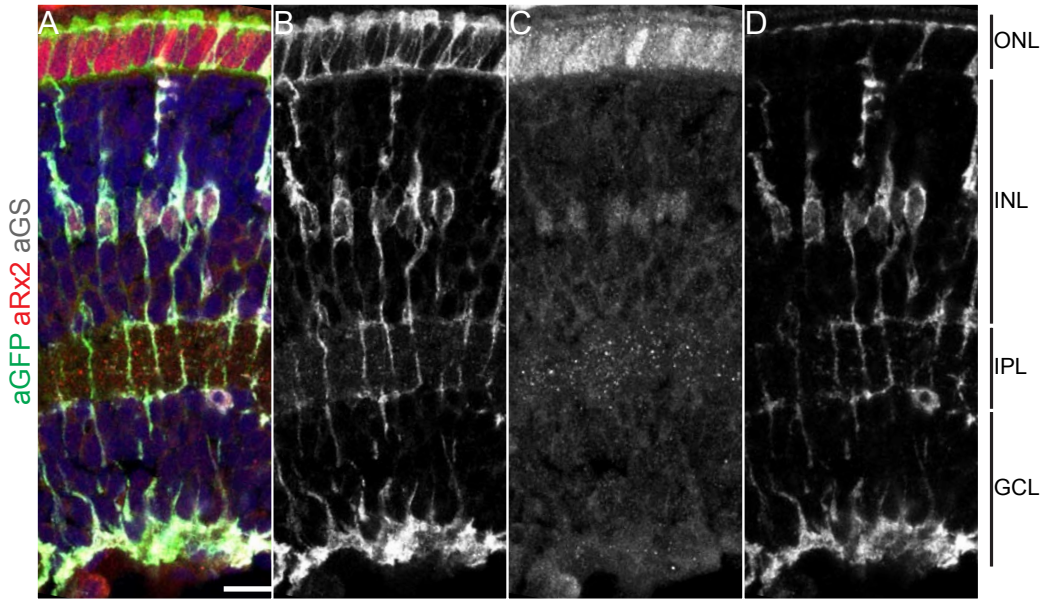

Figure 6. Rx2 labels MGCs in the central retina.
(A-D) Confocal stacks of frontal sections on the retina of transgenic *Rx2* reporter (*Rx2::Tub-GFP*) embryo at stage 34. Transgenic reporter expression driven by *Rx2* CRE (B, green) and Rx2 protein (C, red) co-localizes in the INL with glutamine synthetase immunostaining (D, grey) in the INL. Scale bar: 10 µm.

2.1.3 Identification of regulators of *Rx2* expression

To identify genes controlling RSC-specific features, we investigated the regulatory input guiding *Rx2* expression. For the systematic survey for regulators upstream of *Rx2* the *trans*-regulation screen was employed. This cell culture-based method involves the co-transfection of a reporter construct, which has the luciferase coding sequence downstream of the regulatory region of interest, together with candidate regulators. The luciferase reporter assays provide insight into the strength of the interaction and the actual regulatory function (e.g., activating) of the candidate protein. Rapid transfection under high-throughput conditions allows screening of large quantities of candidate genes in parallel on one or multiple regulatory regions. This approach reliably identified *de novo* upstream regulators of *Atoh7* expression (Souren *et al.* 2009). We took advantage of the relatively short *Rx2* CRE, which is sufficient to recapitulate the entire expression pattern of *Rx2 in vivo* as described above, and tested 1151 individual full length cDNA clones representing a large complement of the putative medaka TF in a dual luciferase-based screen in cultured mammalian (BHK21) cells (Table 1). Activating or repressing candidates were validated by their expression relative to the expression of *Rx2*. Among the 51 genes analyzed, *Sox2* was the top activator expressed in the mature retina. *Gli3* and *Her9* were the regulators with the strongest repressive activities. *Tlx*, not present in the full-length TF library, was included because its particular expression in the CMZ and its role in NSCs (Yu *et al.* 1994; Monaghan *et al.* 1995; Shi *et al.* 2004).

Ratio	Ensembl ID	Protein name
6.8223	ENSORLG00000013930	MAFB (2 of 2)
6.3932	**ENSORLG00000011685**	**SOX2**
5.6326	ENSORLG00000009709	
5.0471	ENSORLG00000005001	SOX4
4.8001	ENSORLG00000012110	SOX1
4.3921	ENSORLG00000006390	P53_ORYLA
4.3592	ENSORLG00000012314	RND1
4.2939	ENSORLG00000017977	
4.2580	ENSORLG00000001780	Q9PT76_ORYLA
4.2226	ENSORLG00000000325	TRIM24
4.0101	ENSORLG00000014996	SOX11
3.9707	ENSORLG00000014398	TBL1XR1
3.8176	ENSORLG00000014335	
3.8015	ENSORLG00000007859	
3.7558	ENSORLG00000011491	MYCBP2
3.6907	ENSORLG00000011362	DUSP4
3.5596	ENSORLG00000014065	
3.5320	ENSORLG00000003250	
3.5207	ENSORLG00000007960	
3.5159	ENSORLG00000012362	

Ratio	Ensembl ID	Protein name
0.2745	ENSORLG00000008319	
0.2724	ENSORLG00000010756	CYR61
0.2673	ENSORLG00000014942	
0.2661	ENSORLG00000019628	
0.2638	ENSORLG00000007548	ACVRL1
0.2633	ENSORLG00000013006	
0.2612	ENSORLG00000017539	CDK5
0.2593	ENSORLG00000004561	DLX5
0.2588	ENSORLG00000001137	MYST1
0.2570	ENSORLG00000004126	ROBO4 (1 of 2)
0.2508	ENSORLG00000003221	IFRD2
0.2428	ENSORLG00000010055	Q7T1Q8_ORYLA
0.2360	ENSORLG00000007641	Q9PT79_ORYLA
0.2334	ENSORLG00000008072	
0.2333	ENSORLG00000015121	Q1XHL4_ORYLA
0.2285	ENSORLG00000010717	PDCD2
0.2259	ENSORLG00000013422	ARG1
0.2247	ENSORLG00000009030	RAB6C
0.2210	ENSORLG00000008054	
0.2156	ENSORLG00000003982	GADD45G (1 of 3)
0.2035	ENSORLG00000017855	TBL1Y
0.2010	ENSORLG00000014546	DLK1
0.1989	ENSORLG00000013231	GADD45B (1 of 2)
0.1981	ENSORLG00000004319	COL1A2
0.1959	ENSORLG00000006591	IFT57
0.1939	ENSORLG00000009381	CHUK (2 of 2)
0.1918	ENSORLG00000017412	PAX1
0.1906	ENSORLG00000018979	STAU1
0.1752	ENSORLG00000004166	
0.1666	**ENSORLG00000005453**	**HER9**
0.1031	**ENSORLG00000012490**	**GLI3**

Table 1. Candidate regulators of *Rx2* identified in the TRS.
Normalized ratios, Ensembl gene IDs and protein names are shown for the putative activators and repressors. Tested factors with normalized ratio of equal or more than 3.388 were considered as putative activators (left). Normalized ratios of equal or less 0.2755 were assigned as putative repressors (right). Factors are listed in descending order according to their normalized ratios. The TFs Sox2, Her9 and Gli3 (bold) were the strongest regulators expressed in the post-embryonic CMZ and therefore tested for the ability to regulated Rx2 *in vivo*.

2.1.4 *Rx2*, *Sox2*, *Tlx*, *Her9* and *Gli3* are co-expressed in the post-embryonic CMZ

To address the function of our candidate genes, we first examined the expression of *Sox2*, *Tlx*, *Gli3* and *Her9* with respect to *Rx2*. Expression of the pan-neural determinant *Sox2* was detected throughout the CMZ, from cells residing distally in the periphery, to more centrally located rapidly proliferating progenitors, to differentiating cells closest to the differentiated central retina (Figure 7A-C). *Tlx* and *Her9*, which were both expressed in the central CMZ, partially overlapped with the *Rx2* expression domain (Figure 7D-I). Tlx- and Her9-positive cells that were Rx2-negative were found more centrally in

the CMZ, where cells express PCNA and rapidly incorporate BrdU. In contrast, highest levels of *Gli3* transcripts were found in the peripheral RPE surrounding the CMZ, while lower levels of *Gli3* were also observed in the peripheral post-embryonic CMZ (Figure 7J-L). Two-color WISH confirmed the presence of *Gli3* transcripts in the peripheral-most *Rx2*-expressing cells inside the CMZ (arrowhead in Figure 7L).

Taken together the expression of all *Rx2* candidate regulators is tightly associated with the expression of *Rx2* in distinctive domains of the post-embryonic retina and where they partially overlap with *Rx2* in the CMZ.

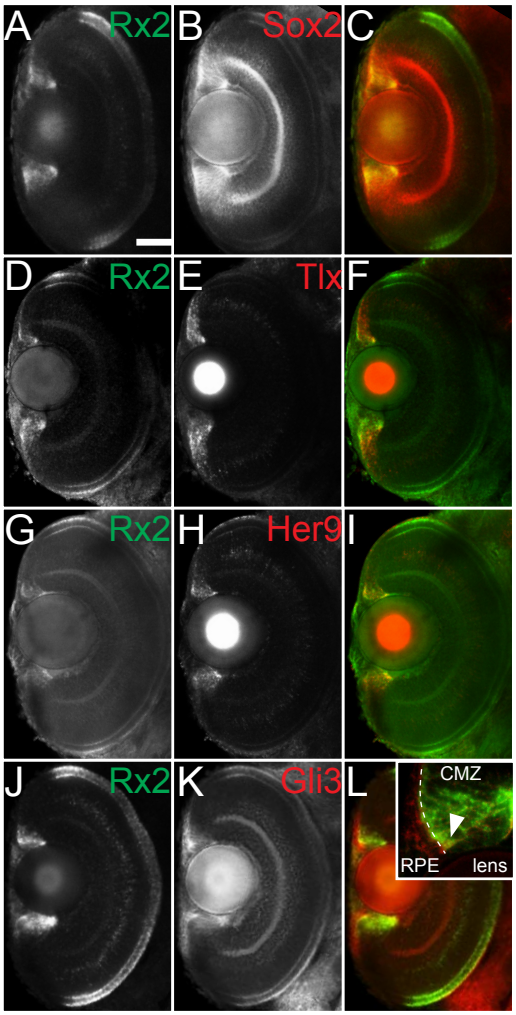

Figure 7. Spatial expression pattern of *Rx2* regulators in the post-embryonic retina of medaka.
(A-L) Confocal stacks of whole-mount two-color fluorescence *in situ* hybridizations with probes against *Sox2* (B, red), *Tlx* (E, red), *Her9* (H, red), *Gli3* (K, red) and *Rx2* (A, D, G, J, green) on stage 35 embryos. *Rx2* (A, D, G, J, green) transcripts are found in the CMZ, INL and ONL. *Sox2* (B, red) is expressed throughout the CMZ. *Tlx* (E, green), *Her9* (H, green) have similar expression patterns in the central CMZ at stage 35, overlapping partially with *Rx2* expression. *Gli3* mRNA (K, red) is expressed primarily in the pigmented epithelium adjacent to the CMZ (inset in L). *Gli3* mRNA in the CMZ is present in the peripheral-most *Rx2*-expressing cells (white arrowhead). Dashed line demarcates boundary between RPE and CMZ. Scale bar: 50 µm.

2.1.5 The *Sox2*, *Tlx* and *Her9 cis*-regulatory elements recapitulate endogenous gene expression

To analyze the expression of *Sox2*, *Tlx* and *Her9* in the CMZ in more detail, transgenic reporter lines were generated. Based on the conservation in comparison to orthologous sequences, non-coding genomic fragments were tested for their *cis*-regulatory activity in the post-embryonic medaka retina (Ramialison *et al.* 2012). Reporter expression driven by the 2.4 kb fragment identified upstream of *Sox2* was located in the entire CMZ (Figure 8A-D). The expression clearly overlapped with staining for Rx2 in the periphery and was extended into the central domain of the CMZ. Consistent with the expression analysis for the transcripts of *Tlx* and *Her9*, the respective transgenic reporter lines were expressed in the CMZ. Expression of both transgenic reporters was detected in the central-most *Rx2* domain. Similar to *Sox2*, both *Tlx* (Figure 8E-H) and *Her9* (Figure 8I-L) reporter activity appeared also in Rx2-negative cells of the central CMZ. In contrast, neither *Tlx::GFP* nor the *Her9::GFP* transgenic fish did express GFP in the most distal Rx2-positive cells.

To put these findings into relation, the transgenic *Atoh7* reporter, labeling the central-most CMZ (Del Bene *et al.* 2007), was added (Figure 9). Transgenic fish carrying three reporter transgenes were analyzed for the expression of nuclear monomeric RFP (*Rx2*), cytoplasmatic GFP (*Tlx*) and membrane-bound YFP (*Atoh7*). Cross sections through the eye of hatchlings revealed three distinct domains: Consistent with previous findings, the cells in the most distal domain expressed the *Rx2* reporter only (1). The next domain, which is located more centrally, was occupied by cells labeled with *Rx2* and *Tlx*, but not by *Atoh7* (2). The third domain, which did not express the *Rx2* reporter, was entirely populated by memYFP-positive cells due to activity of the *Atoh7* reporter transgene (3). At the transition from the second to the third domain *Tlx* was still expressed but did not spread as close as *Atoh7* towards post-mitotic neurons.

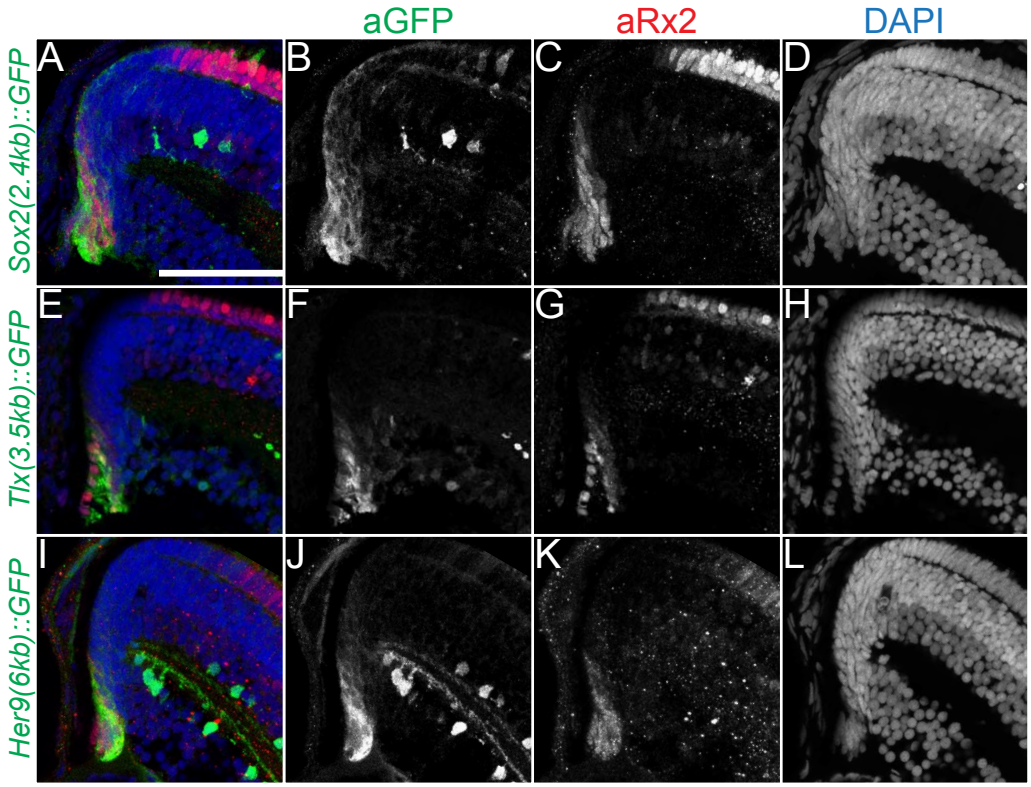

Figure 8. Transgenic reporters for *Sox2*, *Tlx* and *Her9* are expressed in the CMZ.

Confocal stacks of frontal sections on the retina of transgenic hatchlings. Peripheral CMZ is to the left, central retina is to the right.

(A-L) Expression of transgenic *Sox2* (B), *Tlx* (F) and *Her9* (J) reporter overlaps in part with Rx2 protein (C, G, K) in the CMZ. Scale bar: 50 µm.

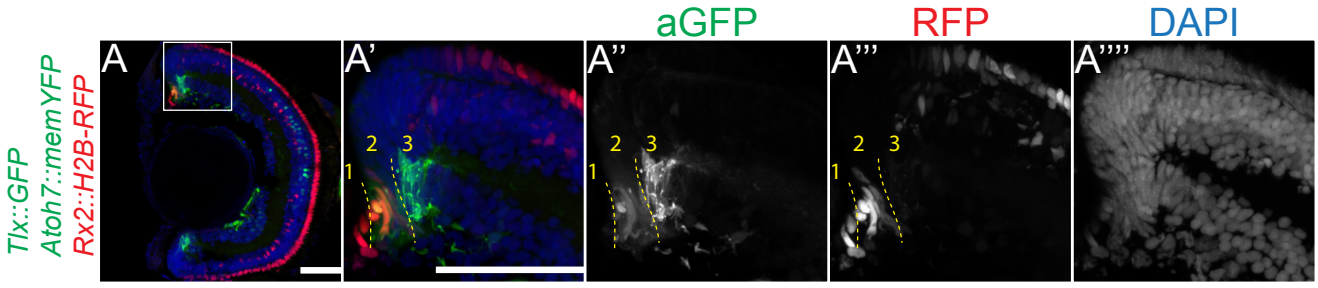

Figure 9. Transgenic *Rx2*, *Tlx* and *Atoh7* reporter lines label different domains in the post-embryonic CMZ.

(A) Confocal stacks of frontal sections on the retina of a triple-transgenic (*Rx2::H2B-mRFP*, *Tlx::GFP* and *Atoh7::memYFP*) hatchling. Higher magnifications of boxed region in (A) highlight the partially overlapping expression in the CMZ of all three reporter lines. *Rx2::H2B-mRFP* occupies the peripheral-most CMZ (1) and overlaps in part with *Tlx::GFP* (2). *Tlx* reporter expression extends into the most central part of the CMZ, labeled by *Atoh7::memYFP* (3). *Rx2::H2B-mRFP* at this stage does not overlap with the *Atoh7::memYFP*. Dashed (yellow) lines demarcate borders between peripheral and central-most *Tlx* reporter expression domain. Scale bars: 50 µm.

2.1.6 Conditional clonal analysis in the post-embryonic medaka retina

Since the *in vitro* characterization and the overlapping expression pattern of *Sox2* and *Tlx* with *Rx2* consistently argued for an activating function of *Sox2* and *Tlx*, their interaction was addressed by a clonal gain-of-function approach in the post-embryonic retina.

For this, we employed a conditional, steroid-inducible expression system, which provided spatio-temporal control over the expression of the gene of interest (Emelyanov and Parinov 2008) and tested the consequences of acute clonal activation of *Sox2* (*cska::LexPR LexOP::Sox2*) and *Tlx* (*cska::LexPR LexOP::Tlx*) gain-of-function through DNA microinjection into fertilized oocytes (Figure 10A). Positive clones were labeled by the expression of fluorescent proteins (*LexOP::H2A-Cherry* or *LexOP::Cherry*), encoded by co-injected reporter plasmids. Injection of the plasmids into a single cell at two-cell-stage in combination with the ubiquitous *cska* promoter (Grabher *et al.* 2003) facilitated randomized mosaic expression throughout all three nuclear layers. Expression of the candidate factors was hormonally induced (4 dpf) when the majority of cells in the central retina had exited the cell cycle and already differentiated into the neuronal and glial cell types (Figure 10B). Transgenic *Rx2::Tub-GFP* embryos, having reporter expression controlled by the same *Rx2* CRE used in the TRS, were used as a sensitive read-out *in vivo* (Figure 10C).

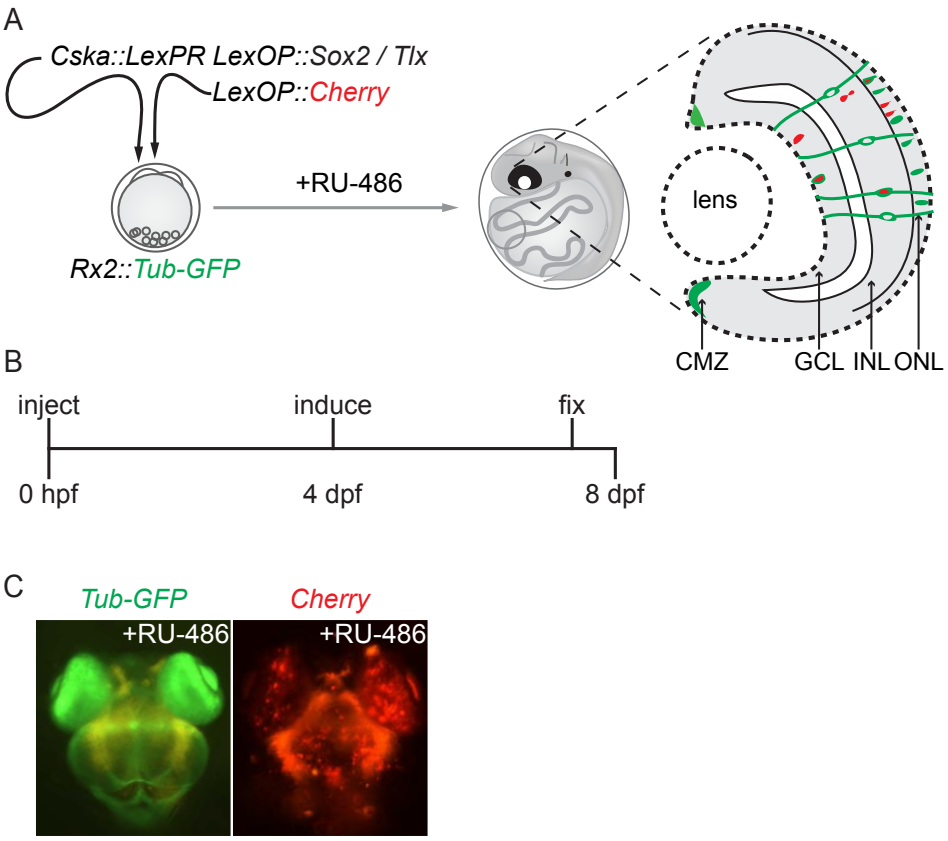

Figure 10. Clonal gain-of-function in the central retina.

(A) Scheme outlining functional assays for clonal expression Rx2 activators. Driver (*cska::LexPR LexOP::Sox2*; *cska::LexPR LexOP::Tlx*) and effector (*LexOP::Cherry*) plasmids are co-injected into transgenic *Rx2* reporter embryos (*Rx2::Tub-GFP*). Treatment with mifepristone results in mosaic expression pattern in the retinae of the embryos. Schematic cross section of the differentiated medaka retina with *Rx2::Tub-GFP* expression (green) in the CMZ, INL and ONL. Gain-of-function clones are randomly introduced into the central retina and identified via the co-expressed fluorescent protein (red) and examined for *Rx2* CRE *trans*-activation (clones that are both green and red).

(B) Experimental timeline of clonal gain-of-function assay.

(C) Transgenic *Rx2::Tub-GFP* embryo after injection with control plasmids (*cska::LexPR* and *LexOP::Cherry*) and subsequent mifepristone treatment as outlined above. Anterior is up, posterior is down. Mosaic cherry expression is spread randomly throughout the head and eyes, while Tub-GFP expression continues unperturbed in the retina.

2.1.7 *Sox2* and *Tlx* activate *Rx2* expression *in vivo*

Sections of transgenic embryos at 7 dpf showed that the combined expression of *Sox2* and *Tlx* resulted in strong *Rx2* reporter activation (40/48, 83.33%) in all three nuclear layers (Figure 11). In addition to reporter expression outside of the *Rx2* expression domain, enhanced levels of *Rx2* were observed indicated by the *Rx2* reporter (*Rx2::Tub-GFP*) in MGCs and photoreceptor cells, which co-expressed *Sox2* and *Tlx*.

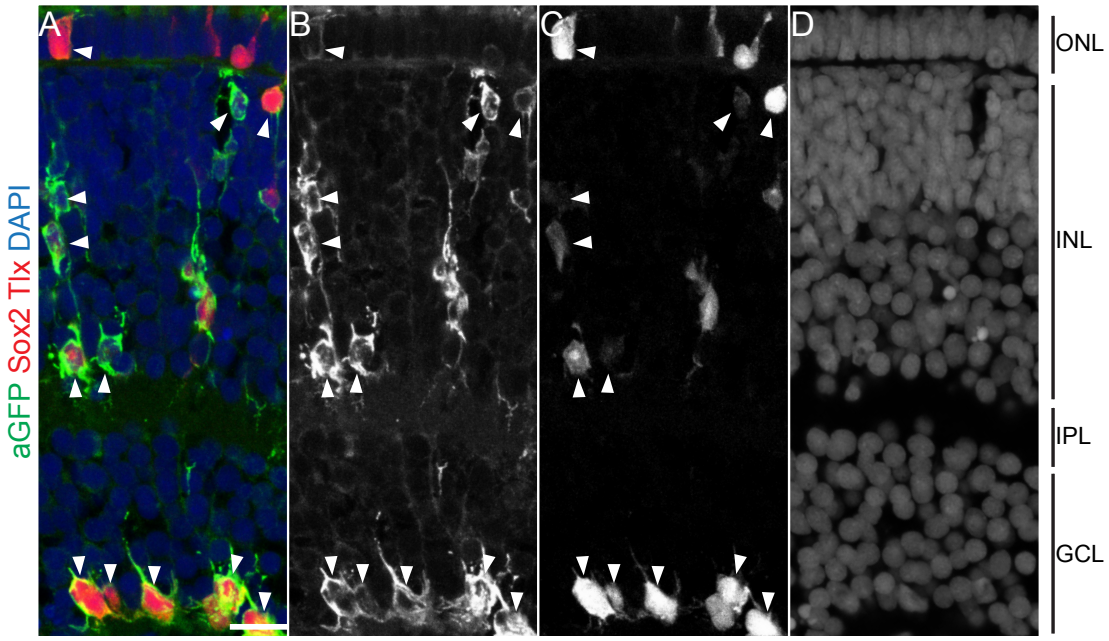

Figure 11. Co-expression of *Sox2* and *Tlx trans*-actives the *Rx2* reporter in the central retina.
(A-D) Confocal stacks of frontal sections on the central retina of transgenic fish (*Rx2::Tub-GFP*) at 7 dpf. Cells in all three nuclear layers of the NR (GCL, INL and ONL) over-expressing *Sox2* and *Tlx* together (C, red), show ectopic *Rx2* reporter activity (B, green). White arrowheads point to representative co-localizing cells. Scale bar: 10 µm.

2.1.8 *Sox2* and *Tlx* individually activate *Rx2* expression *in vivo*

Similarly, clonal miss-expression of *Sox2* (32/48, 66.67%; Figure 12A-D) or *Tlx* (142/173, 82.08%; Figure 12F-I) individually resulted in ectopic *Rx2* reporter activation. To corroborate that *Sox2* and *Tlx* activate the endogenous *Rx2* expression *in vivo*, WISH and immunohistochemistry were combined in whole-mount preparations (stage 30). DNA microinjection into two-cell stage wild-type embryos created mosaic expression in the central retina. Clones expressing *Sox2* (53/62, 85.48%; Figure 12E-E'") or *Tlx*, (34/56, 60.71%; Figure 12J-J'"), co-expressed ectopic *Rx2* mRNA, which was never detected in controls (co-injection of *cska::LexPR LexOP* and *LexOP::H2B-EGFP*). These results revealed that *Sox2* or *Tlx trans*-activate the endogenous *Rx2* promoter as well as the *Rx2* reporter *in vivo* and thus trigger *Rx2* expression in differentiated cells of all three nuclear layers.

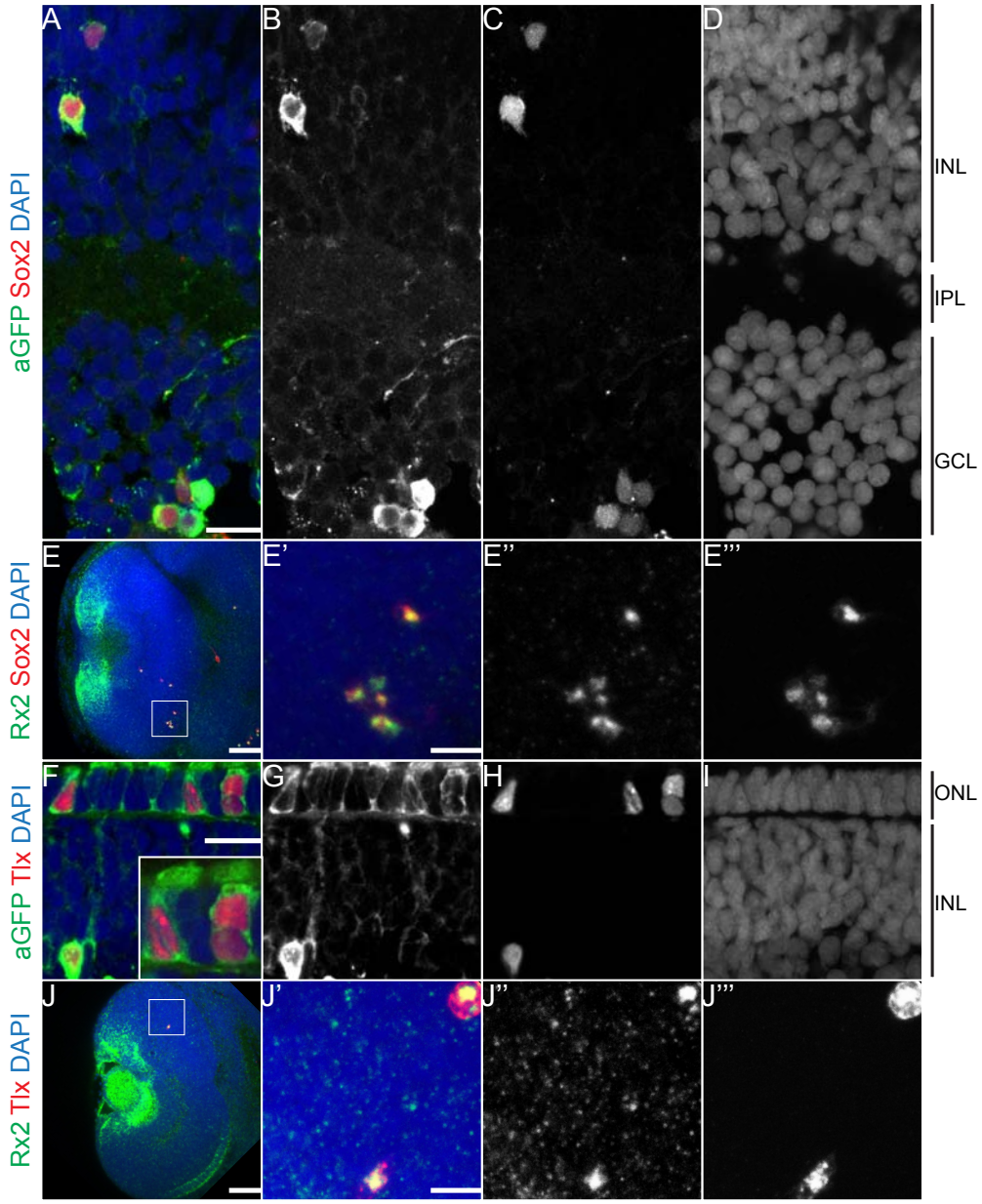

Figure 12. *Sox2* or *Tlx* gain-of-function clones activate *Rx2* reporter expression and ectopic *Rx2* expression in the central retina.

(A-D) Confocal stacks of frontal sections showing the central retina of *Rx2::Tub-GFP* embryo 7 dpf. Cells in the GCL and INL expressing *Sox2* (C, red) show ectopic *Rx2* reporter activity (B, green).

(E-E''') Confocal stacks of whole-mount embryo show co-localization of Sox2 (E''', false-colored red) and *Rx2* mRNA (E'', false-colored green) in the central retina at stage 30 (E).

(F-I) Confocal stacks of frontal sections showing the central retina of *Rx2::Tub-GFP* embryo 7 dpf. Cells in the ONL expressing *Tlx* (H, red) show ectopic *Rx2* reporter activity in the INL and increased activity in the ONL (G, green). Tlx-positive clones of the ONL exhibit modified cell morphology in comparison with wild-type cells (inset in F).

(J-J''') Confocal stacks of whole-mount embryo show co-localization of *Tlx* (J''', false-colored red) and *Rx2* mRNA (J'', false-colored green) in the central retina at stage 30 (J). Scale bars: 10 µm in A, E', F and J'; 50 µm in E and J.

2.1.9 Clonal analysis reveals promotion of RSC-specific features by Sox2 and Tlx *in vivo*

The rationale behind investigating the regulation of *Rx2* was the possibility to identify transcriptional RSC modulators. Given that *Sox2* and *Tlx* are activators of *Rx2 in vivo*, we addressed whether clonal activation of *Rx2* expression by *Sox2* and *Tlx* coincided with the induction of other RSC features. In response to ectopic *Sox2* or *Tlx* expression, changes in cell shape were observed, for instance in photoreceptors lacking the characteristic cone- or rod-like shape (inset in Figure 12F). To evaluate whether clonal activation of *Rx2* expression by *Sox2* or *Tlx* coincided with the induction of other RSC features, we first examined the mitotic state in those cells. Gain-of-function clones were induced as described above and analyzed for the expression of PCNA. In sections of the central retina of controls analyzed at 7 dpf, PCNA-positive clones were never detected. In contrast, both, the expression of *Sox2* (7/11, 63.63%; Figure 13A-E) as well as *Tlx* (3/23, 13.04%; Figure 13F-J) resulted in enhanced mitotic activity as indicated by PCNA staining. This shows that clonal ectopic expression of *Sox2* or *Tlx* re-activated the proliferative potential and shifted cells back into the mitotically active state. PCNA-positive clones were observed in the INL and ONL, indicating that de-differentiation was widespread and not restricted to one particular type of retinal neurons.

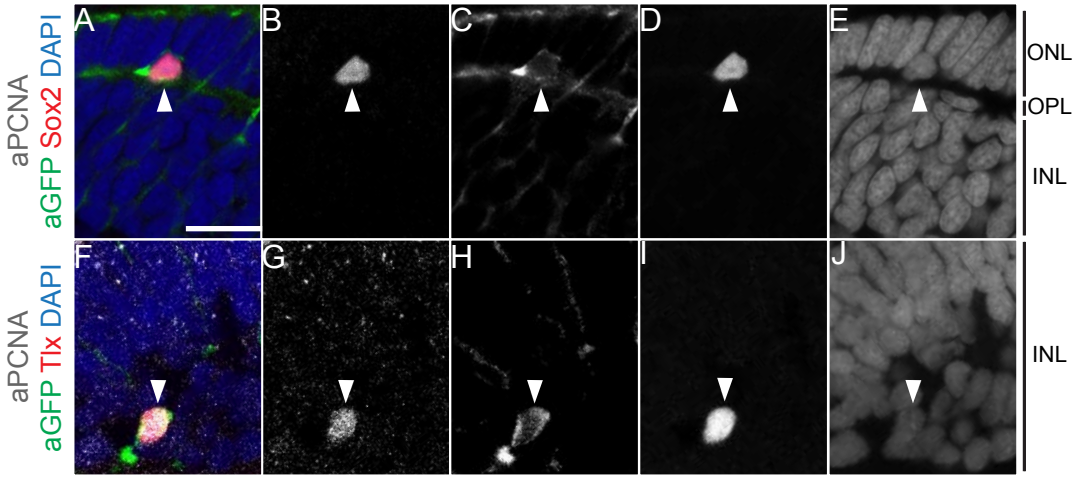

Figure 13. Expression of *Sox2* or *Tlx* promotes stem cell features in terminally differentiated neurons.
(A-J) Confocal stacks of frontal sections showing the central retina of transgenic *Rx2::Tub-GFP* embryo 7 dpf. *Sox2* (D, red) activates *Rx2* reporter expression (C, green) and coincides with PCNA staining (B, grey) in the ONL. Sox2-positive cell of the ONL shows modified cell morphology in comparison with adjacent wild-type cells (E, blue). Likewise, a proportion of Tlx-expressing neurons (I, red), which activate the *Rx2* promoter (H, green), co-localize with staining for PCNA (G, grey). Scale bar: 10 µm.

2.1.10 Transient exposure to Tlx transforms neurons into label- retaining cells

Label-retention over extended periods of time has been shown to be a common feature of bona fide stem cells in different animal niches (Bickenbach 1981; Tumbar *et al.* 2004). The tools for conditional gene expression described earlier allowed us to transiently mis-express *Rx2* activators and fluorescent proteins in the same cells *in vivo*. To address the label-retaining potential in cells expressing *Rx2* in response to the clonal activation of *Tlx*, the retention of fluorescent protein 49 days after the transient induction of *Tlx* was analyzed. The clonal expression of *Tlx* was repeated as described above in *Rx2::Tub-GFP* transgenic embryos. Limited expression of *Tlx* was activated by a hormone pulse (d4-d7) and the fish were allowed to grow for 7 additional weeks in the absence of the inducing hormone (Figure 14A). Strikingly, 49 days after end of the transient induction fluorescently labeled cells were still observed. Those cells were positive for ectopic GFP and cherry (Figure 14B-E). Overlap of the green and red fluorescence in the central retina indicated that transient activation of the *Rx2* CRE was successful at 7 dpf and that these cells retained both labels for almost 50 days. Control retinae, where cherry expression was induced in parallel, did not retain any ectopic label in the central retina. Taken together, this analysis highlighted the potential of *Sox2* and *Tlx* to trigger stem cell features in differentiated retinal cells, which are highly reminiscent of RSCs.

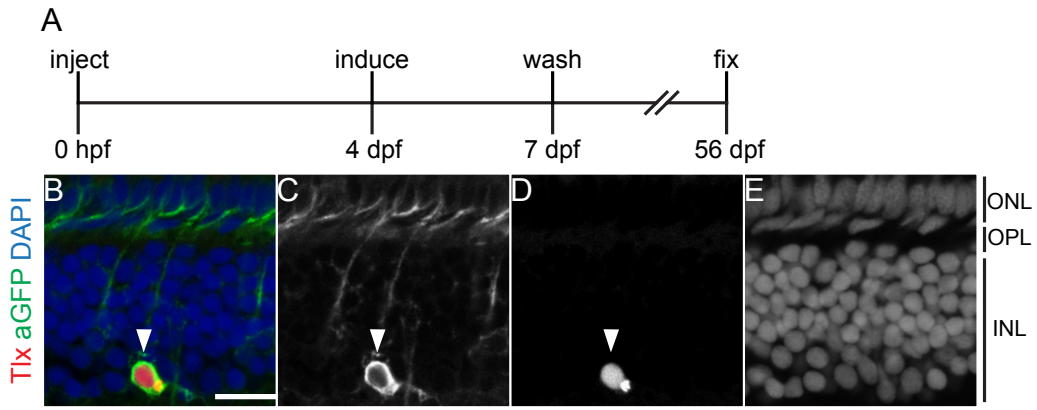

Figure 14. Expression of *Tlx* promotes label retention in terminally differentiated neurons.
(A) Experimental timeline of short-term clonal over-expression followed by long-term chase.
(B-E) Confocal stacks of frontal sections showing the central retina of transgenic *Rx2::Tub-GFP* fish 56 dpf. 49 days after end of mifepristone treatment, which induced clonal *trans*-activation of the *Rx2* reporter through *Tlx*, cells still retain red (C, red) and green fluorescent proteins (D, green). White arrowheads point to representative co-localizing cells. Scale bar: 10 µm.

2.1.11 Gli3 and Her9 repress *Rx2* in the CMZ

To assess whether *Gli3* and *Her9* act as transcriptional repressors of *Rx2 in vivo*, their clonal expression in cells endogenously expressing *Rx2* was triggered. As described above, Rx2-positive cells resided

in the peripheral CMZ, centrally and peripherally flanked by the *Her9* and *Gli3* expression domains respectively (Figure 15B). *Gli3* transcripts were primarily detected distantly in the adjacent RPE. *Her9* mRNA conversely was found in the centrally adjacent CMZ. Therefore the *Gli3* and *Her9* expression was shifted into the *Rx2* domain using inducible clonal expression in transgenic fish (Figure 15C-D). The clones were traced via a co-expressed nuclear GFP (H2B-EGFP) (Figure 15A). An Rx2 antibody was employed to assess Rx2 protein presence and levels. Clonally increased *Gli3* expression in the peripheral CMZ (*Rx2::LexPR LexOP::Gli3 LexOP::H2B-EGFP*), resulted in the loss of Rx2 protein in almost 40% of the ectopic Gli3-positive cells (13/33, 39.39%; Figure 16E-H). Of the clones expressing ectopic *Her9* within the *Rx2* domain (*Rx2::LexPR LexOP::Her9 LexOP::H2B-EGFP*), 20% showed decreased levels of Rx2 protein (7/35, 20.00%; Figure 16I-L). In contrast, Rx2 protein expression remained unaffected (1/34, 2.94%; Figure 16A-D) in the control (*Rx2::LexPR LexOP::Her9 LexOP::H2B-EGFP*). These findings are consistent with hypothesis that the domain of Rx2-positive stem cells is established and maintained by the activity of *Sox2* and *Tlx*, is centrally (NR) and peripherally (RPE) confined by the expression of *Her9* and *Gli3*.

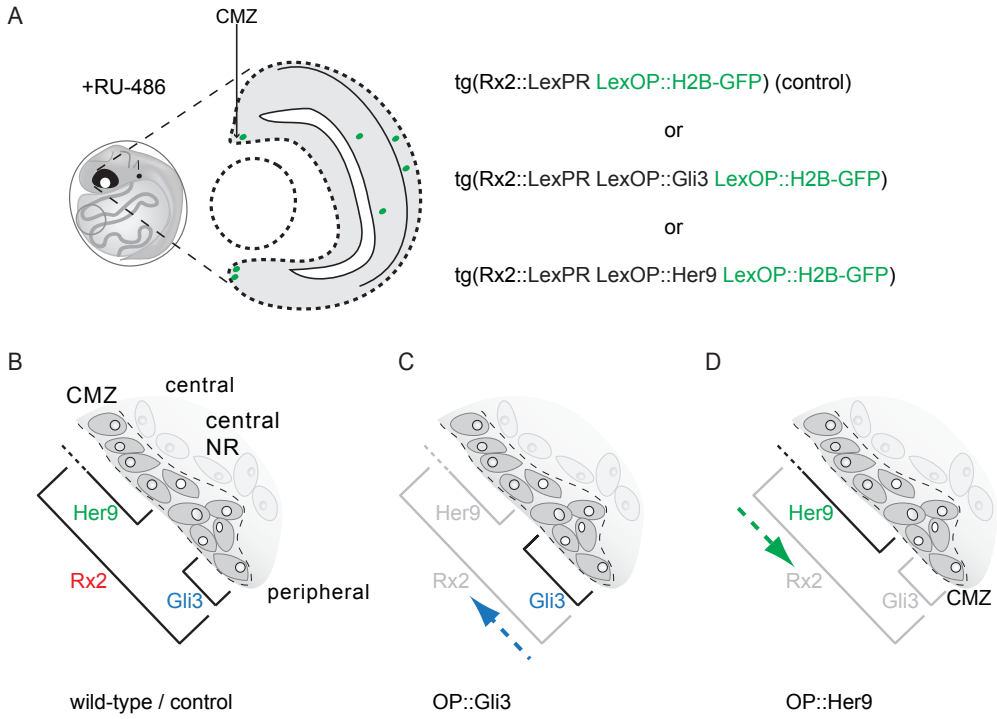

Figure 15. Conditional clonal gain of Gli3 and Her9 in the CMZ.

(A) Schematic cross section of the mature retina upon induction of clonal expression as indicated by H2B-EGFP under the *Rx2* CRE.

(B-D) Close up of the post-embryonic CMZ outlines the expression domains of RSC-marker *Rx2*, *Gli3* and *Her9* (B) in the controls, upon increased *Gli3* (C) or *Her9* (D) expression in the peripheral *Rx2* domain.

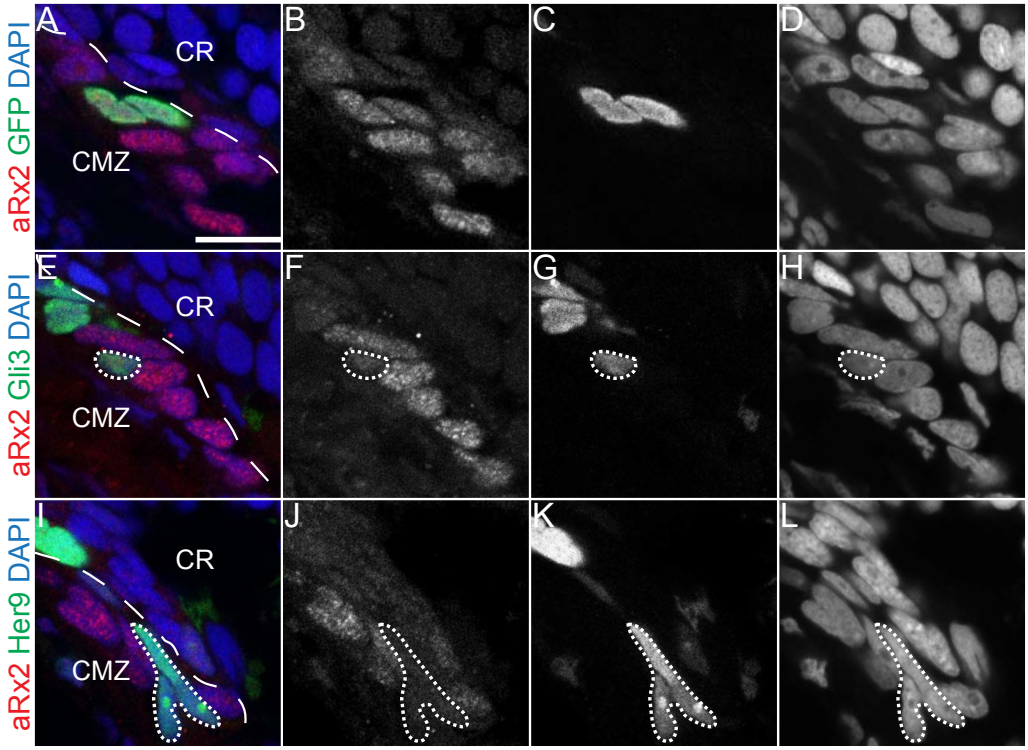

Figure 16. Clonal over-expression of *Gli3* or *Her9* in the CMZ reduces Rx2 protein levels.

(A-L) Confocal stacks of transversal sections on transgenic retinae (*Rx2::LexPR LexOP LexOP::H2B-EGFP*; *Rx2::LexPR LexOP::Gli3 LexOP::H2B-EGFP*; *Rx2::LexPR LexOP::Her9 LexOP::H2B-EGFP*) with immunostaining against the Rx2 protein at 9 dpf.

(A-D) In control experiments (*Rx2::LexPR LexOP LexOP::H2B-EGFP*), Rx2 is detected in the peripheral-most cells of the CMZ (B, red) despite sustained expression of H2B-EGFP (C, green).

(E-H) Clonal expansion of the *Gli3* (G, green) expression domain in the CMZ reduces levels of Rx2 protein (F, red) in transgenic fish (*Rx2::LexPR LexOP::Gli3 LexOP::H2B-EGFP*).

(I-L) Similarly, sections on transgenic fish (*Rx2::LexPR LexOP::Her9 LexOP::H2B-EGFP*) reveal reduction or loss of Rx2 staining (J, red) in the peripheral CMZ is observed in clones expressing *Her9* (K, green). Dashed lines demarcate Rx2 domain in the CMZ. Dotted lines highlight affected clones. Scale bar: 10 µm.

2.1.12 Sustained expression of Gli3 and Her9 represses proliferation in the CMZ

Having shown that *Rx2* activators *Sox2* and *Tlx* promote RSC-specific behavior, we asked whether expression of *Rx2* repressors mediates the opposite phenotype. To test this hypothesis the mitotic activity of clones expressing *Gli3* or *Her9* was investigated through PCNA immunostaining. Gain-of-function clones were generated and traced as described above (Figure 15). In sectioned control retinae of embryos at 9 dpf, homogenous presence of PCNA protein was detected throughout the central domain of the CMZ, unaffected by expression of H2B-EGFP (3/38, 7.89%; Figure 17A-D). In contrast, in *Gli3* gain-of-function clones PCNA was markedly reduced. Less or no PCNA protein was found in more than 36% of the H2B-EGFP-positive (indicative of Gli3 expression) cells (39/106, 36.79%; Figure

17E-H). Similarly, PCNA staining was strongly reduced or completely absent in more than 30% of the *Her9* over-expressing cells (21/64, 32.81%), indicating that entry of RPCs or RSCs cells into S-phase of the cell cycle was prevented (Figure 17I-L). Taken together these results indicate that ectopic *Gli3* and *Her9* expression in the CMZ antagonize both, *Rx2* expression and proliferation in adult RSCs.

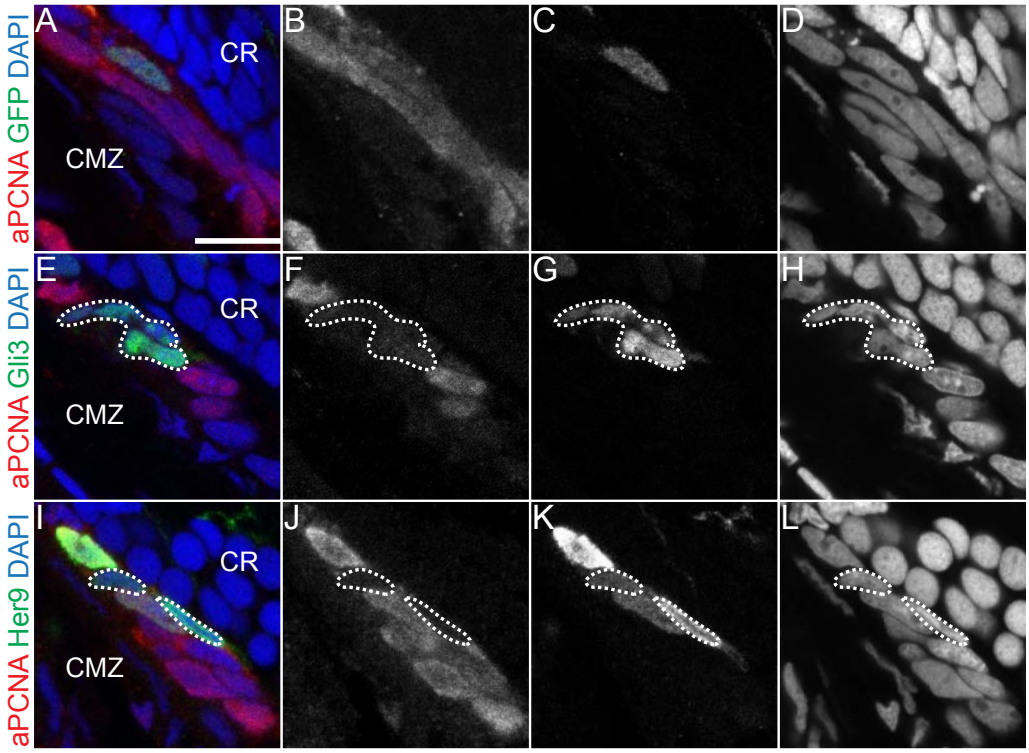

Figure 17. Clonal over-expression of *Gli3* or *Her9* in the CMZ reduces proliferation.
(A-L) Confocal stacks of transversal sections on transgenic retinae (*Rx2::LexPR LexOP LexOP::H2B-EGFP*; *Rx2::LexPR LexOP::Gli3 LexOP::H2B-EGFP*; *Rx2::LexPR LexOP::Her9 LexOP::H2B-EGFP*) with immunostaining against the PCNA protein at 9 dpf.
(A-D) PCNA labels a continuous group of mitotically active, undifferentiated cells in the CMZ (B, red).
(E-H) *Gli3* gain-of-function clones (G, green) show frequently lowered PCNA staining (F, red) compared to control cells.
(I-L) *Her9* gain-of-function clones (K, green) have less PCNA protein (J, red). Dotted lines highlight affected clones. Scale bar: 10 µm.

2.1.13 Sox- and Gli-binding sites are necessary for the functionality of the *Rx2* CRE

To further address the significance of the identified *trans*-regulators for the accurate expression of *Rx2*, we analyzed the architecture of the *Rx2* CRE. Applying evolutionary footprinting to uncover putatively functional, non-coding DNA elements by their conservation, binding sites for Sox, the strongest activator in the *in vitro* assay, as well as for Gli, the strongest repressor were identified. Alignment of non-coding

genomic DNA sequences upstream of the *Rx2* transcriptional start site showed conservation between teleost fish species (Figure 18A). Despite low overall similarities of the entire medaka CRE to higher vertebrates, a conserved putative Sox-binding site was identified (Figure 18B).

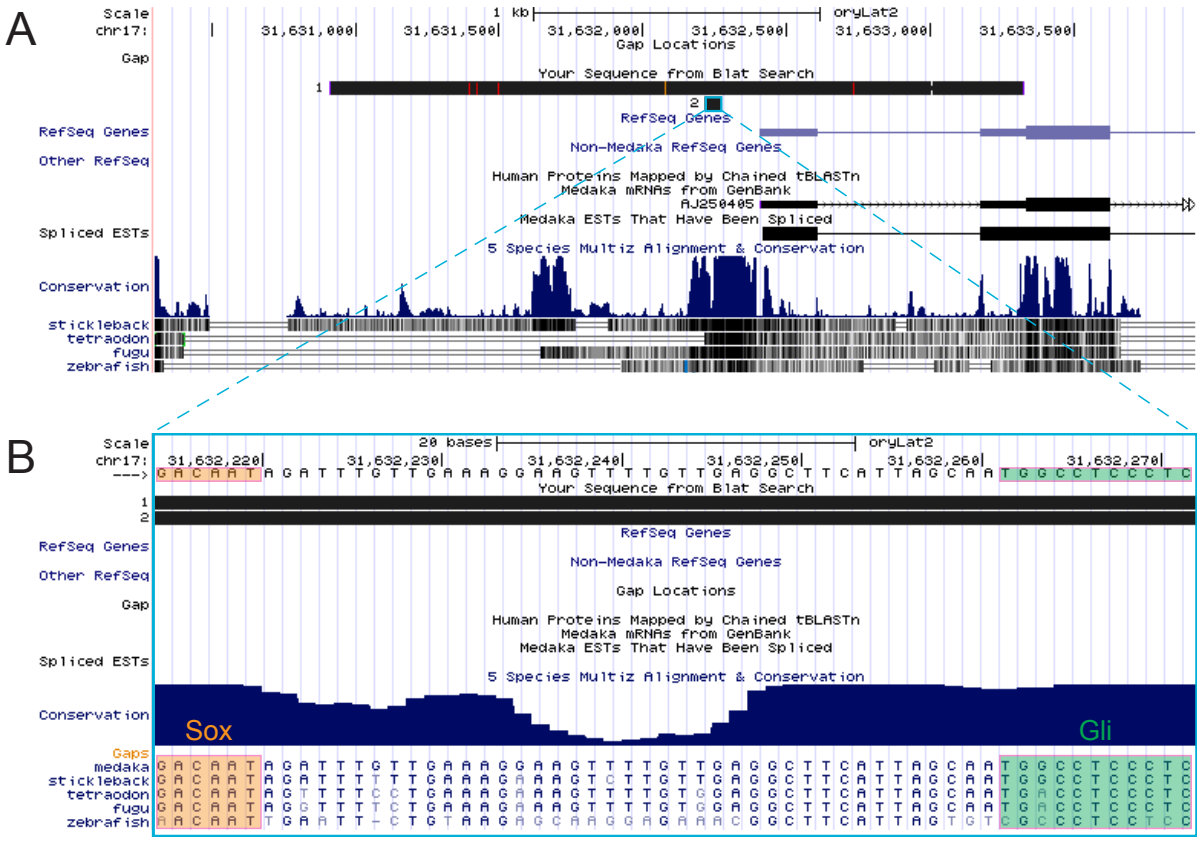

Figure 18. The *Rx2* CRE contains conserved Sox- and Gli-binding sites.
(A-B) Result of BLAT search for the 2.4kb medaka *Rx2* CRE using the UCSC Genome Browser (1 in A). The region (2 in A), which contains the putative Sox-binding site (orange) and Gli-binding site (green) is conserved (B). Blue peaks indicate conservation of coding and non-coding DNA sequences among teleost species.

The importance of conserved transcription factor binding sites (TFBSs) for the precise spatio-temporal expression coordinated by the *Xenopus Rx* CRE has been implicated previously (Danno *et al.* 2008; Martinez-De Luna *et al.* 2010). Given that the TF Sox2 is able to *trans*-activate expression of genes downstream of the medaka *Rx2* CRE *in vivo*, we addressed whether alterations in the putative Sox-binding site affect *Rx2* reporter expression. To address this, two point mutations (Danno *et al.* 2008) were introduced into the core of the predicted Sox-binding site (*Rx2::H2B-mRFP mtSox2*) and the activity of the mutated *Rx2* CRE in transgenic medaka embryos was tested. As described above, *Rx2* reporter activity accurately matched the expression of the Rx2 protein in the retina (Figure 19A-B). In contrast, mutations in the Sox TFBS resulted in an altered expression pattern. In sectioned retinae of

stage matched transgenic *Rx2::H2B-mRFP mtSox2* embryos, reporter activity in the CMZ was strongly reduced (Figure 19C-C''''). Also in the INL, where *Rx2* is expressed in MGCs 9 dpf (Figure S2), the number of mRFP-positive cells was reduced (Figure 19D-D'''). Interestingly, *Rx2* reporter expression in photoreceptor cells of the ONL, where *Sox2* is not expressed, was unchanged and identical to the control (Figure 19D-D'''). Strikingly, the mutation in the putative Sox-binding site in the *Rx2* CRE affects all domains of Rx2 expression that overlap with the expression of *Sox2*. The finding that upon mutation of the predicted Sox TFBS expression in the CMZ is strongly reduced, albeit not entirely abolished, highlights the *in vivo* relevance of the Sox-binding site contained within the *Rx2* CRE for the activation of *Rx2* expression in the peripheral CMZ.

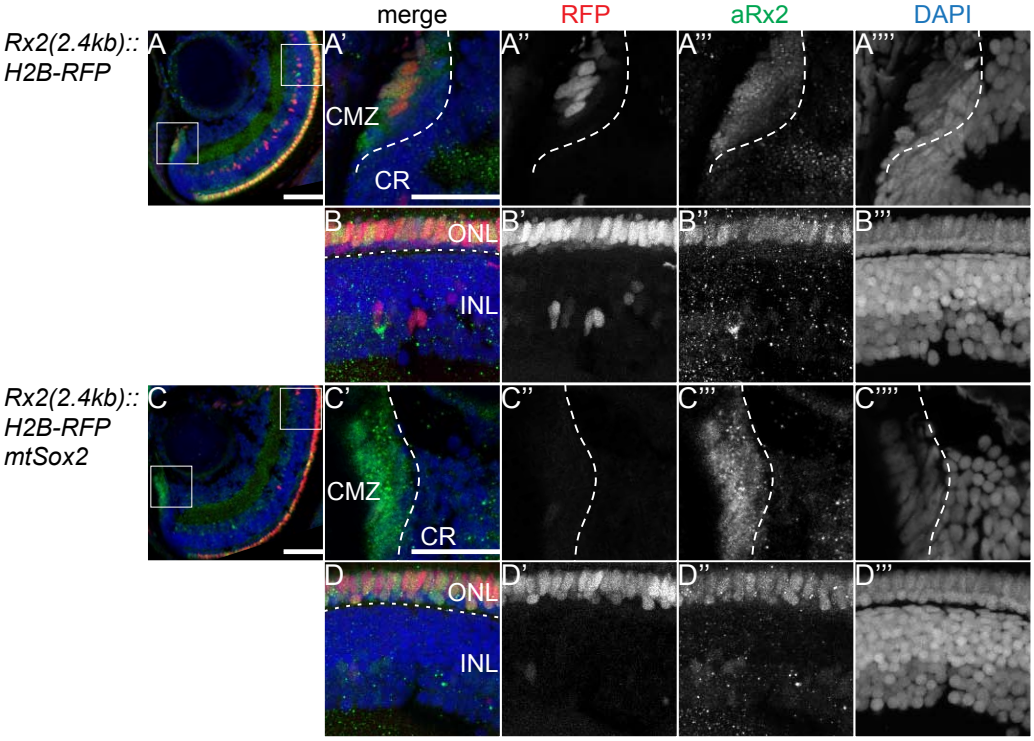

Figure 19. Mutation of Sox-binding site abolishes *Rx2 cis*-regulatory activity in the CMZ.

(A-B''') Confocal stacks of frontal sections on the retina of *Rx2::H2B-mRFP* transgenic embryo 9 dpf. Transgene expression (A, red), driven by *Rx2* CRE, co-localizes with Rx2 protein in the CMZ, INL and ONL (A, green). Higher magnification pictures of boxed regions (A) are shown in (A'-A''''; B-B''').

(C-D''') Confocal stacks of frontal sections on the retina of *Rx2::H2B-mRFP mtSox2* transgenic embryo 9 dpf. Number of cells with transgene expression (C, red), driven by mutated *Rx2* CRE, is markedly reduced in the CMZ and INL in comparison to Rx2 immunostaining (C, green) and control transgene expression (A, red). In contrast, transgene expression in *Rx2::H2B-mRFP mtSox2* fish continues in the photoreceptor cells of the ONL. Higher magnification pictures of boxed regions (C) are shown in (C'-C''''; D-D'''). Dashed line indicates transition from CMZ to CR. Dotted line represents border between layers of the NR. Scale bars: 50 µm in A and C; 25 µm in A' and C'.

Given the ability of *Gli3* to repress *Rx2 in vivo*, it was also investigated whether Gli TFs (like Sox) act as direct transcriptional regulators of the *Rx2* CRE. Following the identification of a putative Gli TFBS (Sasaki *et al.* 1997), 11 bp containing the Gli DNA motif were deleted from the *Rx2* CRE (Figure 18B). Analysis of transgenic medaka fish (*Rx2::H2B-mRFP delGli*) revealed a marked shift in reporter expression from the peripheral CMZ to the mono-layered RPE (Figure 20B-B'''). Consistent with our previous results from the *Gli3* expression analysis, reporter expression within the RPE was detected only in epithelial cells adjacent to the CMZ in transgenic embryos (*Rx2::H2B-mRFP delGli*). mRFP expression in the transgenic control (*Rx2::H2B-mRFP*) was confined to the NR and absent from the RPE (Figure 20A-A'''). Interestingly, in *Rx2::H2B-mRFP delGli* transgenic fish fewer mRFP-positive cells were observed within the CMZ, suggesting that the loss of the Gli TFBS resulted in a shift of expression towards the RPE rather than an expansion. These results demonstrate that inhibitory factors confine *Rx2* to the RSCs in the CMZ and prevent expression in the proliferating cells of the RPE. Furthermore, the Gli-binding site is of importance within the CMZ for the *trans*-activation of *Rx2*.

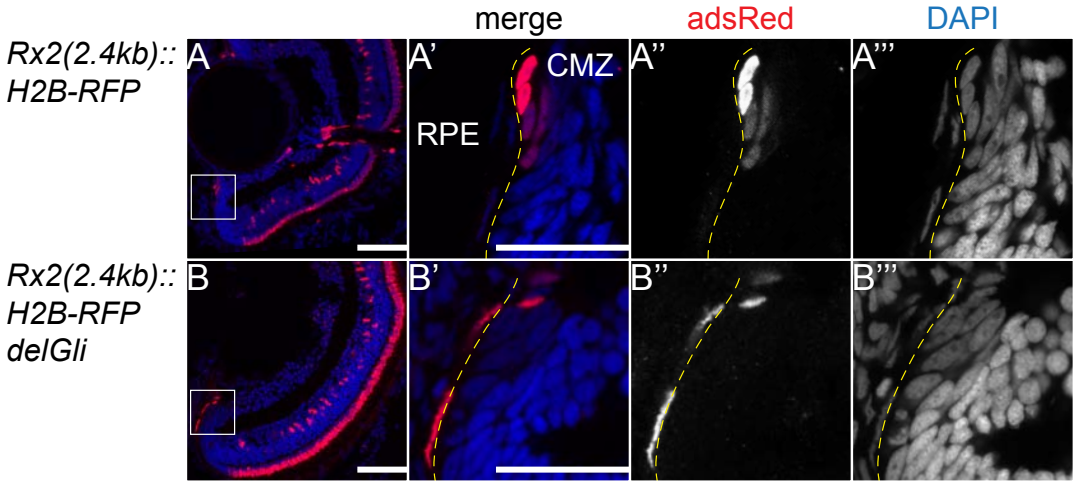

Figure 20. Loss of the Gli-binding site in the *Rx2* CRE shifts reporter expression into the RPE.
(A-A''') Confocal stacks of frontal sections on the retina of *Rx2::H2B-mRFP* transgenic embryo 9 dpf. Immunostaining against nuclear mRFP shows transgene expression in the controls as expected in the CMZ, INL and ONL (A, red). Expression of the transgene is confined to the CMZ and does not extend to the RPE (A'', red). Higher magnification pictures of boxed regions (A) are shown in (A'-A''').
(B-B''') Confocal stacks of frontal sections on the retina of *Rx2::H2B-mRFP delGli* transgenic embryo 9 dpf. Deletion of putative Gli-binding site in the *Rx2* CRE causes ectopic transgene expression in cells of the RPE and reduces expression in the CMZ (B''). Higher magnification pictures of boxed regions (B) are shown in (B'-B'''). Yellow dashed line demarcates border between RPE and CMZ. Scale bars: 50 µm in A and B; 25 µm in A' and B'.

2.2 Elucidating *Rx2* function

2.2.1 Gain of *Rx2* in the medaka retina

To address the function of *Rx2* itself, the effect of *Rx* mis-expression was studied *in vivo*. For this purpose, a single mRNA encoding *Rx2* and *mRFP* separated by a sequence for a viral T2A cleavage site was engineered (Rx2-T2A-mRFP), resulting in the equal proportions of (separate) Rx2 and mRFP proteins. The regulatory element of *Atoh7* (Del Bene *et al.* 2007) was chosen to express Rx2-T2A-mRFP. *Atoh7* is involved in specification of RGCs during early neurogenesis in the retina (Kanekar *et al.* 1997; Brown *et al.* 2001; Wang *et al.* 2001; Kay *et al.* 2005) and, as described above, later demarcates the central-most CMZ, where cells exit the cell cycle and terminally differentiate (Cerveny *et al.* 2010). In addition the *Atoh7* CRE is also active in a fraction of differentiated cells of the post-embryonic retina. As a result, the transgene *Atoh7::Rx2-T2A-mRFP* was expressed in post-mitotic precursors (at embryonic and post-embryonic stages) as well as neurons in the GCL and INL.

2.2.1.1 *Rx2* gain-of-function in the *Atoh7* domain results in morphological changes in the GCL and INL

Cross-sections of transgenic *Atoh7::Rx2-T2A-mRFP* hatchlings were characterized by apical extensions of the GCL. Furthermore, the INL was extended towards the GCL (basally), resulting in irregular spacing between the two layers. These extensions were inhabited by mRFP-positive cells and distributed at similar positions in GCL and INL along the dorsal-ventral axis of the sectioned retinae (Figure 21A-D). In the most severe cases, the IPL, usually free of cell nuclei, was populated by cells, which formed continuous connections between the GCL and INL (Figure 21E-H). In all retinae analyzed, multiple extensions were found along the apical surface of the GCL and basal surface of the INL. On average, 3.67 positions across the IPL were irregular spaced per section (3.67±1.37, six sections). Two independent transgenic lines with the same transgene (*Atoh7::Rx2-T2A-mRFP*) were established, similar in pattern but different in level of mRFP expression due to their varying copy-numbers and different positions of insertion into the genome. While embryos of both lines displayed the phenotype described above, the length of the extensions along the apico-basal axis entering the IPL was increased in offspring with stronger *mRFP* expression (not shown). Since Rx2 and mRFP originate from the same mRNA and therefore the translation of both proteins is stoichiometrically equivalent, increased expression of *mRFP* is indicative of higher *Rx2* levels. Enucleated eyes from *Atoh7::Rx2-T2A-mRFP* transgenics were undistinguishable from control eyes in their external morphology.

To test whether proliferation is altered in retinae over-expressing *Rx2*, a 24 h (at day 9) pulse of BrdU

was provided without a chase (fixed at day 10). With the exception of the cells inside and surrounding the optic nerve, no BrdU-positive cells were detected in the central retina of *Atoh7::Rx2-T2A-mRFP* transgenics (Figure 21E-H). These findings were similar to wild-type controls treated in parallel (not shown). Inside the CMZ, where ectopic *Rx2* was expressed in the central-most cells, incorporation of BrdU was limited to the transit-amplifying domain (white arrowhead in Figure 21I-L). Similarly, a short pulse resulted mainly in BrdU uptake in rapidly dividing progenitors in between peripheral and central CMZ of control retinae. The irregular spacing of the nuclear layers was not accompanied by cell divisions in cells expressing Rx2-T2A-mRFP, hinting at either ectopic proliferation occurring earlier during development or that the phenotype seen in *Atoh7::Rx2-T2A-mRFP* transgenics is established independent of changes in proliferation.

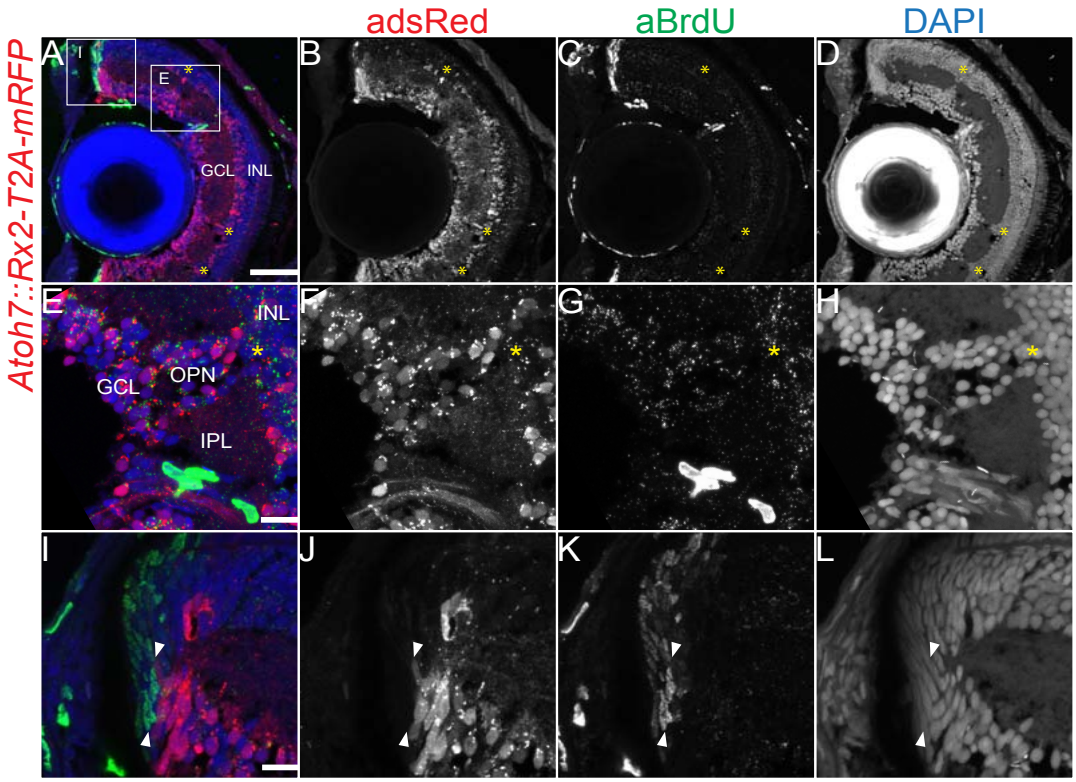

Figure 21. Gain of *Rx2* in the *Atoh7* domain does not coincide with enhanced proliferation.
(A-L) Confocal stacks of frontal sections showing the central retina of transgenic *Atoh7::Rx2-T2A-mRFP* fish 10 dpf. BrdU was provided for 24 h prior to fixation. Rx2-T2A-mRFP (B, F, J, red) expression induces irregular spacing between the GCL and INL. No cell divisions outside of the CMZ and optic nerve occurred during the 24 h BrdU pulse (C, G, K, green). Higher magnification pictures of boxed regions (A) are shown in (E-H and I-L). Asterisks (yellow) indicate irregular layering. White arrowheads highlight outer margin of the *Atoh7* expression domain. Scale bars: 50 µm in A; 10 µm in E and I.

2.2.1.2 *Rx2* gain-of-function does not alter proliferation and morphology during the beginning of retinal differentiation

To assess the dynamics in the phenotype caused by Rx2 mis-expression, earlier stages of eye development, in particular during the onset and progression of retinal neurogenesis were examined in *Atoh7::Rx2-T2A-mRFP* transgenic embryos.

At 2.5 dpf Rx2-T2A-mRFP was ectopically expressed throughout the GCL and in very few cells on the basal surface of the future INL (Figure 22A-H). Similarly, transgene expression at 3.5 dpf was detected in the GCL and INL (Figure 22I-P). At both stages analyzed, *mRFP*-expressing cells clustered together in small groups at the basal surface of the INL (yellow asterisks in Figure 22). Additionally, weak mRFP signal was detected in a small number of individual cells of the ONL. Compared to retinae at 2.5 dpf, more mRFP-positive cell cluster were detected in the INL at 3.5 dpf.

Cells passing through the S-phase of the cell cycle were localized at the periphery of the NR at 2.5 dpf and 3.5 dpf (Figure 22). Neither during 24 h (fixed at 2.5 dpf) nor 48 h pulses (fixed at 3.5 dpf) was BrdU incorporated in *Rx2* over-expressing cells. In terms of morphology and proliferation these retinae did not differ from stage-matched wild-type controls (not shown). In particular, the spacing between GCL and INL was similar to the controls, arguing for the phenotype being established at later stages of embryonic retinogenesis.

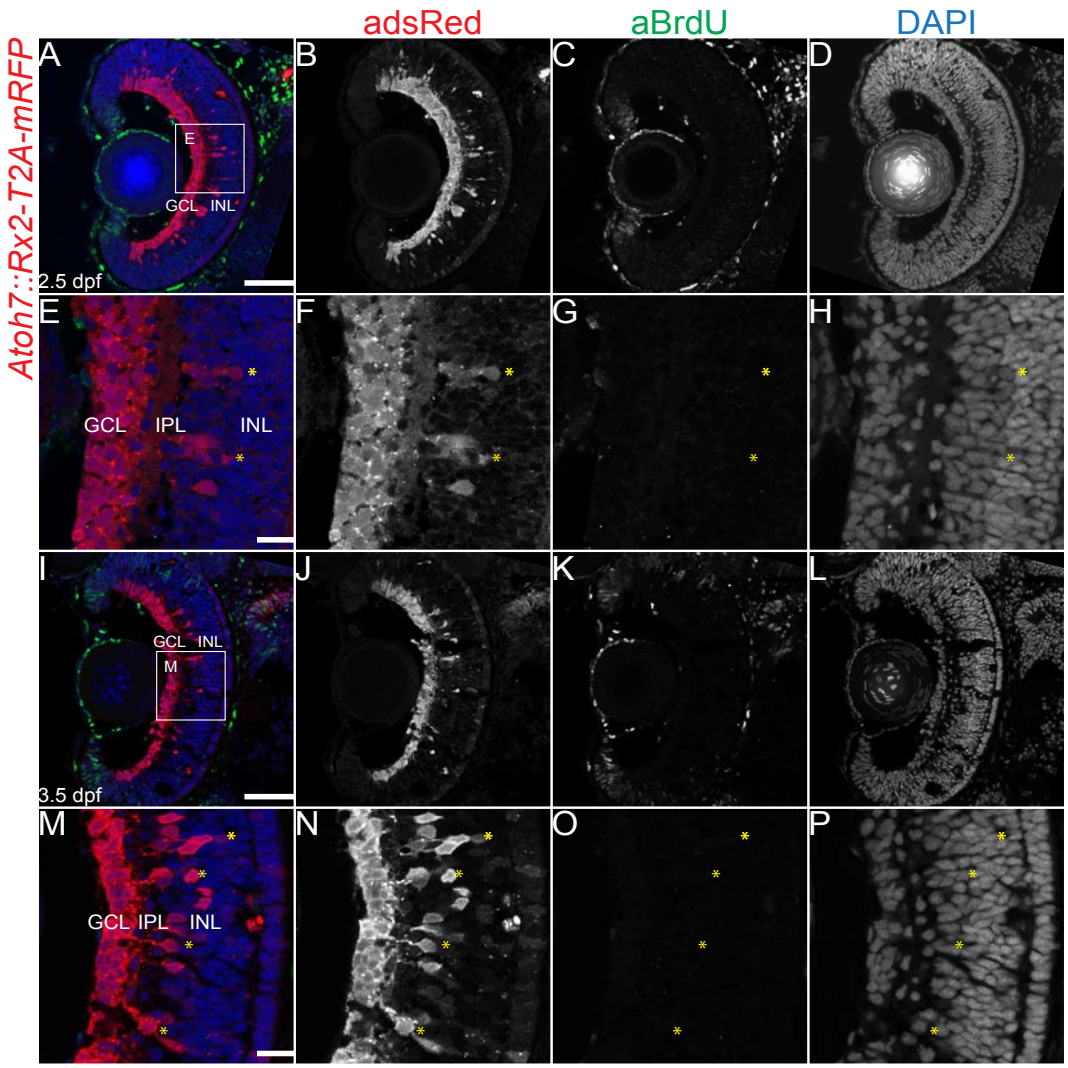

Figure 22. The *Rx2*-mediated layering phenotype is not established during early retinogenesis.
(A-H) Confocal stacks of transversal sections showing the central retina of transgenic *Atoh7::Rx2-T2A-mRFP* fish 2.5 dpf. BrdU was provided for 24 h prior to fixation. Rx2-T2A-mRFP-expressing (red, B, F) cells occur in cluster in the INL. No cell divisions outside of the CMZ were observed in the NR.
(I-P) Confocal stacks of transversal sections showing the central retina of transgenic *Atoh7::Rx2-T2A-mRFP* fish 3.5 dpf. BrdU was provided for 48 h prior to fixation. Rx2-T2A-mRFP-expressing (red, J, N) cells occur in cluster in the INL. No cell divisions outside of the CMZ were observed in the NR. Higher magnification pictures of boxed regions (A and I) are shown in (E-H and M-P). Asterisks (yellow) indicate irregular layering. Scale bars: 50 µm in A and I; 10 µm in E and M.

2.2.1.3 *Rx2* expression under the *Atoh7* CRE coincides with reduced expression of markers for neural differentiation of RGCs

The proneural gene *Atoh7* encodes a basic helix-loop-helix TF crucial for the genesis of RGCs. Atoh7 has the ability to activate itself through an auto-regulatory feedback loop; the TF recognizes and binds

the *Atoh7* CRE to mediate expression (Matter-Sadzinski *et al.* 2001; Del Bene *et al.* 2007). Other known targets of Atoh7 include Hu antigen C (HuC, ELAV-like 3) Brn3C and CD166. *Atoh7* is able to trans-activate HuC expression via direct binding to an E-box motif in the proximal regulatory element (Del Bene *et al.* 2007). To investigate the molecular mechanism behind the phenotype in the post-embryonic retina of *Atoh7::Rx2-T2A-mRFP* transgenics, HuC as a known Atoh7 target gene and Islet as a RGCs marker (Martinez-Morales *et al.* 2001) were assessed through immunostainings. At 10 dpf when embryonic neurogenesis was concluded, cells in GCL with strong *Rx2* expression (as indicated by the mRFP) had reduced levels of HuC/D protein (Figure 23A-A''''). Similarly, weak immunostainings for Islet coincided with high *mRFP* expression, while high Islet levels occurred in cells with no or little *mRFP* expression (Figure 23B-E).

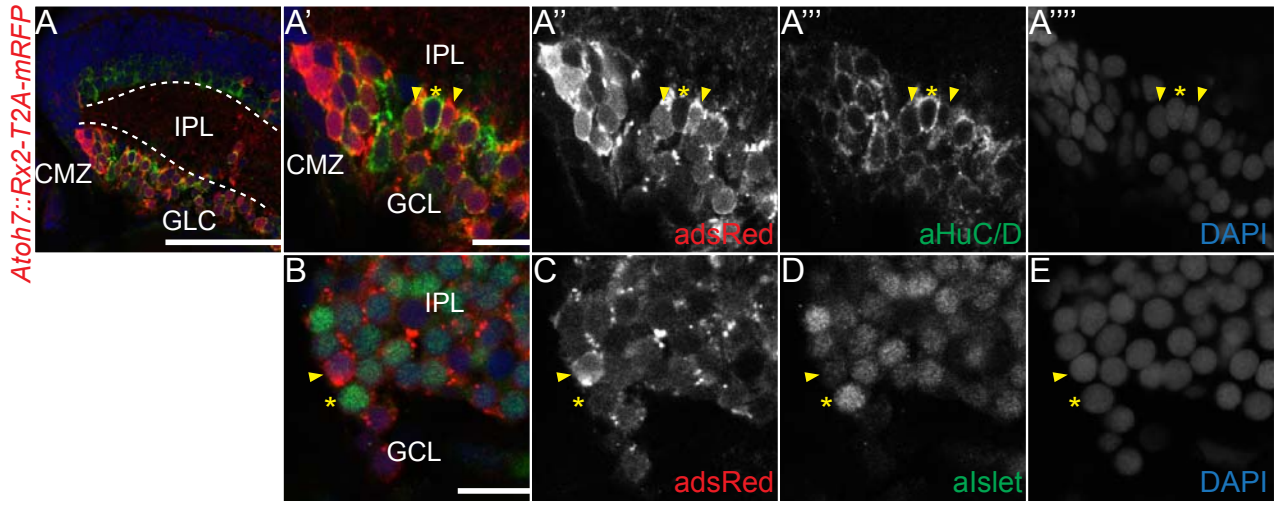

Figure 23. *Rx2* overexpression in RGCs coincides with reduced expression of markers for RGCs.
(A-E) Confocal stacks of transversal sections showing the central retina of transgenic *Atoh7::Rx2-T2A-mRFP* fish 10 dpf.
(A-A'''') Rx2-T2A-mRFP (red, A'') expression coincides with reduced staining for the RGC-marker HuC/D (green, A''').
(B-E) Rx2-T2A-mRFP (red, C) expression coincides with reduced staining for the RGC- and AC-marker Islet (green, D). Asterisks (yellow) indicate absence of Rx2-T2A-mRFP in strongly HUC/D- or Islet-positive cells in the GCL. Yellow arrowheads indicate Rx2-T2A-mRFP-expressing cells with no or less HuC/D (or Islet) in the GCL. Scale bars: 50 µm in A; 10 µm in A' and B.

2.2.1.4 Reduced activity of the *Shh* regulatory element in the GCL coincides with *Rx2* gain-of-function

Having shown above that downstream mediators of the *Hh* pathway regulate *Rx2* expression, the impact of gain of Rx2 in cells with active *Hh* signaling was evaluated. For this purpose double transgenic offspring from a cross between *Atoh7::Rx2-T2A-mRFP* and *Shh::GFP* carriers were analyzed. Siblings

expressing only *Shh::GFP* were used as the control. The zebrafish regulatory element of *Shh* (Neumann and Nuesslein-Volhard 2000) introduced upstream of GFP resulted in reporter gene expression in the GCL and INL in hatchlings (Figure 24A-H). Thus, the observed reporter expression in transgenic medaka embryos was consistent with studies in other vertebrate species detailing *Shh* expression in the NR (Wallace 2008). Given that the *Atoh7* CRE is primarily active in the RGCs, offspring carrying both transgenes should co-express Rx2-T2A-mRFP and GFP in the GCL. On average 12.5 GFP-positive cells (12.5±2.43, six sections) were detected in the GCL of *Shh::GFP* hatchlings (yellow asterisks in Figure 24A-H). In contrast, this number was reduced to 2.5 cells (2.5±1.05, six sections) in the GCL of *Atoh7::Rx2-T2A-mRFP* / *Shh::GFP* transgenics (yellow asterisks in Figure 24I-P). The number of GFP-positive cells in INL of double-transgenic hatchlings (13.67±2.88, six sections) was similar to the average number in control siblings (13±4.56, six sections). The findings show that the non-conditional expression of *Rx2* coincided with lower activity of the *Shh* promoter.

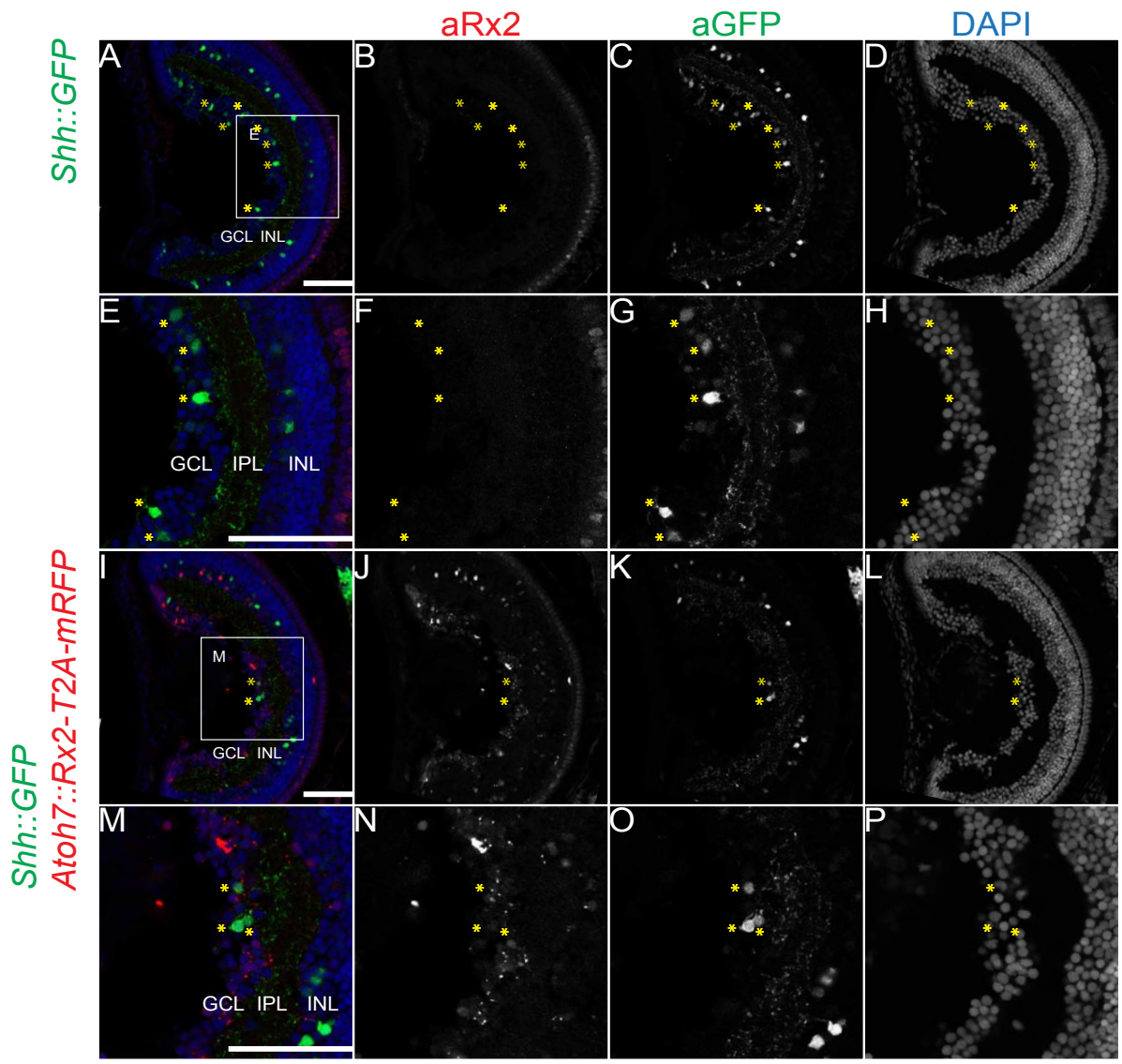

Figure 24. Expression of Rx2 in the GCL reduces *Shh* promoter activity.
(A-H) Confocal stacks of transversal sections showing the central retina of transgenic *Shh::GFP* fish 9 dpf. The *Shh* promoter (green, C, G) is active in the GCL and INL.
(I-P) Confocal stacks of transversal sections showing the central retina of double transgenic *Atoh7::Rx2-T2A-mRFP* and *Shh::GFP* fish 9 dpf. Rx2-T2A-mRFP expression (red, J, N) coincides with reduced number of cells with Shh reporter expression (green, K, O). Higher magnification pictures of boxed regions (A and I) are shown in (E-H and M-P). Asterisks (yellow) indicate GFP-positive cells in GCL. Scale bars: 50 µm.

2.2.2 *Rx2* loss-of-function

Rx2 has been established as a molecular marker for multipotent NSCs in the adult fish retina. However, the function of *Rx2* remains unknown. To accurately gauge the role of *Rx2*, loss-of-function studies are inevitable. Morpholino oligonucleotides directed against the start codon of *Rx2* failed to produce

phenotypes (not shown). Instead of changing Rx2 protein levels by means of mRNA knockdown strategies, we aimed for the permanent genetic inactivation of *Rx2* through locus-specific disruptive mutations.

For this purpose two customized TALEN pairs were designed against the coding sequence of the *Rx2* gene. TALENs 128 and 129 TALEN consist of DNA binding domains matching the first coding exon of *Rx2* (Figure 25A). The TAL effectors of pair 106/107 were designed to bind the second exon (Figure 25A). Analysis of the protein domains encoded in the *Rx2* gene showed TAL effectors 128 and 129 binding in between the sequence of the octapeptide domain and the homeobox (Figure 25B). TALENs 106 and 107 were binding in the middle of the homeobox. Depending on the nature of mutations, TALEN-mediated changes in the exonic sequences could result different truncated protein variants.

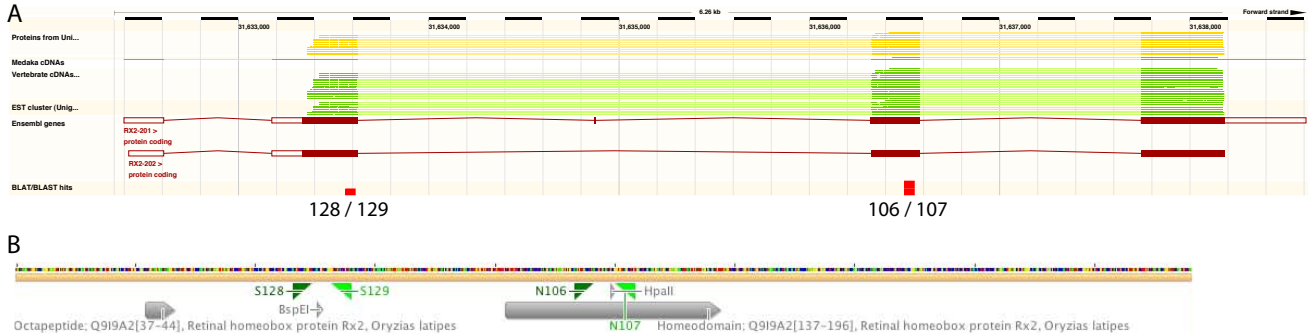

Figure 25. TALEN pairs 106/107 and 128/129 align perfectly with the *Rx2* coding sequence.

(A) Result of BLAST search for the two TALEN pairs against the medaka genome in the Ensembl browser. The *Rx2* gene is located on chromosome 17 of the genome and the transcript consists of three coding exons (dark red). One small additional coding exon is included in an alternative Rx2 transcript. All four TALEN DNA binding domains (red) align free of mismatches to exonic *Rx2* sequences.

(B) The annotated coding sequence of *Rx2* results in a single ORF (orange). The binding sequences (green) of 106/107 align to the sequence encoding the homeodomain (grey). 128 and 129 (green) bind upstream of the homeobox and downstream of the octapeptide domain (grey). Restriction enzymes BspEI and HpaII (grey triangular pyramids) were used for the band-retaining assays.

2.2.2.1 TALEN pairs 106/107 and 128/129 introduce locus-specific DNA breaks in the *Rx2* coding sequence

To test whether the TALENs are able to accomplish the desired genomic modifications, wild-type embryos were co-injected with TALEN mRNAs at one-cell stage and genotyped prior to hatching. For the genotyping process genomic DNA from injected embryos was isolated. The predicted TALEN target regions were specifically amplified and tested in restriction digest-based band-shift assays (Figure 26). Mutations in sub-cloned retained bands were confirmed in sequencing reactions.

One clone (1/1, 100%) for the pair 128/129 was sequenced, aligned with the *Rx2* locus and carried a

mutation (Figure 27A). The deletion in between the predicted TALEN binding sites was 5 base pairs, which resulted in a frame shift and a truncated Rx2 protein with 101 amino acids (wild-type Rx2 protein consists of 328 amino acids). For TALENs 106 and 107, 15 out of 16 (15/16, 93.75%) sequenced clones from seven individual embryos contained mutations in between the binding sites (Figure 27B). The mutations were deletions of either 4 or 10 base pairs, all causing frame shifts in the ORF and in theory producing truncated Rx2 proteins. This shows that both TALEN pairs induce disruptive mutations in their respective binding domains of the *Rx2* coding sequence upon injection at one-cell stage.

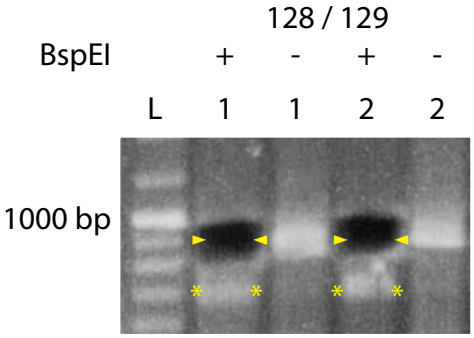

Figure 26. Band-retaining assay on isolated genomic DNA of injected medaka fish.
Amplified PCR products from injected fish (F0) were digested with a restriction enzyme cutting in between the binding sites of the TALENs (HpaII for TALENs 106/107, BspEI for 128/129). Retained bands (identical in size to the undigested PCR product) were isolated from the gel (yellow arrowheads), sub-cloned and confirmed through sequencing. A fraction of the amplified products were not mutated and therefore digested by the restriction enzyme (yellow asterisks). L, ladder; bp, base pairs.

Figure 27. Alignments of sequenced clones (F0) with the *Rx2* coding sequences.
(A) Genomic DNA isolated from injected embryo contains deletion of base pairs between binding sites of TALENs 128 and 129.
(B) Several sequenced clones show a variety of modifications caused by TALEN (106 and 107) co-injection. One clone is aligned perfectly with the *Rx2* sequence of interest, meaning no modification was created on this genomic DNA.

2.2.2.2 TALENs 106/107 and 128/129 induce heritable *Rx2* mutations

In order to determine whether the customized TALENS efficiently create mutations in the endogenous *Rx2* gene in medaka germ cells and in turn pass them on to the following generation, the offspring of injected fish were genotyped. Injected F0 embryos were raised to adulthood and crossed to wild-type fish. Collected offspring (F1) from each cross were divided in two halves; one group was raised to adulthood, while the rest was pooled and genotyped as outlined above for the F0 generation. This approach was chosen to detect whether the injected fish are carriers and therefore the TALENs induced genomic modifications in the germline. Eight outcrosses with TALEN 106 and 107 injected fish were genotyped (Table 2). In four of these crosses alteration in the target region were detected. All deletions observed in the sequencing process were 10 base pairs in size. Regarding putative founders from 128/129 injections, two out of two crosses produced offspring with mutations in *Rx2*. Sequencing revealed at least two different types of mutations (6 and 9 base pair deletions) in the offspring of the two founders (Figure 28). The observed deletions of 6 and 9 base pairs were both in frame, therefore resulting in the deletion of entire amino acids instead of a shift in the ORF. The analyses of the F1 generation revealed heritable targeted gene disruption can be created with both pairs of TALENs.

individual outcrosses	n clones mapping to the *Rx2* gene	n of clones with mutations	percentage of mutations identified
1.	**7**	**1**	**14.29**
2.	6	0	0
3.	**8**	**4**	**50**
4.	**5**	**1**	**20**
5.	**6**	**3**	**50**
6.	5	0	0
7.	6	0	0
8.	4	0	0
total	**47**	**9**	**19.15**

Table 2. Overview of analyzed offspring from outcrosses between fish injected with TALENs 106/107 and wild-type fish.

The offspring from four (bold) of the eight injected (TALENs 106/107) fish inherited lesions in the targeted *Rx2* sequence.

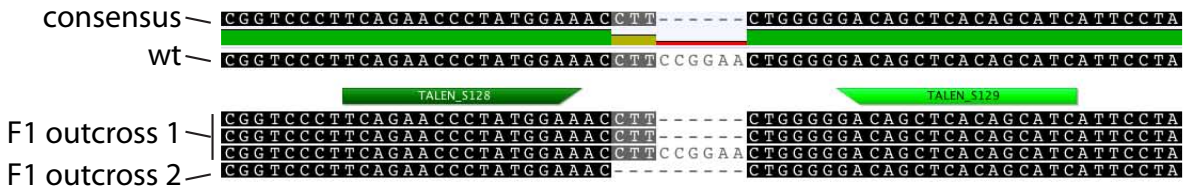

Figure 28. Alignments of sequenced clones (F1) with the *Rx2* coding sequences.
Two adult medaka fish were (injected with TALENs 128 and 129) were outcrossed to wild-type fish and their progeny were genotyped. The sequenced clones show a variety of heritable modifications. One clone is a false-positive and aligns perfectly with the *Rx2* sequence of interest, meaning no modification was created on this genomic DNA.

2.2.2.3 TALENs 106 and 107 show mutagenesis activity on the homeobox of *Rx1* and *Rx2*

The homeodomain is a well-conserved protein structure among various animals, including vertebrates (Gehring 1992). Given that *Rx2* has two paralogs (*Rx1* and *Rx3*) in the medaka genome, we explored whether the TALENs designed for *Rx2* recognize other *Rx* coding sequences. Alignment of the homeoboxes of *Rx1* and *Rx2* with the TALE effector binding sites showed perfect match with TALEN 106. For TALEN 107, three mismatches were found when compared with *Rx1* (Figure 29A). Nevertheless, we addressed whether this particular TALEN pair is able to induce lesions in this specific region of the *Rx1* gene. The genotyping process (genomic DNA was isolated from the fins of adults) on the F1 generation was repeated using specific primers for the *Rx1* homeobox. Sequencing of picked DNA clones revealed deletions in *Rx1* in within the predicted target region of the homeobox flanked by TALE effectors 106 and 107 (Figure 29B), arguing for the chance to induce TALEN-mediated mutation with partially mismatching binding domains. Furthermore, this opens the possibility to generate and analyze *Rx1* mutant fish.

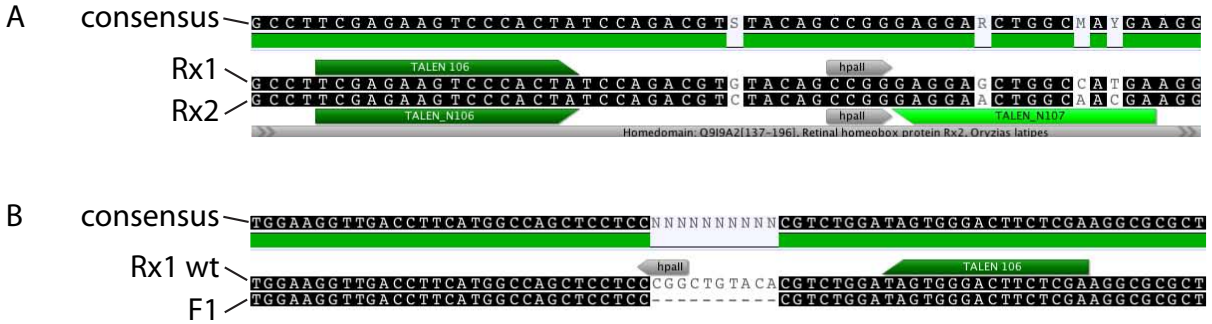

Figure 29. TALENs 106/107 introduce heritable modifications in the *Rx1* homeobox.

(A) Alignment of *Rx1* and *Rx2* coding sequences for the TALE effector binding sites. TALEN 106 matches perfectly to *Rx1* and *Rx2*, while TALEN 107 only aligns without mismatches to *Rx2*.

(B) Amplification of *Rx1* homeobox sequence from genomic DNA of adult fish (F1) was sub-cloned and sequenced. Disruptive mutation in *Rx1* was caused by TALEN (106 and 107) co-injection and passed on through the germline.

The fraction of the offspring (F1) collected from the injected F0 generation, which were grown to adulthood, was genotyped (genomic DNA isolated from the fins) (Table 3). Out of the twelve mutant fish eleven had deletions in *Rx1* and four in *Rx2*. With the exception of the *Rx2* target site of carrier 8, all deletions in the predicted target sites were 10 bases in size. Translation of the mutant sequences *in silico* contained frame-shifts, resulting in truncated Rx1 or Rx2 proteins. The deleted 6 bp in *Rx2* of mutant fish 8 were in frame, removing two amino acids in the homeodomain. A low frequency of sequenced clones contained single base pair substitutions or indels upstream or downstream of the predicted TALEN target region. These unexpected modifications were present in sequences with and without the desired modifications in the *Rx1* or *Rx2* target site. F1 mutant carriers with the intended modifications in the *Rx1* target sequence were occasionally accompanied by additional deletions of 6 consecutive bases. All instances of these unpredicted genetic events in *Rx1* mapped at the same position, approximately 60 nucleotides upstream of the TALEN 106 binding site. In contrast, sequencing reads of the *Rx1* homeobox free of genomic modifications in the TALEN target site, which were false-positives from the band-retaining assay, never missed 6 base pairs upstream or downstream of the predicted TALEN binding sites.

The fish carrying mutations leading to a frame shift in *Rx1* or *Rx2* were outcrossed to wild-type medaka. The offspring (F2) of genotyped individual F1 carriers of *Rx1* and *Rx2* mutations are currently being raised to adulthood. For the molecular analysis of the *Rx1* or *Rx2* genes, heterozygous siblings (F2) will be intercrossed to homozygosity. So far, the phenotype of homozygous *Rx1* and *Rx2* mutant fish remains to be determined.

F1 fish	gene	n of mapped clones	n of clones with mutations	size of deletion in the target sequence	other genomic modifications
1.	***Rx1***	**3**	**1**	**10 bp**	additional 6 bp del
	Rx2	**3**	**2**	**2 bp**	additional A nt
2.	***Rx1***	**3**	**1**	**10 bp**	additional 6 bp del
	Rx2	7	0		
3.	***Rx1***	**3**	**2**	**10 bp**	
	Rx2	**3**	**3**	**10 bp**	
4.	***Rx1***	**4**	**4**	**10 bp**	
	Rx2	1	0		
5.	***Rx1***	**2**	**2**	**10 bp**	additional 6 bp del
	Rx2	5	0		
6.	***Rx1***	**3**	**2**	**10 bp**	
	Rx2	0	0		
7.	***Rx1***	**3**	**3**	**10 bp**	
	Rx2	4	0		one clone with additional T
8.	***Rx1***	**3**	**2**	**10 bp**	same reads having 10 bp del have also 1 nt substituted
	Rx2	**3**	**2**	**6 bp**	
9.	*Rx1*	5	0		
	Rx2	**2**	**1**	**10 bp**	same read having 10 bp del has also 1 nt substituted
10.	***Rx1***	**3**	**2**	**10 bp**	
	Rx2	6	0		
11.	***Rx1***	**4**	**3**	**10 bp**	
	Rx2	1	0		
12.	***Rx1***	**3**	**1**	**10 bp**	
	Rx2	3	0		

Table 3. Overview of *Rx1* and *Rx2* mutations in genotyped adult F1 (F0 injected with TALENs 106/107). Summary of the results obtained from genotyping. Genomic modifications in each individual fish were determined for the predicted target region in the *Rx1* and *Rx2* homeoboxes (bold). The number of modified nucleotides inside the target as well as outside is listed.

2.2.2.4 TALEN-induced mutants recapitulate *eyeless* phenotype

When injected F0 fish were raised to adulthood and inter-crossed, a fraction of the progeny (F1) from some of these crosses repeatedly exhibited a phenotype in the eye. These embryos were identified by small or absent optic cups during embryogenesis. Embryos screened at late gastrula and early neurula stages showed incompletely formed or missing optic vesicle, resembling phenotypes of mutants for genes involved in early eye field patterning and vesicle evagination such as *Rx3* or *Pax6*. Given that TALENS 106 and 107, which targeted the homeobox of *Rx2*, produced mutations in *Rx1* as well as *Rx2*, it was a strong possibility that disruptive lesions were introduced in the coding sequence of *Rx3*. To test this hypothesis without the genotyping process, fish co-injected with TALEN 106 and 107 mRNAs at one-cell stage (F0) were crossed to wild-type fish. In the following generation (F1), the offspring were crossed, without prior genotyping, to heterozygous *eyeless* mutant carriers. *Eyeless* mutants harbour a recessive, temperature-sensitive mutation in the *Rx3* locus. Homozygous *eyeless* embryos raised at the restrictive temperature show smaller or absent eyes (Winkler *et al.* 2000; Loosli *et al.* 2001). Out of all the F1 fish outcrossed to known *eyeless*$^{+/-}$ carriers so far, one (out of 12) produced offspring with an eye phenotype. All embryos collected from this particular cross of TALEN 106/107 fish and *eyeless* founders were raised at the permissive temperature, however, more than 22% (5/22, 22.73%) of the collected offspring morphologically resembled Rx3$^{-/-}$ mutants and showed phenotypes ranging from small eyes to the complete lack of eyes (Figure 30). As early as neurula stage embryos exhibited phenotypes in the forming eye (not shown), the most severe cases showing a complete failure to form optic vesicles. Mutants with small optic cups (Figure 30B) failed to develop normal sized retinae, instead the eye remained small yet underwent pigmentation (Figure 30D), while the overall body shape and size (excluding the eyes) was similar to wild-type or heterozygous siblings (Figure 30C). This morphological analysis of the offspring from a cross between TALEN 106/107$^{+/-}$ and *eyeless*$^{+/-}$ founders recapitulates the phenotype described for homozygous *Rx3* mutants.

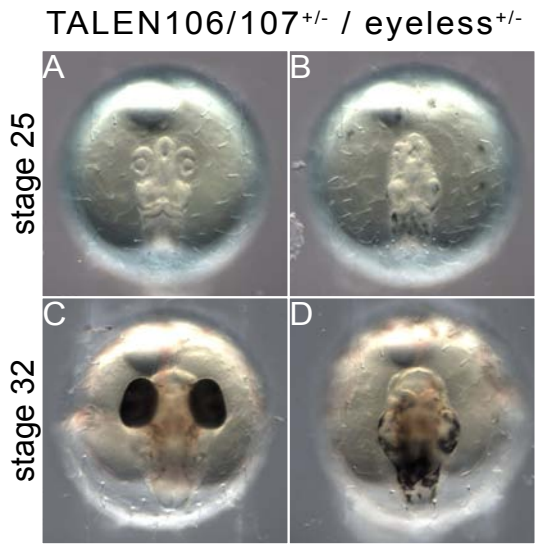

Figure 30. Cross of TALEN 106/107-injected progeny and heterozygous *Rx3* carriers results in *eyeless* phenotype.

(A-D) Dorsal view of medaka embryos in the brightfield. Close to a quarter of the siblings at optic cup stage exhibit small or absent optic cups (B), while the remaining collected embryos show wild-type morphology (A). The mutant embryos continue development with small or no eyes (D), as the siblings go through retinogenesis and form a properly differentiated eye (C). All images were obtained with the same magnification.

DISCUSSION AND OUTLOOK

3 Discussion

3.1 A regulatory framework containing Sox2, Tlx, Gli3 and Her9 controls stem cell features in the retina

3.1.1 *Sox2* and *Tlx* positively regulate stem cell features in the retina

Previous studies have highlighted the importance of *Sox2* and *Tlx* for NSCs and progenitors. *Sox2* plays a crucial role in maintaining neural precursors in an undifferentiated state and suppressing terminal differentiation (Bylund *et al.* 2003; Graham *et al.* 2003; Van Raay *et al.* 2005; Taranova *et al.* 2006). Consistent with reports of the pan-neural determinant *Sox2* being expressed in self-renewing and multipotent adult NSCs in the brain (Suh *et al.* 2007), expression in the retina labeled the CMZ including the Rx2 domain. *Tlx* has been demonstrated to be expressed in neural progenitors in the developing retina and brain, as well as mitotically active cells in the adult brain of mammals (Yu *et al.* 1994; Monaghan *et al.* 1995; Shi *et al.* 2004). Genetic inactivation has highlighted the role of *Tlx* in retinal development as well as in keeping adult NSCs and precursors in a proliferative state (Yu *et al.* 2000; Shi *et al.* 2004). *Tlx* expression was partially overlapping with *Rx2,* but mainly observed in the centre of the CMZ, where the transiently amplifying progenitors are located, reminiscent of the expression reported in the mouse brain (Obernier *et al.* 2011).

The present study provides evidence that both *Sox2* and *Tlx* have the ability to induce RSC characteristics in terminally differentiated neurons of the post-embryonic retina. We found the RSC-specific marker *Rx2* upregulated in clonal overexpression assays, with the highest rate of *trans*-activation achieved by co-expression of *Tlx* and *Sox2*. Sox proteins are involved in a great variety of cell specifications and depend on interaction with process-specific partner proteins (Kondoh and Kamachi 2010). For instance, ectopic *Rx* CRE activity had previously been shown to be the result of the collaborative effort between *Sox2* and *Otx2*; however, in contrast to our findings regarding the medaka *Rx2* CRE, *Sox2* overexpression on its own was not sufficient to *trans*-activate the Xenopus *Rx* CRE (Danno *et al.* 2008). *Otx2*, which has been reported to play a critical role in photoreceptor cell development in the embryonic mouse retina (Nishida *et al.* 2003), could still be involved in regulation of *Rx2* expression at early developmental stages or in post-mitotic cells. Interestingly, studies in mice on the *Otx2* regulatory element revealed *Rx* as an activator (Muranishi *et al.* 2011), which suggests an independent regulatory network governing commitment of RPCs towards photoreceptor cell fate. Recent studies carried out in NSCs have shown that *Sox2* expression induces *Tlx* expression (Shimozaki *et al.* 2012). Furthermore, direct interaction between Sox2 and Tlx proteins relieved a negative feedback loop on the *Tlx* promoter.

Therefore, it is possible that a similar protein-protein interaction between Sox2 and Tlx synergistically regulates *Rx2* expression in the context of the retina. While it has been shown that Tlx in general acts as a transcriptional repressor through interaction with HDACs to maintain neural precursors in an undifferentiated state (Sun *et al.* 2007), the TF Tlx is also able to directly activate target genes when associated with co-activators instead of HDACs (Elmi *et al.* 2010). Thus, it is possible that *Tlx* induces *Rx2* expression either through activation of transcription or repression of an *Rx2* repressor.

Upon clonal activation of *Rx* activators, terminally differentiated cells lost their differentiation markers, re-entered S-phase and rested in a proliferatively quiescent state, a general hallmark of adult stem cells (Orford and Scadden 2008). The appearance of mitotic markers and morphological changes in differentiated neurons argues for loss of neuronal identity. Moreover, after transient exposure to *Tlx*, cells retained fluorescent labels for multiple weeks, suggesting altered cell metabolism or protein turnover. In comparison, in the control experiments no transiently expressed fluorescent labels were retained in post-mitotic neurons several weeks after the expression was discontinued.

However, we did not observe increase in clone size or cell divisions, even when *Sox2* and *Tlx* were co-expressed. Instead, neurons showed RSC-specific features without proliferating. This is agreement with results from previous reports, where *Sox2* or *Tlx* gain-of-function experiments were conducted in undifferentiated stem cells or progenitors of the CNS, even though not in differentiated neurons as in the present study. Although it has been recently demonstrated that *Sox2* is sufficient to convert mouse and human fibroblasts into induced NSCs (Ring *et al.* 2012), *Sox2* overexpression in retinal progenitors of frog and mouse does not induce proliferation, instead, progenitors increasingly commit to post-mitotic MGC fate (Agathocleous *et al.* 2009; Lin *et al.* 2009). In mammalian neural progenitors and stem cells, *Tlx* overexpression has been shown to transiently enhance proliferation; however, even there sustained *Tlx* expression is necessary for persisting effects and was not tested in terminally differentiated neurons (Elmi *et al.* 2010; Liu *et al.* 2010).

In light of the results presented here, we hypothesize that transient gain of *Sox2* or *Tlx* mediates de-differentiation into a quiescent RSC-like state, but is not sufficient to trigger proliferation of terminally differentiated neurons. Rather, prolonged expression or combination with other factors, for instance cell cycle activators (Agathocleous *et al.* 2009), is required for post-mitotic neurons to complete the entire cell cycle and divide.

3.1.2 *Gli3* and *Her9* overexpression in the CMZ antagonizes Rx2 and stem cell proliferation

In the frog retina ligands of the Hh signaling pathway are expressed in the GCL and the central RPE. The key transcriptional regulators of the cascade, zinc-finger containing Gli TFs, are expressed at a distance to the source at the boundary between NR and RPE (Borday *et al.* 2012). Consistently, we found full-length *Gli3*, which encodes a repressor and activator-domain, expressed in the peripheral RPE and peripheral CMZ. In absence of Hh signaling, Gli3 is proteolytically cleaved and functions as a transcriptional repressor of Hh target genes. In the event of Hh signal transduction, proteolytic processing is inhibited, and Gli3 translocates to the nucleus to activate Hh target gene transcription (Humke *et al.* 2010). Clonal expression of *Gli3* in the peripheral CMZ repressed *Rx2* transcription arguing for only restricted Hh signaling activity in that domain. Additionally, we found a decrease of RSCs in S-phase after exposure to Gli3, reminiscent of results in the chicken neural tube, where dominant-negative *Gli3* delays cell cycle progression and decreases expression of mitotic markers (Cayuso *et al.* 2006). Consistent with our findings in the CMZ, *Gli3* regulates the proliferative expansion of mesenchymal progenitors through restriction of their entry into S-phase during chondrogenesis (Lopez-Rios *et al.* 2012). Similarly, the blocking of the Hh cascade has been reported to impact on the cell cycle exit of retinal progenitors cells in fish and frogs (Locker *et al.* 2006). Interestingly, pharmacological inhibition of Hh signaling is not sufficient to modulate *Rx* expression in the CMZ of frog (Locker *et al.* 2006; Borday *et al.* 2012). The finding that *Gli3* and *Rx2* share expression in the peripheral CMZ, while the peripheral RPE is simultaneously occupied by *Gli3* only, suggests a dual role for the TF Gli3 as activator and repressor.

In our gain-of-function assays full-length Gli3 acted as a repressor of *Rx2* and inhibited proliferation, although it also encoded an activator domain. This indicates limited levels of Hh signaling likely due to the distance to the source of Hh ligands in the GCL (Neumann and Nuesslein-Volhard 2000; Stenkamp *et al.* 2000), resulting in an accumulation of Gli3 in the repressive form.

Similarly, acute and sustained expression of *Her9*, a *Hes1* ortholog in fish, in the peripheral CMZ reduced Rx2 levels and proliferation. This finding is surprising since *Hes* genes have generally been reported to antagonize proneural function and are required to keep neural progenitor cells in a proliferative state (Kageyama *et al.* 2007). However, it has been demonstrated that persistent and high levels of *Hes1* expression inhibit both cell proliferation and differentiation (Baek *et al.* 2006). Furthermore both, sustained gain or loss of *Hes1* activity causes G1 phase retardation, resulting in reduced cell proliferation (Yoshiura *et al.* 2007). Thus, the loss of proliferation upon exposure to high levels of *Her9* likely represents a pausing of cell cycle progression and failure to enter S-phase. We did

not detect apoptosis in clones with reduced proliferation in response to *Gli3* or *Her9* over-expression (not shown). Furthermore, these cells did not express any markers characteristic for neurons or glia (not shown), again arguing for a pausing of the cells.

3.1.3 The RSC-specific expression of *Rx2* is sustained through conserved Sox- and Gli-binding sites

Our analysis of the *Rx2* CRE indicated that Sox-binding is crucial for *Rx2* expression in RSCs of the CMZ as well as for MGCs. Mutations in a Sox-binding site of the *Rx2* CRE resulted in the massive reduction of reporter expression in the CMZ and MGCs, consistent with the expression of *Sox2* transcripts in the CMZ and INL described above. In contrast, the expression in photoreceptors, where *Sox2* is not expressed, remained unaffected. Our data are consistent with and extending previous studies on the CRE of *Xenopus Rx*. Combined mutations in the Sox- and Otx-binding sites resulted in reduced reporter activity in the frog CMZ (Martinez-De Luna *et al.* 2010), however, the impact of mutations in either the Sox- or Otx-motif was not shown. Experiments carried out in cultured cells have shown that physical interaction and binding of the TFs Sox2 and Otx2 sustain activity of the *Xenopus Rx* CRE (Danno *et al.* 2008). However, *Otx2* transcripts were absent from the mature medaka CMZ (not shown). Since a putative *Otx*-binding has been predicted in the medaka *Rx2* CRE (M. Ramialison, unpublished), it is a possibility that *Otx trans*-acting factors are involved in *Rx2* regulation, for instance during embryonic stages of eye development.

The finding that reporter expression controlled by the mutated CRE was not fully absent suggests that *Rx2* expression in the CMZ is not entirely dependent on *trans*-acting factors, which utilize the Sox-binding site, but rather that *Rx2* expression in the CMZ is the result of multiple regulatory inputs. Given the ability of *Tlx* to activate the *Rx2* regulatory element and their overlapping expression domains, it is possible that *Tlx* is also directly involved in *Rx2* regulation in the NR. Future experiments predicting and testing Tlx-binding motifs will address the role of direct Tlx-binding for correct *Rx2* expression. Alternatively, the base pair substitutions in the Sox-binding site might not be sufficient to completely abolish Sox protein interaction with the *Rx2* CRE. Analyzing Rx2 reporter expression after deletion of the entire Sox-motif could test this hypothesis. Out of the three members of the *Sox* B1 sub-group only *Sox2* was expressed in the CMZ, supporting the hypothesis that Sox2 is the TF acting through the mutated binding site *in vivo*. Interestingly, mutation of the Sox-binding site also affected *Rx2* reporter expression in the MGCs, the reservoir of quiescent stem cells in the central NR (Bernardos *et al.* 2007). With *Rx* being necessary for wound-regeneration in the Xenopus retina (Martinez-De Luna *et al.* 2011), this finding indicates a similar regulatory scaffold governing quiescence in the peripheral

CMZ and injury-free NR.

Conversely, upon deletion of a putative Gli-binding site, reporter expression was shifted towards the RPE. Here it was restricted to cells adjacent to CMZ, the domain of *Gli3* expression. In contrast to cells in the central RPE, they continue to proliferate beyond the conclusion of embryogenesis, similar to RSCs in the CMZ. Combined with the results showing that Gli3 is a *Rx2* repressor *in vivo*, it is tempting to speculate that Gli3 is the TF acting through the deleted binding-site and responsible for preventing *Rx2* CRE activity in the RPE. This way it confines *Rx2* expression to the CMZ and blocks it from entering the RPE. The shift of *Rx2* reporter expression in the CMZ upon deletion of the Gli-binding site is intriguing. It indicates a dual function of this Gil-binding site, mediating repressive activity in the RPE as well as transcriptional activation in the directly adjacent CMZ. Upon deletion of the Gli-binding site, the loss of repression resulted in the gain of *Rx2* reporter expression in the RPE, while the loss of activation in the CMZ abolishes *Rx2* reporter expression in that domain. As an alternative to Gli3, the reduced activation in the CMZ could also be attributed to another *trans*-acting factor requiring the deleted DNA motif. For instance, the transcriptional activator Gli1 is expressed in the CMZ (not shown) and has been shown to share overlapping activating functions with Gli3 during vertebrate neurogenesis (Tyurina *et al.* 2005). Further, it has been demonstrated that input from both Gli1 and Sox2 is required for precise neural enhancer activity in the mammalian neural tube (Peterson *et al.* 2012), raising the possibility that similar cross talk between signal transduction cascades and neural determinants takes place in the context of RSCs and retinal progenitors. Future experiments addressing the identity of the protein binding to the Gli-motif (e.g., chromatin immunoprecipitation or electrophoretic mobility shift assays) will be required to determine whether these activating and repressing functions are mediated by one or more factors binding to the site identified.

Given that our data indicates Gli TFs as activators in the CMZ, it is possible that the weak activity of the Sox2 mutant *Rx2* CRE is mediated through the Gli-motif. This could be tested in a transgenic strain carrying an *Rx2* reporter with both, altered Sox- and Gli-binding sites, and analyzing whether this results indeed in total loss of reporter expression in the CMZ.

Based on the evidence collected, we propose a model for the confinement of post-embryonic RSCs to the peripheral post-embryonic CMZ, which incorporates the regulatory cues of transcriptional activators and repressors.

The *Rx2*-positive RSC population located within the CMZ is defined by both activators (*Sox2*, *Tlx*) and repressors (*Gli3*, *Her9*) (Figure 31), which have the ability to modulate stem cell features upon ectopic expression. Our data demonstrate that *Sox2*, similar to setting up neural competence in mammalian NSCs, induces *Rx2* expression and stem cells fate in the CMZ (Figure 31A) and also ectopically. High

levels of the *Her9* repressor in the central CMZ normally limit slow-cycling RSCs and consequently *Rx2* expression towards the differentiated central retina. On the peripheral side, *Gli3* in its repressive form restricts *Rx2* and prevents it from extending into the mitotically active domain of the adjacent RPE. *Tlx*, overlapping with *Sox2* and in part *Her9*, specifies transiently amplifying neural precursors in the central part of the CMZ. The transcriptional confinement of *Rx2* to the CMZ by the activity of the regulatory scaffold presented here (Figure 31B) connects the stem cells of the NR and those of the RPE and thus sheds light on the mechanism specifying this composite stem cell niche. We hypothesize that the combined activities of those factors within the *Rx2* expression domain coordinate the proliferation and commitment towards neural lineages (either to the NR or the RPE) of the stem cells in the retina.

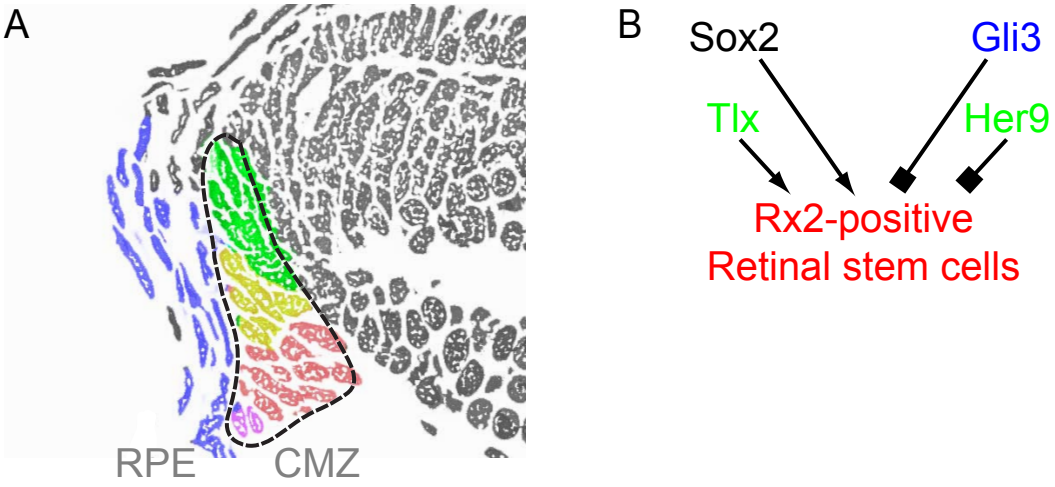

Figure 31. A proposed model summarizing spatial regulation of *Rx2* expression and RSC-specific features by *Sox2*, *Tlx*, *Gli3* and *Her9*.

(A) Schematic illustration outlining the spatial distribution of *Rx2* (red), *Sox2* (black dashed line), *Tlx* (green), *Her9* (green) and *Gli3* (blue) in the medaka CMZ and RPE. Magenta indicates overlap between red and blue; yellow indicates overlap between red and green.

(B) A model summarizing our findings on the regulation of multipotent *Rx2*-positive RSCs by Sox2, Tlx, Gli3 and Her9.

3.2 Expression of *Rx2* might antagonize activity of the *Shh* pathway in the CMZ

Constitutive expression of *Rx2* under the *Atoh7* CRE did not alter proliferation in the stages analyzed. Rather, this approach resulted in a phenotype affecting the patterning of the RGC and INL. How this phenotype was established is presently unknown. Already before the phenotype was visible, *Rx2*-expressing cells in the INL appeared in small clusters. One of the paralogs of *Rx2*, *Rx3*, has been shown to influence cell migration by transcriptionally antagonizing *Nlcam* expression (Brown *et al.*

2010). Molecules belonging to the Alcam family, which Nlcam is part of, have been shown to participate in cell-cell adhesion and to mediate cell migration (Heffron and Golden 2000). Ectopic expression of *Rx2* might transcriptionally regulate the expression of cell adhesion molecules and encourage affected cells to form clusters. 4D imaging of the transgenic retinae could address whether this is an active process of *Rx2*-positive cells (labeled by RFP) migrating towards each other. Long-term *in vivo* imaging might also determine how the phenotype is established and whether only *Rx2*-expressing cells are involved.

In frog, injections of *Rx* mRNA have been shown to expand retinal tissues, resulting in the formation of folds and rosette-like structures within the layered retina (Wu *et al.* 2009). Although this phenotype, where multiple layers fold in parallel, differs from the one observed in the *Atoh7*::Rx2-T2A-mRFP retinae, both show defects in layering of the central NR. Consistent with our findings, *Rx* mis-expression did not induce ectopic proliferation (Wu *et al.* 2009). Conditional clonal gain-of-function assays based on the same tools used for *Sox2*, *Tlx*, *Gli3* and *Her9* will be necessary to address whether *Rx2* itself is able to trigger stem cell features. Although the increased Rx2 levels coincided with reduced expression of molecular markers for RGCs, those experiments need to be quantified and compared to control retinae (e.g., *Atoh7::mRFP*). In studies in mouse and frog, it has been reported that Rx TFs regulate genes involved in photoreceptor specification (Pan *et al.* 2010; Muranishi *et al.* 2011). Morphologically, none of the *Rx2*-expressing cells resembled cones or rods in their shape; however, it still needs to be tested through expression profiling whether photoreceptor-specific genes are activated ectopically. Unlike *Six3*, which has been described to be involved in an auto-regulatory feedback-loop (Loosli *et al.* 1999), gain of *Rx2* did not activate ectopic *Rx2* reporter expression (not shown). Similarly, transgenic reporters for *Sox2*, *Tlx* and *Her9* were unaffected by *Rx2* overexpression in the *Atoh7* domain (not shown). This finding is consistent with the proposed role of *Rx2* in our model as the RSC-specific component in the described regulatory scaffold, downstream of neural determinants.

Surprisingly, expression controlled by the zebrafish *Shh* promoter was reduced in the GCL. The downregulation in *Shh* reporter expression is intriguing, since it indicates a possible cross-regulation between Rx2 and the *Shh* signal pathway. The relationship between *Rx2* and the *Shh* CRE is presently unclear and needs to be addressed in detail. Computational analysis of the sequence of the *Shh* CRE could be used to predict putative Rx binding sites (Brown *et al.* 2010), which then could be modified to investigate the response in reporter expression. Future gene expression analyses of components of the *Shh* signal pathway, in particular the ligand itself and the *Gli* family members, in the *Rx2* mutant will address whether loss of *Rx2* achieves the opposite effect of *Rx2* mis-expression, resulting in a more widespread secretion of Shh ligands and the expression of downstream mediators.

It is tempting to speculate that endogenous *Rx2* in RSCs prevents expression of the *Shh* ligand in the CMZ, thus, restricting broader expression of *Gli* genes and their transcriptional activity on target genes. Our data from *in vitro* and *in vivo* assays have shown that transcriptional regulators downstream of the *Shh* pathway regulate *Rx2* expression; Rx2 is activated in the CMZ and prevented from expanding into the RPE, thus, confined to the peripheral CMZ. In turn, Gli TFs activating *Rx2* could trigger a negative feedback loop, with Rx2 limiting the range of *Shh* signaling. In experiments carried out in *Xenopus*, it was demonstrated that balanced proliferation of retinal precursors depends on *Hh* and *Wnt*/*beta-catenin* signaling pathways negatively regulating each other (Borday *et al.* 2012). Notably, expression Wnt ligands reduced transcriptional activity of the *Rx2* CRE in the trans-regulation assays (not shown). Consistently, a previous study in mouse has linked *Rx* and canonical Wnt signaling by demonstrating that genetic inactivation of *beta-catenin* resulted in expanded expression of *Rx* at the expense of RPE-markers (Fujimura *et al.* 2009). Combining those results into a speculative model suggests that coordinated spatial interplay between *Hh*, *Wnt* and *Rx* is fine-tuning stem cell behavior and balancing their commitment towards either NR or RPE.

3.3 *Rx* mutants

3.3.1 TALEN pairs 106/107 and 128/129 produce disruptive mutations in *Rx2*

The data presented here demonstrate the success of targeted mutagenesis in medaka. By applying chimeric nucleases, we were able to induce stable, heritable genetic marks in specific sites of the endogenous *Rx2* locus. Already transient expression of the TALEN pairs was sufficient to induce modifications in the genome of injected embryos. In zebrafish, the efficiency of TALEN mRNA injections has been described as potent enough to phenocopy morpholino-based knockdowns of previously described genes (Bedell *et al.* 2012). DNA fragments containing genetic alterations caused through erroneous NHEJ-mediated repair were detected in the band-retaining assay. Although this method has been used to determine the efficiency of targetable nucleases in injected embryos, we still identified false-positive sub-cloned fragments with an unchanged target site, underscoring the importance of confirmation through sequencing reaction. It has been suggested that TALEN mRNAs induce mutations in a dose-dependent manner (Ansai *et al.* 2013); whether increased mRNA concentration of the TALENs against *Rx2* would decrease the occurrence of unmutated retained bands needs to be determined. Together with reports of biallelic changes in somatic cells in the injected zebrafish embryos (Bedell *et al.* 2012), this raises the possibility to study gene function by assessing phenotypes of the F0 generations. While the enzymatic restriction digest allows estimating mutagenesis activity,

mutations inside the target sequence not affecting the palindromic recognition sequence will not result in a retained band. Instead, the band will be digested and in the case of small insertions or deletions appear identical to cleaved wild-type bands, resulting in false-negatives. Interestingly, both pairs of TALENs created varying sizes of modifications in the respective genomic target sites, however, all of them were deletions. Other types of genetic modifications such as substitutions or insertions were absent from the sequenced clones. In both medaka and zebrafish, TALENs have been reported to produce mixtures of genomic changes through the homology-free repair pathway (Sander *et al.* 2011; Ansai *et al.* 2013). The bias towards deletions in our analyses could be explained through the relatively small sample size. For instance, for 128/129 TALEN-injected embryos only one clone (a mutant) was successfully sequenced. The target size of TALENs 106/107 is 19 base pairs in the *Rx2* homeobox, while the recognition sequence of HpaII is 4 bases. For example, if insertions occur preferentially adjacent to the HpaII restriction site, the amplified DNA fragment will be cleaved and not sequenced. Thus, selecting a different restriction enzyme could lead ultimately to a different set of mutant carriers. However, the potential bias of the *Rx2* TALENs to produce deletions did not present a disadvantage since the targetable nucleases were intended to induce disruptive lesions in exonic *Rx2* sequences and produce mutants with frame-shifts or premature stop codons. The most promising F1 carriers revealed in the genotyping assays contained mutations in the centre of the homeobox in exon 2 of *Rx2*. While the majority were frame-shifts resulting in truncated proteins with only half of the homeodomain, one mutation removed two amino acids in the middle of the homeodomain. Whether the mutations do disrupt Rx2 protein function completely or create hypomorphic alleles needs to be determined by analyzing the phenotypic consequences in the homozygous progeny. Taken together, both *Rx2* TALENs efficiently induced heritable genetic modifications within the intended exonic regions and yielded mutant carriers for future functional studies.

3.3.2 Off-target activities of TALENs 106 and 107 can generate *Rx1* mutants

Although the high binding specificity of TALENs has been demonstrated in a plethora of studies, unintended cleavages have to be taken into consideration. The most widespread method to assess off-target activity of TALENs is based on identifying and testing sequences in the genome similar to the binding site or target sites of choice. Several studies following this approach reported that off-target events accompanied cleavage in the desired genomic modifications at a low frequency (Hockemeyer *et al.* 2011; Mussolino *et al.* 2011; Tesson *et al.* 2011). Additionally, computational programs have been developed to improve genome-wide predictions of potential off-target sites (Grau *et al.* 2013).

For the TALEN pair 106/107, which in contrast to pair 128/129 binds in the conserved homeobox,

off-target events were assessed in the paralogs of *Rx2*. The sites of potential off-target activity of the TALENs were determined by pair-wise alignment of the *Rx1* coding sequence and binding domains of 106 and 107. The genotyping of the predicted *Rx1* target site in F1 fish revealed the existence of TALEN-induced off-target deletions similar to those in the *Rx2* homeobox. Since the F1 generation instead of the injected fish was tested, it is impossible to determine in which *Rx* gene TALENs 106 and 107 preferentially induced DSBs. Interestingly, the genomic modifications in *Rx1* were accompanied infrequently by additional deletions, which occurred always at the same position and affected the identical number of nucleotides. None of the sequencing reads for *Rx2* were affected by similar unwanted modifications, arguing for this phenomena being linked to the TALEN-induced alterations in *Rx1* locus, potentially due to the imperfectly binding TALEN 107, rather than general off-target events mediated by TALENs 106 and 107. All tested F1 fish with alterations in the *Rx1* homeobox, both those with and without deletions upstream of the target site, were frame-shift mutants, resulting in shortened and partially incorrect Rx1 proteins. Thus, all the *Rx1* mutants can still be tested for *Rx1* loss-of-function phenotypes. However, the molecular pathway causing these additional yet specific deletions upstream of the target site in *Rx1* remains unknown.

In general, we observed single nucleotide modifications at low frequency in individual sequencing reads with and without the desired genetic modifications during the genotyping, arguing for those mutations being introduced in the polymerase-based cloning process. Unidentified off-target mutations accompanying the desired modifications can be removed by consecutively crossing founders to wild-type animals, provided that the unintended alterations are not closely linked to the desired mutation.

While off-target effects represent a serious problem, they open the opportunity to interrogate the function of similar genes with a limited number of TALENs.

For instance, the promiscuity shown by TALENs designed against *Rx2* could be exploited for in a small-scale mutagenesis screen targeting genes similar to *Rx*, in particular those containing a homeobox. Not all *Rx1* mutants identified in the F1 generation were carriers of *Rx2* mutations and vice versa, arguing for independent instances of erroneous repair processes being the cause for the alterations in the individual *Rx* genes. Furthermore, the unintended deletions in *Rx1* occurred in the predicted target site or in case of the additional off-target deletions, adjacent to it. Thus, alignments of the used TAL effectors with the protein-coding genes could be used as reference points for the genotyping assays in such a mutagenesis screen.

3.3.3 Phenotypic analysis suggests TALENs 106 and 107 might disrupt genes involved in early eye development

The F1 of TALEN 106/107-injected fish, which crossed to heterozygous *eyeless* mutants, produced offspring in expected mendelian ratios without eyes, are likely to carry a mutation in the *Rx3* locus. In that case it is reasonable to assume that these alterations occurred inside the homeobox of *Rx3*. Aligned with the sequence of *Rx3*, TALENs 106 and 107 produced two and four mismatches, respectively, flanked a window of 19 nucleotides. Through the sequencing of the *Rx1* homeobox, it was confirmed that TALENs 106 and 107 have the ability to induce lesions, despite TALEN 107 containing three mismatches in the binding domain, giving *in vivo* evidence for the functionality of partially mismatching TAL effectors. An alternative explanation for the absence of eyes is presented by the possibility that these were transheterozygous mutants with one mutant *Rx3* allele (from the *eyeless* carriers) and one mutated *Rx1* or *Rx2* allele (from the TALEN 106/107 F1). That the TALEN pair 106/107 has the potential to induce mutations in *Rx1* or *Rx2* has been confirmed by the genotyping done on injected fish. This theory could be tested by examining the offspring of a cross between the genotyped $Rx1^{+/-}$ or $Rx2^{+/-}$ mutants with heterozygous *eyeless* carriers. Consequently, transheterozygous progeny ($Rx1^{+/-}$ / $Rx3^{+/-}$ or $Rx1^{+/-}$ / $Rx2^{+/-}$) should have the *eyeless* phenotype. However, *Rx1* and *Rx2* gene expression begins later than *Rx3* expression, after the optic vesicles are established, arguing for the *eyeless* phenotype being caused by mutations in genes actively expressed during optic vesicle morphogenesis (e.g., *Rx3*). Ultimately, genotyping will be required to determine where the mutations contributing to the *eyeless* phenotype were introduced in the TALEN 106/107-injected fish.

3.3.4 The function of *Rx2* remains unknown

Morpholino oligonucleotides directed against *Rx1* and *Rx2* did not yield any specific phenotypes. Morpholino-mediated knockdowns can be a powerful tool to inhibit gene function, however, since the morpholino oligonucleotides are delivered via microinjections at one-cell stage, they are designed to interfere with genes expressed during early embryogenesis. For instance, *Rx3* morphants phenocopy the morphology of *eyeless* mutants and recover during later, when the morpholino nucleotides are diluted after multiple rounds of cell divisions, growing eyes identical in size to the uninjected siblings (L. Centanin and J. Wittbrodt, unpublished). As described above, *Rx1* and *Rx2* gene expression begins later than *Rx3*, arguing for a lack of phenotypes due to the inefficiency of the morpholinos during embryonic and adult stages when *Rx1* and *Rx2* might play a role. The knockdown of *Rx1* and *Rx2* transcripts was not evaluated through PCR or Northern analysis. While inefficient knockdown will not be a concern

in the *Rx1* or *Rx2* mutants, once these are crossed to homozygosity, there are a number of issues that could explain the lack of phenotype in the morphants, which might also concern the analyses of the mutants. *Rx1* and *Rx2* share similar expression domains and have related sequences, probably as a result of the teleost-specific genome duplication event, and therefore might have overlapping or partially redundant functions. As a consequence, disruption of a single *Rx* gene might result in no or subtle phenotypes only. The potential redundancy could be addressed by generating double-knockout mutants ($Rx1^{-/-}$ / $Rx2^{-/-}$) by crossing the existing *Rx1* and *Rx2* carriers, preventing one *Rx* gene from compensating for the loss of the other one.

Systematic analysis of over 1200 zebrafish mutants revealed that less than 10% of the mutated genes caused a phenotype during development (Kettleborough *et al.* 2013). While redundancy of duplicated genes might contribute to the low percentage of phenotypes, other factors such as presence of maternal transcripts and loss-of-function phenotypes not resulting in external morphological changes have to be considered. Similarly, the phenotype of *Rx1* or *Rx2* mutants, even of the double-knockout mutants, could be very subtle compared to the dramatic phenotype of *Rx3* mutants. Thus, phenotypic consequences caused by *Rx1* or *Rx2* loss-of-function might only be evident in assays providing single-cell resolution, such as transplantation experiments, where labeled mutant cells are transplanted to wild-type host and vice versa at blastula stage.

Interestingly, during the incrossing of TALEN-injected F0 fish, where we identified the embryos resembling *eyeless* mutants, we also observed the occurrence of embryos with small eyes, although not in mendelian ratios. The phenotype became apparent at optic cup stage and while the eyes continued to grow in size, they were smaller than those of phenotypically normal siblings or stage-matched wild-type embryos (not shown). These mutant embryos were grown to adulthood without genotyping and will be incrossed to test whether the progeny are affected by similar anatomical abnormalities. It is tempting to speculate about the connection between the functions of *Rx* genes and altered mitotic activity of retinal progenitors being the cause for small optic cups in the mutant embryos.

Rx genes are molecular markers of quiescent stem cells in the post-embryonic amphibian retina - *Rx2* labels RSCs in the peripheral CMZ and *Rx* genes are expressed in the MGCs located the central NR. If *Rx* genes indeed play a functional role in maintaining multipotent stem cells in a quiescent state, loss of *Rx* could result in increased short-term proliferation in the CMZ, depleting the pool self-renewing cells, which would interfere with the steady supply of new neurons required for the constant growth of the fish retina. Small-eyed zebrafish mutants with an enlarged CMZ containing very few proliferative active cells have previously been reported (Wehman *et al.* 2005). In case of a similarly enlarged CMZ in the TALEN-induced small eye mutants, this would argue for *Rx* being required for restricting the

population of quiescent cells in the CMZ and potentially interfering transciptionally with their cell cycle progression. However, so far the correlation between phenotype and genotype, as well as shape of the CMZ, if any exists, is unknown.

Complementary to the analyses of the morphological consequence, the regulatory network orchestrated by *Rx* genes could be delineated in the stable mutants. Gene expression profiling of the *Rx* mutants through transcriptome assembly from RNA deep sequencing data would give insight into the biological processes and genetic programs *Rx2* is involved in. Chromatin immunoprecipitation followed by microarray analysis or deep sequencing could predict the direct targets forming the transcriptional network downstream of *Rx2*. For this purpose, tagged Rx2 fusion proteins, which exist in the laboratory (D. Inoue and J. Wittbrodt, unpublished), will be inserted as transgenes in the genome of the *Rx2* mutants. The expressed fusion protein would then allow the immunoprecipitation with commercial antibodies for the genome wide mapping of Rx2 bindings sites.

3.3.5 Applications of nuclease-based genome editing in fish

The findings that TALEN-induced stable genetic marks in medaka are feasible raises the possibility to carry out more advanced nuclease-induced genetic engineering in the fish model. While the type of mutation generated by incorrect NHEJ is unpredictable, the majority is likely to cause frame-shifts through small indels. On the other hand, homology directed repair offers precise control over genetic editing and opens the opportunity to a variety of different applications. By simultaneously providing a DNA donor with homology flanks matching the target region and locus-specific nucleases, the type and position of modification can be freely orchestrated with single-nucleotide resolution. Insertions of up to 8000 base pairs have been reported (Moehle *et al.* 2007). Experiments carried out in ESCs and IPSCs provided evidence for the efficiency and precision of genome editing with TALENs being similar to ZFNs (Hockemeyer *et al.* 2011). TALEN-mediated genome editing has already been successfully utilized to insert a *lox*-site in the zebrafish genome, which presents a crucial step to carry out advanced genetic studies of conditional alleles in fish (Bedell *et al.* 2012). In particular, TALEN-mediated homology directed repair to generate functional fusion proteins *in vivo* without being disruptive is desirable and will be beneficial for a wide range of applications. As it has been demonstrated for the endogenous *Oct4* locus in ESCs, nuclease-mediated integration of a splice acceptor-EGFP into an intron or replacement of the stop codon can yield in frame fusion proteins expressed in physiological levels (Hockemeyer *et al.* 2011). Due to their accurate spatio-temporal expression, transgenic reporter lines generated in this manner could one day replace traditional expression reporter designs based on recombined BACs or isolated regulatory elements. Although improved protocols allow immunohistochemistry in medaka

and zebrafish based on antibodies against conserved proteins from other species (Inoue and Wittbrodt 2011), the lack of fish-specific antibodies has been a long-standing problem. Proteins fused either with a fluorescent protein or a small exogenous tag will be a valuable resource in particular for studies requiring specific antibodies, such as cell-type specific immunoprecipitations or protein-localization studies.

Using targeted nucleases to generate loss-of-function mutants and tag the gene of interest provides a powerful resource to study direct downstream targets. Similar to what has recently been demonstrated with RNA-guided nucleases in transgenic GFP-expressing zebrafish, where the GFP coding sequence was replaced with RFP (Auer *et al.* 2013), existing tissue-specific fluorescent reporter strains caused through positional effects could be exploited by exchanging the existing reporter cassettes with Cre or Flp coding sequences supplied by the donor DNA.

3.4 Outlook

By investigating the regulatory input on the *Rx2*, the molecular marker for multipotent RSCs, we identified a regulatory framework defining the stem cell compartment of the post-embryonic NR, the CMZ. However, many aspects have to be addressed in detail to fully understand the definitive mechanisms underlying this regulatory network.

The potential of undifferentiated cells in the RPE is poorly understood. Studying the composition of clones originating from individual Gli3-positive cells will address whether these cells are stem cells or progenitors with a limited capacity to self-renew. Particularly, lineage-tracing of the cells co-expressing *Rx2* and *Gli3* in the CMZ will delineate the contribution of the stem cells of the NR and those of the RPE; thus, shed light on the mechanism coordinating those adjacent stem cell domains. Making use of the rapidly evolving methods allowing targeted genome modifications, conditional clonal loss of *Sox2*, *Tlx*, *Gli3* or *Her9* will give insight into the molecular mechanism governing multipotency and mitotic activity in RSCs. Examining the outcome of sustained clonal expression of *Tlx* or *Her9* in the peripheral *Rx2*-domain will help us to understand how the commitment of individual RSCs to the NR or the RPE is regulated. Analyzing the behavior of RSCs in the TALEN-induced *Rx2* mutants will address the functional role *Rx2* in the regulatory scaffold. In particular investigating the progeny of individual mutant stem cells will reveal whether *Rx2* coordinates stemness in both the NR and the RPE.

MATERIALS AND METHODS

4 Materials and Methods

4.1 Materials

4.1.1 Buffers

All buffers not specifically described in this section were prepared according to standard protocols (Sambrook *et al.* 1989) using highly deionized water (Millipore), unless indicated differently. Sterilization was achieved by autoclaving.

6x DNA loading buffer

ficoll (type 400, Pharmacia) 15 % (w/v)

bromphenol blue 0.05 % (w/v)

xylene cyanol FF 0.05 % (w/v)

Embryonic Rearing Medium (ERM)

NaCl (Merck) 0.1 % (w/v)

KCl (Merck) 0.003 % (w/v)

$CaCl_2 \times 2H_2O$ (Merck) 0.004 % (w/v)

$MgSO_4 \times 7H_2O$ (Merck) 0.016 % (w/v)

Fin clip buffer

Tris (Sigma)-HCl (Merck), pH8.0 400 mM

EDTA (Merck), pH8.0 5 mM

NaCl 150 mM

SDS 0.1 % (v/v)

LB agar

Agar 15 g/l in LB medium

dissolved by boiling

LB medium (Luria-Bertani)

tryptone 10 g/l

yeast extract 1 g/l

NaCl 10 g/l

to pH7.0 with 5N NaOH (Merck), autoclaved

Hatching medium

NaCl (Merck) 0.1 % (w/v)

KCl (Merck) 0.003 % (w/v)

$CaCl_2 \times 2H_2O$ (Merck) 0.004 % (w/v)

$MgSO_4 \times 7H_2O$ (Merck) 0.016 % (w/v)

Methylene blue 0.0002 % (w/v)

PBS

NaCl 10 mM

KCl (Merck) 195 mM

Na_2HPO4 (Merck) 5.9 mM

KH_2PO4 (Merck) 1.1 mM

pH adjusted to 7.3

PTW

PBS containing 0.1 % Tween 20

TAE buffer

Tris 40 mM

acetic acid (Merck) 20 mM

EDTA 1 mM

TE buffer

Tris-HCl, pH8.0 10 mM

EDTA, pH8.0 1 mM

4.1.2 *Oryzias latipes* stocks

Wild-type *Oryzias latipes* from a closed stock at the COS were kept as described (Koster *et al.* 1997). Transgenic lines *Rx2::H2B-mRFP* (Inoue and Wittbrodt 2011), *Rx2::Tub-GFP* (generated by Juan-Ramon Martinez-Morales) Atoh7::mYFP (Filippo Del Bene) and *Shh::GFP* (generated by Beate

Wittbrodt) were used in this study. The *eyeless* mutants were kept as described (Winkler *et al.* 2000; Loosli *et al.* 2001).

4.1.3 Laboratory equipment and instruments

Binoculars and Stereo Microscopes

DM5000 scope (Leica) with a DFC500 camera (Leica)

Stemi 2000-C (Zeiss)

Stemi SV 11 (Zeiss)

Centrifuges

5417 C (Eppendorf)

5430 R (Eppendorf)

5810 R (Eppendorf)

Cryostat

CM3050S (Leica)

Electroporator

Micro Pulser electroporator (Bio-Rad)

Fluorescence binoculars

Olympus MVX10 MacroView (Olympus)

Incubators

Hera CO_2 cell incubator 150 (Heraus)

Hybaid OmniGene (MWG-Biotech)

Innova 44 Incubator Shakers (New Brunswick Scientific)

Rumed (Rubarth Apparate)

Laminar flow hood

Hera safe HS12 (Heraus)

Laser scanning confocal microscope

(Inverted) TCS SPE (Leica)

Luminescence Counter

Victor Light 1420 (PerkinElmer)

Microinjector

InjectMan NI 2 (Eppendorf)

Microinjector 5242 (Eppendorf)

Nanodrop

Nanodrop Spektrophotometer ND-1000 (peqlab Biotechnologie)

Thermocycler

PTC-200 Peltier Thermal Cycle (Bio-Rad)

Thermomixer

Thermomixer compact (Eppendorf)

4.1.4 Reagents

Alkaline Phosphatase (Roche)

dNTP Mixture, 2.5mM each (Takara)

Fast Red Tablets (Roche)

GeneRuler Ladder Mix (Fermentas)

House Taq Polymerase (EMBL)

innuPREP Gel Extraction kit (Analytik Jena)

innuPREP PCRpure kit (Analytik Jena)

Klenow (Roche)

Ligation buffer (Fermentas)

mMessage machine (SP6) kit (Ambion)

Pfu DNA Polymerases (Stratagene)

Phusion® DNA Polymerase (Thermo Scientific)

QIAfilter Plasmid Maxi kit (Qiagen)

QIAquick Gel Extraction kit (Qiagen)

QiaQuick Nucleotide Removal kit (Qiagen)

QuikChange™ Site-Directed Mutagenesis Kit (Stratagene)

Restriction enzyme buffer (Fermentas, Roche, New England Biolabs)

Restriction enzymes (Fermentas, Roche, New England Biolabs)

RNA Polymerase (SP6, T7) (Roche)

RNeasy Mini kit (Qiagen)

T4 DNA ligase (Fermentas)

TSA™ Plus Fluorescein System (PerkinElmer)

4.1.5 Miscellaneous Materials

Agarose (Sigma)

GC100F-10 Borosilicate glass capillaries with filament (Clark Electromedical Instruments)

4.1.6 Chemicals

5-bromo-4-chloro-3-indolyl-phosphate (Roche)

Aceton (Sigma)

Anti-Digoxigenin-AP, Fab fragments (Roche)

Anti-Fluorescein-POD, Fab fragments (Roche)

Blocking reagent (Roche)

Cover slips (24 mm x 60 mm) (Roth)

DAPI (Sigma)

Digoxigenin-UTP (Roche)

Fast Red Tablets (Roche)

Fluorescein-UTP (Roche)

Formamide (Sigma)

Glass Bottom Culture Dishes (35mm) (MatTek)

Glycerol (Merck)

Glycin (Merck)

Heparin sodium salt (Sigma)

Methanol (Merck)

Nitro blue tetrazolium chloride (Roche)

Proteinase K, 20mg/ml (Roche)

Ribonucleic acid from torula yeast, type VI (Sigma)

SeaPlaque GTG agarose (FMC BioProducts)

Sheep serum (Sigma)

Sodium citrate (Sigma)

Sucrose (Sigma)

Superfrost Plus (Thermo Scientific)

Tissue Freezing Medium (Jung)

TSA™ Plus Fluorescein System (PerkinElmer)

Tween 20 (Sigma)

4.1.7 Cell culture and DNA plasmid transfection

Dishes Nunclon (Nunc)

DMSO (Merck)

Dual-Luciferase Reporter Assay System (Promega)

Dulbecco's Modified Eagle Medium (1x), liquid (High Glucose), 4500 mg/l D-Glucose, without Sodium Pyruvate and L-Glutamine (Invitrogen)

Foetal Bovine Serum, Qualified, Heat-Inactivated (Invitrogen)

FuGENE6 Transfection Reagent, (Roche)

L-Glutamine 200 mM (100x), liquid (Invitrogen)

Opti-MEM® I Reduced Serum Medium (1X), liquid - with L-Glutamine (Invitrogen)

OptiPlate-96, White Opaque 96-well Microplate, (PerkinElmer)

Penicillin-Streptomycin-Glutamine (100x), liquid (Invitrogen)

Stericup-GP, 0.22 um (Millipore)

Trypsin-EDTA Solution (1x) (Sigma)

4.1.8 Antibodies

Primary antibodies

chicken anti-GFP (1:500, Invitrogen)

mouse anti-PCNA (1:100; Santa Cruz)

mouse anti-BrdU (1:50, Becton Dickinson)

mouse anti-Islet (1:250, DSHB)

mouse anti-Zpr1 (1:250, ZIRC)

mouse anti-GS (1:50, Chemicon)

rabbit anti-Phospho-Histone3 (1:500; Upstate)

rabbit anti-OlRx2 (1:500)

rabbit anti-DsRed (1:250, Clontech)

Secondary antibodies

anti-chicken (1:500, DyLight488, DyLight549 and DyLight647, Jackson)

anti-mouse (1:500, DyLight488, DyLight549 and DyLight647, Jackson)

anti-rabbit (1:500, DyLight488, DyLight549 and DyLight647, Jackson)

4.1.9 Cell line

Syrian Hamster Fibroblast (BHK21)

4.1.10 Electrocompetent cells

Electro MAX DH10B cells (Stratagene)

4.1.11 Embryo injection plates

Petri dishes were filled with liquid 1.5 % (w/v) agarose (Sigma) in H_2O. Afterwards, plastic molds were added to create the injection trenches during agarose solidification.

4.1.12 TALEN

The TALENs designed to bind the *Rx2* coding sequence were provide by (Jean-Paul Concordet) in pCS2$^+$ backbones with the following DNA binding domains: N106: TCGAGAAGTCCCACTA; N107: TCGTTGCCAGTTCCTC; S128: TCAGAACCCTATGGAA; S129: GATGCTGTGAGCTGTC.

4.2 Methods

4.2.1 Generation of medaka unigene cDNA library

Full-length cDNA clones were generated based on total RNA extracted from medaka embryos of different developmental stages as previously described (Souren *et al.* 2009). The cDNAs were inserted into a pCMVSport6.1 vector, end-sequenced, clustered based on sequence alignments and collected in a consolidated unigene library. Based on GO annotations a subset of developmental relevant genes and genes encoding TFs were collected in a library consisting of 1151 cDNA clones (Thorsten Henrich).

4.2.2 Molecular cloning

A cassette containing the LexOP operator upstream of the Cherry coding sequence was extracted from *pDs(cry:C-LOP:Ch)*. The Cherry coding sequence was replaced with H2B-EGFP and H2A-Cherry. Effectors: *LexOP::H2A-Cherry*; *LexOP::H2B-EGFP*; *LexOP::Cherry*. A cassette containing the coding sequence for the LexPR trans-activator followed by the LexOP operator was released from *pDs(krt8:LPR-LOP:G4)* and inserted downstream of the *Rx2* CRE (Inoue and Wittbrodt 2011). Coding sequences for *Gli3* and *Her9* were inserted downstream of the LexOP operator. A second LexOP operator followed by H2B-EGFP coding sequence was added (released from *LexOP::H2B-EGFP*). Driver-Effectors: *Rx2::LexPR LexOP::Gli3 LexOP::H2B-EGFP*; *Rx2::LexPR LexOP::Her9 LexOP::H2B-EGFP*; *Rx2::LexPR LexOP LexOP::H2B-EGFP*.

A cassette containing the coding sequence for the LexPR trans-activator followed by the LexOP operator was introduced downstream of the *cska* promoter (Grabher *et al.* 2003). Coding sequences for *Sox2* and *Tlx* were inserted downstream of the LexOP operator. Drivers: *Cska::LexPR LexOP::Sox2*; *Cska::LexPR LexOP::Tlx*,; *Cska::LexPR LexOP*.

LexPR and LexOP cassettes were derived from *pDs(krt8:LPR-LOP:G4)* and *pDs(cry:C-LOP:Ch)* to generate driver, effector or driver-effector constructs (Emelyanov and Parinov 2008). The 2.4 kb *Rx2* CRE was released through restriction digest and cloned upstream of the luciferase gene in to the pGL3 luciferase reporter vector (Promega).

Coding sequences for *Sox2*, *Gli3* and *Her9* were derived from a full-length cDNA library based on the pCMV-Sport6.1 vector (Souren *et al.* 2009), *Tlx* cDNA was derived from a Lambda ZAP cloning vector (Felix Loosli). Full-length *OlRx2* coding sequence (NP_001098373.1) for antibody generation was cloned by PCR from medaka stage 32 cDNA using the following primers: forward primer: 5'-GGAATTCCATATGATGCATTTGTCAATGGATAC-3'; reverse primer: 5'-CGGGATCCTCACATGTGCTGCCAGG-3'. PCR products were digested with restriction enzymes

NdeI and BamHI, ligated into the pET15b (Merck Millipore), which was cleaved with the same enzymes. pET15b-*OlRx2* was used to bacterially express *OlRx2* protein as the antigen for generation of OlRx2 antibody (Daigo Inoue). All constructs generated for transient expression or transgenesis were based on a pBluescript plasmid containing two I-SceI sites flanking the insert.

The gene regulatory regions of *Tlx*, *Sox2* and *Her9* were amplified via PCR from genomic DNA using the following primers for *Tlx* (ENSORLG00000013426): forward primer: 5'-GGCGGAATATTTAATGAACTGTAGATACGTTGATCA-3'; reverse primer: 5'-CTCACACGGCAGTGACGTAAGG-3'; *Sox2* (ENSORLG00000011685): forward primer: 5'-TTTACAAGTGGTCCGAGGGAG-3'; reverse primer: 5'-CAGGGAAAATTTTAACTTTTCGCTGGG-3'; and *Her9* (ENSORLG00000005453): forward primer: 5'-AGCGCTTCATTAGTGTGGGCG-3'; reverse primer: 5'-GCGCACAGCAGCTCTCCACA-3'. The corresponding PCR products were cloned into a pBluescript-based transgenesis vector containing two recognition sites for the meganuclease I-SceI (New England Biolabs) flanking a multiple cloning site followed by a cassette containing an enhanced GFP and a SV40-polyadenylation signal.

Fusion PCR

The *Rx2* coding sequence was amplified excluding the last three nucleotides (stop codon) from *Rx2* cDNA with the following primers:

Rx2 forward primer: 5'-ATGCATTTGTCAATGGATACCC-3'; reverse primer: 5'-AGGGCCGGGATTCTCCTCCACGTCACCGCATGTTAGAAGACTTCCTCTGCCCTCTCCCATGT-GCTGCCAG-3', underlined overhangs encode T2A (Kim *et al.* 2011). In a separate PCR the mRFP coding sequence was obtained from the linearized *Vsx3::H2B-mRFP* (Marcel Souren) vector with the following primers: forward primer: 5'-GAGGGCAGAGGAAGTCTTCTAACATGCGGTGACGTGGAGG-AGAATCCCGGCCCTATGGCCTCCTCCGAGG-3', underlined overhangs encode T2A; reverse primer: 5'-AACAAAAGCTGGAGCTCCA-3'. A single fusion PCR was performed on the resulting PCR products with the *Rx2* forward primer and mRFP reverse primer. Afterwards, the Rx2-T2A-mRFP fragment was cut with NotI (recognition site in mRFP reverse primer not shown) and ligated into *Atoh7::mYFP* (Filippo Del Bene), which was digested with SnaBI and NotI to release the mYFP and provide a complementary overhang. All PCR fragments were amplified with identical PCR steps (30 sec 98°C, (20 sec 98°C, 45 sec 60°C, 1 min 15 sec 72°C) repeated for 4 cycles, (20 sec 98°C, 45 sec 58°C, 1 min 15 sec 72°C) repeated for 9 cycles, (20 sec 98°C, 45 sec 56°C, 1 min 15 sec 72°C) repeated for 14 cycles, followed by 72°C 5 min) and purified with the innuPREP Gel Extraction kit (Analytik Jena) or the innuPREP PCRpure kit according to manufacturers protocol.

Site-directed mutagenesis

Amino-acid substitutions or deletions were introduced into the *Rx2* gene regulatory region of *Rx2::H2B-mRFP* by site-directed mutagenesis (3 min 95°C, (30 sec 95°C, 30 sec 55°C, 12 min 30 sec 72°C) repeated for 18 cycles, followed by 15 min 72°C) using the following primers: Sox-binding site, forward primer: 5'-CCACACAAGCCATTATCTTTCAGACGCTAGATTTGTTGAAAGGAAGTTTTGT-3'; reverse primer: 5'-ACAAAACTTCCTTTCAACAAATCTAGCGTCTGAAAGATAATGGCTTGTGTGG-3';
Gli-binding site, forward primer: 5'-GAAGTTTTGTTGAGGCTTCATTAGCAATGTGGTCTGAAAGCAG-3'; reverse primer: 5'-CTGCTTTCAGACCACATTGCTAATGAAGCCTCAACAAAACTTC-3'.
All steps were carried out according to the manufactures protocol (QuikChange™, Stratagene) with the exception of the transformation, which was done using electrocompetent DH10B cells.

mRNA transcription *in vitro*

Supercoiled DNA of the pCS2^{+} plasmid was subjected to restriction digest with NotI and the linearized DNA template was purified using the innuPREP PCRpure kit (Analytik Jena) according to the manufacturers protocol. TALEN N106, N107, S128 and S129 mRNA transcription in vitro from the SP6 promoter was performed using the mMessage machine (Ambion) according to the manufacturers protocol. The mRNA was purified using the RNeasy RNA purification kit (Qiagen) according to the manufacturers protocol and stored at –80°C.

4.2.3 Microinjection

Fertilized eggs were collected from wild-type CAB or transgenic crosses and placed in chilled ddH_2O to slow down development. For microinjections a pressure injector was used. Borosilicate glass capillaries (Clark Electromedical Instruments) were backfilled with the injection solution (final concentration DNA: 30 ng/ul). The injection solution was injected through the chorion into the cytoplasm of the one-cell stage embryos. TALEN mRNAs (N106 and N107; S128 and S129) were co-injected at a concentration of up to 100 ng/ul in ddH_2O. For transient mosaic expression injection solution (DNA) was injected into the cytoplasm at two-cell stage.

4.2.4 Generation of transgenic lines

Transgenic lines were established by co-injection of the DNA plasmid and I-SceI enzyme into one-cell stage medaka eggs as described (Thermes *et al.* 2002). All DNA plasmids used in injections

were isolated from bacterial lysate using Qiagen-tip 500 columns from the QIAfilter Plasmid Maxi kit (Qiagen) according to manufacturers protocol.

4.2.5 BrdU treatment

Embryos were incubated in a solution of 1 g/l BrdU for a varying amount of time and fixed immediately afterwards in 4 % PFA/PTW.

4.2.6 RU486 treatment

Mifepristone (Sigma, Tocris, Cayman) was dissolved in DMSO to a final concentration of 25 mM and stored as stock solution at -20 °C. The stock solution was added to the medium and used at final concentrations up to 20 uM.

4.2.7 pBluescript-TA

A PCR under low-stringency conditions (5 min 95°C, (45s 95°C, 45s 45°C, 1 min 72°C) repeated for 29 cycles, followed by 5 min 72°C) using a single primer (CGGAATTC**CCATGGTTGTGATGG**G, recognition site for EcoRI underlined, XcmI bold) on medaka CAB genomic DNA yielded random fragments of various sizes after standard gel electrophoresis (Beate Wittbrodt). A 500 bp fragment was excised from an agarose gel using the innuPREP Gel Extraction kit according the manufacturers protocol (Analytik Jena). Taq DNA polymerase derived A-overhangs were used to sub-clone the PCR fragment into the pCR®II-TOPO® vector provided by the TOPO® TA Cloning® Kit (Invitrogen) according the manufacturers protocol. The inserted fragment, which retained EcoRI recognition sequences in its flanks from the oligonucleotide, was released from pCR®II-TOPO® vector through enzymatic digest with EcoRI and ligated into an EcoRI-cleaved pBluescript II vector. After restriction digest with XcmI, the 500 bp insert was released from the linearized vector, leaving behind T-overhangs flanked by EcoRI recognition sequences. The fragments were separated by standard gel electrophoresis, the linearized pBluescript-TA vector was excised, purified and stored at -80°C. PCR fragments intended for TA cloning were always freshly prepared. The two EcoRI sites of the pBluescript-TA vector allow rapid identification of clones, which successfully inserted the DNA fragment of interest.

4.2.8 Genotyping

4.2.8.1 Genomic DNA extraction

Single medaka eggs were placed in individual 2 ml tubes, flash-frozen in liquid nitrogen, crushed with sterile pestle and homogenized in 100 µl (for pool of embryos use 300 ul) fin clip buffer containing proteinase K (add 500 µl proteinase K (20 mg/ml) to 10 ml fin clip buffer) (Beate Wittbrodt). The homogenate was incubated o/n at 60 °C. Afterwards 200 µl ddH_2O (500 µl for multiple embryos) were added and the tube gently turned without shaking and incubated for 10 min at 95°C. After a short spin down of the samples, the supernatant was transferred to a fresh tube and stored at 4°C.
For the isolation of genomic DNA from adult tissues, fish were transferred into ice water or 0.4 % Tricaine (4 ml Tricaine in 100 ml fish water), collected with a large plastic spoon and cut at the tailfin. The tissue samples were placed with the aid of forceps in tubes and 100 µl fin clip buffer containing proteinase K was added. The adult fish were kept in 2/3 hatching medium and 1/3 fish water o/n. The remaining steps of the genomic DNA extraction from adults were carried out as described above.

4.2.8.2 Genotyping PCR and restriction digest-based band-retention

The regions of interest for TALEN pair 106/107 were amplified from the isolated genomic DNA with the following primers: *Rx1* forward primer: 5'-ATTCGTCCGTGTGGACCTGT-3'; reverse primer: 5'-TCTCGTCCTCCAAACAGACA-3'; *Rx2* forward primer: 5'-AACAGTGAGTAGCGGGTCGT-3'; reverse primer: 5'-TCTGAGGGATGGAATTCTGG-3'. The PCR amplification was mediated by a proofreading polymerase (*Rx1*: 30s 98°C, (20s 98°C, 45s 67°C, 15s 72°C) repeated for 29 cycles, followed by 5 min 72°C; *Rx2*: 30s 98°C, (20s 98°C, 45s 67°C, 45s 72°C) repeated for 29 cycles, 5 min followed by 72°C) and followed by 15 min at 72°C with Taq polymerase. The resulting PCR products (Rx1: 300 bp; Rx2: 930 bp) were enzymatically digested with HpaII for 1 h. The region of interest for TALEN pair 128/129 was amplified from the isolated genomic DNA with the following primers: *Rx2* forward primer: 5'-GAGTCCAAAGGCAAGTCCAC-3'; reverse primer: 5'-TTTGAACCTCTCGCTGTGA-3'. The PCR amplification was mediated by a proofreading polymerase (*Rx2*: 30s 98°C, (20s 98°C, 45s 67°C, 45s 72°C) repeated for 29 cycles, 5 min followed by 72°C) and followed by 15 min at 72°C with Taq polymerase. The resulting PCR products (1040 bp) were enzymatically digested with BspEI for 1 h. The uncleaved bands retaining original size were purified and through the Taq polymerase derived A-overhangs ligated into a pBluescript-TA vector, with complementary T-overhangs created by the restriction enzyme XcmI. The DNA minipreps were subjected to restriction digest with EcoRI and clones with the correct insert size were selected for sequencing.

4.2.9 WISH

4.2.9.1 Riboprobe preparation

For anti-sense riboprobe synthesis linear templates were produced from full-length cDNA clones either through standard PCR using standard M13 forward and reverse primers (*Sox2*, *Gli3* and *Her9*) or digestion with restriction enzymes cutting 5' of the start codon (*Rx2* and *Tlx*). T7 RNA polymerase-based transcription and incorporation of digoxigenin-UTP or fluorescein-UTP was carried out as previously described (Loosli *et al.* 1998).

4.2.9.2 Single color WISH

Whole-mount in situ hybridizations using NBT/BCIP detection were carried out as previously described (Loosli *et al.* 1998).

4.2.9.3 (Double-) Fluorescent WISH

Fluorescent whole mount in situ hybridizations were performed as previously described (Souren *et al.* 2009). For combined single-color fluorescent whole mount in situ hybridization and immunostaining, embryos were incubated for two days with anti-fluorescein antibody conjugated to horseradish peroxidase (Roche) and anti-GFP antibody at 4°C. After riboprobe detection using TSA-Plus Cyanine 3 System (PerkinElmer) the embryos were incubated with fluorescent-conjugated secondary antibody and DAPI for two days at 4°C. In case of WISH followed by immunostaining, the embryos were subjected to 3 % H_2O_2 (Sigma), 1 % KOH in 1x PTW for 30 minutes at RT after fixation and removal of the chorion.

4.2.10 Immunohistochemistry

4.2.10.1 Rx2 antibody

Anti-OlRx2 antibody was raised against the full-length *OlRx2* (NP_001098373.1) recombinant protein in rabbits (Charles River), and affinity purified as described previously (Barenz *et al.* 2013).

4.2.10.2 Fixation

Embryos were fixed in 4 % PFA/PTW o/n at 4°C.

4.2.10.3 Antigen retrieval and cryosections

Fixed embryos were washed in PTW. In case of embryos fixed at pre-hatch stages, the chorion was removed with forceps. Cryoprotection, heating steps for retrieving antigens and sections were performed as previously described (Inoue and Wittbrodt 2011).

4.2.10.4 Immunostaining on cryosections

Dried cryosections were incubated in aceton for 10 min at -20°C. When necessary, cryosections were subjected to 3 % H_2O_2 (Sigma), 1 % KOH in 1x PTW for 30 minutes at RT prior to the aceton step. The sections were washed and blocked with 10 % sheep serum/PTW for at least 2 h at RT. Afterwards, incubation with the primary antibody followed o/n at 4°C. The cryosections were washed and incubated with the secondary antibody for 90 min at 37°C in the dark. Cell nuclei were counterstained with DAPI (final concentration; 200 mg/ml) for 5 min at RT in the dark. For imaging, the slides were washed, 70 % glycerol and was added. The stained tissues were covered with cover slips and sealed with nail polish. All washing steps were performed with 1x PTW for 10 min for at least three times.
For BrdU detection, cryosections were dried o/n, re-hydrated with 1x PTW and treated with 2N HCL, 0.5 % Triton X-100 in 1x PBS for 90 minutes at RT.

4.2.11 Imaging

Images of sections and whole-mount embryos were acquired using the Leica Application Suite Advanced Fluorescence software and an inverted Leica TCS SPE confocal microscope with ACS APO 10x/0.30, 20x/0.60, 40x/1.15 and 63x/1.30 objective lenses. 405 nm, 488 nm, 532 nm and 635 nm laser lines were used for fluorophore excitation. Whole-mount embryos were mounted as previously described (Ramialison *et al.* 2012). Images were processed using ImageJ software, v.1.41o. Images of NBT/BCIP stainings were taken using a Leica DM5000 scope equipped with a Leica DFC500 camera.

4.2.12 *Trans*-regulation screen

Cell culture, transfection and luciferase read-out were carried out with 1151 cDNA clones (300 ng) on the pGL3 *Rx2::luc2* vector (40 ng) as previously described (Souren *et al.* 2009).

REFERENCES

References

Abad, M., L. Mosteiro, C. Pantoja, M. Cañamero, T. Rayon, I. Ors, O. Graña, D. Megías, O. Domínguez, D. Martínez*, et al.* (2013). "Reprogramming in vivo produces teratomas and iPS cells with totipotency features." Nature **502**(7471): 340-345.

Agathocleous, M., I. Iordanova, M.I. Willardsen, X.Y. Xue, M.L. Vetter, W.A. Harris and K.B. Moore (2009). "A directional Wnt/beta-catenin-Sox2-proneural pathway regulates the transition from proliferation to differentiation in the Xenopus retina." Development (Cambridge, England) **136**(19): 3289-3299.

Amato, M.A., E. Arnault and M. Perron (2004). "Retinal stem cells in vertebrates: parallels and divergences." The International journal of developmental biology **48**(8-9): 993-1001.

Anderson, K.V. (2000). "Finding the genes that direct mammalian development : ENU mutagenesis in the mouse." Trends in genetics : TIG **16**(3): 99-102.

Andreazzoli, M., G. Gestri, D. Angeloni, E. Menna and G. Barsacchi (1999). "Role of Xrx1 in Xenopus eye and anterior brain development." Development (Cambridge, England) **126**(11): 2451-2460.

Ansai, S., T. Sakuma, T. Yamamoto, H. Ariga, N. Uemura, R. Takahashi and M. Kinoshita (2013). "Efficient targeted mutagenesis in medaka using custom-designed transcription activator-like effector nucleases." Genetics **193**(3): 739-749.

Auer, T.O., K. Duroure, A. De Cian, J.P. Concordet and F. Del Bene (2013). "Highly efficient CRISPR/Cas9-mediated knock-in in zebrafish by homology-independent DNA repair." Genome research.

Austin, C.P., D.E. Feldman, J.A. Ida and C.L. Cepko (1995). "Vertebrate retinal ganglion cells are selected from competent progenitors by the action of Notch." Development (Cambridge, England) **121**(11): 3637-3650.

Baek, J.H., J. Hatakeyama, S. Sakamoto, T. Ohtsuka and R. Kageyama (2006). "Persistent and high levels of Hes1 expression regulate boundary formation in the developing central nervous system." Development (Cambridge, England) **133**(13): 2467-2476.

Barenz, F., D. Inoue, H. Yokoyama, J. Tegha-Dunghu, S. Freiss, S. Draeger, D. Mayilo, I. Cado, S. Merker, M. Klinger*, et al.* (2013). "The centriolar satellite protein SSX2IP promotes centrosome maturation." The Journal of cell biology **426**(6966): 570.

Barker, N., M. Huch, P. Kujala, M. van de Wetering, H.J. Snippert, J.H. van Es, T. Sato, D.E. Stange, H. Begthel, M. van den Born*, et al.* (2010). "Lgr5(+ve) stem cells drive self-renewal in the stomach and build long-lived gastric units in vitro." Cell stem cell **6**(1): 25-36.

Barker, N., J.H. van Es, J. Kuipers, P. Kujala, M. van den Born, M. Cozijnsen, A. Haegebarth, J. Korving, H. Begthel, P.J. Peters*, et al.* (2007). "Identification of stem cells in small intestine and colon by marker gene Lgr5." Nature **449**(7165): 1003-1007.

Bedell, V.M., Y. Wang, J.M. Campbell, T.L. Poshusta, C.G. Starker, R.G. Krug Ii, W. Tan, S.G. Penheiter, A.C. Ma, A.Y.H. Leung*, et al.* (2012). "In vivo genome editing using a high-efficiency TALEN system." Nature.

Belliveau, M.J. and C.L. Cepko (1999). "Extrinsic and intrinsic factors control the genesis of amacrine and cone cells in the rat retina." Development (Cambridge, England) **126**(3): 555-566.

Belliveau, M.J., T.L. Young and C.L. Cepko (2000). "Late retinal progenitor cells show intrinsic limitations in the production of cell types and the kinetics of opsin synthesis." The Journal of neuroscience : the official journal of the Society for Neuroscience **20**(6): 2247-2254.

Bernardos, R.L., L.K. Barthel, J.R. Meyers and P.A. Raymond (2007). "Late-stage neuronal progenitors in the retina are radial Müller glia that function as retinal stem cells." The Journal of neuroscience : the official journal of the Society for Neuroscience **27**(26): 7028-7040.

Bernier, G., F. Panitz, X. Zhou, T. Hollemann, P. Gruss and T. Pieler (2000). "Expanded retina territory by midbrain transformation upon overexpression of Six6 (Optx2) in Xenopus embryos." Mechanisms of development **93**(1-2): 59-69.

Bibikova, M., M. Golic, K.G. Golic and D. Carroll (2002). "Targeted chromosomal cleavage and mutagenesis in Drosophila using zinc-finger nucleases." Genetics **161**(3): 1169-1175.

Bickenbach, J.R. (1981). "Identification and behavior of label-retaining cells in oral mucosa and skin." Journal of dental research **60 Spec No C**: 1611-1620.

Bitinaite, J., D.A. Wah, A.K. Aggarwal and I. Schildkraut (1998). "FokI dimerization is required for DNA cleavage." Proceedings of the National Academy of Sciences of the United States of America **95**(18): 10570-10575.

Blancafort, P., D.J. Segal and C.F. Barbas (2004). "Designing transcription factor architectures for drug discovery." Molecular pharmacology **66**(6): 1361-1371.

Boch, J. and U. Bonas (2010). "Xanthomonas AvrBs3 family-type III effectors: discovery and function." Annual review of phytopathology **48**: 419-436.

Boch, J., H. Scholze, S. Schornack, A. Landgraf, S. Hahn, S. Kay, T. Lahaye, A. Nickstadt and U. Bonas (2009). "Breaking the code of DNA binding specificity of TAL-type III effectors." Science (New York, NY) **326**(5959): 1509-1512.

Bonaguidi, M.A., M.A. Wheeler, J.S. Shapiro, R.P. Stadel, G.J. Sun, G.-l. Ming and H. Song (2011). "In vivo clonal analysis reveals self-renewing and multipotent adult neural stem cell characteristics." CELL **145**(7): 1142-1155.

Borday, C., P. Cabochette, K. Parain, N. Mazurier, S. Janssens, H.T. Tran, B. Sekkali, O. Bronchain, K. Vleminckx, M. Locker*, et al.* (2012). “Antagonistic cross-regulation between Wnt and Hedgehog signalling pathways controls post-embryonic retinal proliferation.” Development (Cambridge, England) **139**(19): 3499-3509.

Branda, C.S. and S.M. Dymecki (2004). “Talking about a revolution: The impact of site-specific recombinases on genetic analyses in mice.” Developmental Cell **6**(1): 7-28.

Bravo, R., R. Frank, P.A. Blundell and H. Macdonald-Bravo (1987). “Cyclin/PCNA is the auxiliary protein of DNA polymerase-delta.” Nature **326**(6112): 515-517.

Brenner, S. (1974). “The genetics of Caenorhabditis elegans.” Genetics **77**(1): 71-94.

Brown, K.E., P.J. Keller, M. Ramialison, M. Rembold, E.H. Stelzer, F. Loosli and J. Wittbrodt (2010). “Nlcam modulates midline convergence during anterior neural plate morphogenesis.” Developmental Biology **339**(1): 12-12.

Brown, N.L., S. Patel, J. Brzezinski and T. Glaser (2001). “Math5 is required for retinal ganglion cell and optic nerve formation.” Development (Cambridge, England) **128**(13): 2497-2508.

Bylund, M., E. Andersson, B.G. Novitch and J. Muhr (2003). “Vertebrate neurogenesis is counteracted by Sox1-3 activity.” Nature neuroscience **6**(11): 1162-1168.

Carl, M. and J. Wittbrodt (1999). “Graded interference with FGF signalling reveals its dorsoventral asymmetry at the mid-hindbrain boundary.” Development (Cambridge, England) **126**(24): 5659-5667.

Cavodeassi, F., F. Carreira-Barbosa, R.M. Young, M.L. Concha, M.L. Allende, C. Houart, M. Tada and S.W. Wilson (2005). “Early stages of zebrafish eye formation require the coordinated activity of Wnt11, Fz5, and the Wnt/beta-catenin pathway.” Neuron **47**(1): 43-56.

Cayuso, J., F. Ulloa, B. Cox, J. Briscoe and E. Martí (2006). “The Sonic hedgehog pathway independently controls the patterning, proliferation and survival of neuroepithelial cells by regulating Gli activity.” Development (Cambridge, England) **133**(3): 517-528.

Centanin, L., B. Hoeckendorf and J. Wittbrodt (2011). “Fate restriction and multipotency in retinal stem cells.” Cell stem cell **9**(6): 553-562.

Cermak, T., E.L. Doyle, M. Christian, L. Wang, Y. Zhang, C. Schmidt, J.A. Baller, N.V. Somia, A.J. Bogdanove and D.F. Voytas (2011). “Efficient design and assembly of custom TALEN and other TAL effector-based constructs for DNA targeting.” Nucleic Acids Research **39**(12): e82.

Cerveny, K.L., F. Cavodeassi, K.J. Turner, T.A. de Jong-Curtain, J.K. Heath and S.W. Wilson (2010). “The zebrafish flotte lotte mutant reveals that the local retinal environment promotes the differentiation of proliferating precursors emerging from their stem cell niche.” Development (Cambridge, England) **137**(13): 2107-2115.

Chang, N., C. Sun, L. Gao, D. Zhu, X. Xu, X. Zhu, J.-W. Xiong and J.J. Xi (2013). “Genome editing with RNA-guided Cas9 nuclease in Zebrafish embryos.” Cell research **23**(4): 465-472.

Chiang, C., Y. Litingtung, E. Lee, K.E. Young, J.L. Corden, H. Westphal and P.A. Beachy (1996). “Cyclopia and defective axial patterning in mice lacking Sonic hedgehog gene function.” Nature **383**(6599): 407-413.

Chow, R.L., C.R. Altmann, R.A. Lang and A. Hemmati-Brivanlou (1999). “Pax6 induces ectopic eyes in a vertebrate.” Development (Cambridge, England) **126**(19): 4213-4222.

Clayton, E., D.P. Doupé, A.M. Klein, D.J. Winton, B.D. Simons and P.H. Jones (2007). “A single type of progenitor cell maintains normal epidermis.” Nature **446**(7132): 185-189.

Colbert, T., B.J. Till, R. Tompa, S. Reynolds, M.N. Steine, A.T. Yeung, C.M. McCallum, L. Comai and S. Henikoff (2001). “High-throughput screening for induced point mutations.” Plant physiology **126**(2): 480-484.

Collas, P. and J.A. Dahl (2008). “Chop it, ChIP it, check it: the current status of chromatin immunoprecipitation.” Frontiers in bioscience : a journal and virtual library **13**: 929-943.

Cong, L., F.A. Ran, D. Cox, S. Lin, R. Barretto, N. Habib, P.D. Hsu, X. Wu, W. Jiang, L.A. Marraffini*, et al.* (2013). “Multiplex genome engineering using CRISPR/Cas systems.” Science (New York, NY) **339**(6121): 819-823.

Cooley, L., R. Kelley and A. Spradling (1988). “Insertional mutagenesis of the Drosophila genome with single P elements.” Science (New York, NY) **239**(4844): 1121-1128.

Cotsarelis, G., T.T. Sun and R.M. Lavker (1990). “Label-retaining cells reside in the bulge area of pilosebaceous unit: implications for follicular stem cells, hair cycle, and skin carcinogenesis.” CELL **61**(7): 1329-1337.

Cremisi, F., A. Philpott and S.-i. Ohnuma (2003). “Cell cycle and cell fate interactions in neural development.” Current opinion in neurobiology **13**(1): 26-33.

Danno, H., T. Michiue, K. Hitachi, A. Yukita, S. Ishiura and M. Asashima (2008). “Molecular links among the causative genes for ocular malformationtion: Otx2 and Sox2 coregulate Rax expression.” Proceedings of the National Academy of Sciences of the United States of America **105**(14): 5408-5413.

Davis, R.L., H. Weintraub and A.B. Lassar (1987). “Expression of a single transfected cDNA converts fibroblasts to myoblasts.” CELL **51**(6): 987-1000.

Del Bene, F. (2011). “Interkinetic nuclear migration: cell cycle on the move.” The EMBO Journal **30**(9): 1676-1677.

Del Bene, F., L. Ettwiller, D. Skowronska-Krawczyk, H. Baier, J.-M. Matter, E. Birney and J. Wittbrodt (2007). “In vivo validation of a computationally predicted conserved Ath5 target gene set.” PLoS genetics **3**(9): 1661-1671.

Deltcheva, E., K. Chylinski, C.M. Sharma, K. Gonzales, Y. Chao, Z.A. Pirzada, M.R. Eckert, J. Vogel and E. Charpentier (2011). “CRISPR RNA maturation by trans-encoded small RNA and host factor RNase III.” Nature **471**(7340): 602-607.

Doyon, Y., J.M. McCammon, J.C. Miller, F. Faraji, C. Ngo, G.E. Katibah, R. Amora, T.D. Hocking, L. Zhang, E.J. Rebar*, et al.* (2008). “Heritable targeted gene disruption in zebrafish using designed zinc-finger nucleases.” Nature Biotechnology **26**(6): 702-708.

Driessens, G., B. Beck, A. Caauwe, B.D. Simons and C. Blanpain (2012). “Defining the mode of tumour growth by clonal analysis.” Nature **488**(7412): 527-530.

Driever, W., L. Solnica-Krezel, A.F. Schier, S.C. Neuhauss, J. Malicki, D.L. Stemple, D.Y. Stainier, F. Zwartkruis, S. Abdelilah, Z. Rangini*, et al.* (1996). “A genetic screen for mutations affecting embryogenesis in zebrafish.” Development (Cambridge, England) **123**: 37-46.

Dyer, M.A., F.J. Livesey, C.L. Cepko and G. Oliver (2003). “Prox1 function controls progenitor cell proliferation and horizontal cell genesis in the mammalian retina.” Nature genetics **34**(1): 53-58.

Eivers, E., K. McCarthy, C. Glynn, C.M. Nolan and L. Byrnes (2004). “Insulin-like growth factor (IGF) signalling is required for early dorso-anterior development of the zebrafish embryo.” The International journal of developmental biology **48**(10): 1131-1140.

Ekker, S.C., A.R. Ungar, P. Greenstein, D.P. von Kessler, J.A. Porter, R.T. Moon and P.A. Beachy (1995). “Patterning activities of vertebrate hedgehog proteins in the developing eye and brain.” Current Biology **5**(8): 944-955.

El Yakoubi, W., C. Borday, J. Hamdache, K. Parain, H.T. Tran, K. Vleminckx, M. Perron and M. Locker (2012). “Hes4 controls proliferative properties of neural stem cells during retinal ontogenesis.” STEM CELLS **30**(12): 2784-2795.

Elmi, M., Y. Matsumoto, Z.-j. Zeng, P. Lakshminarasimhan, W. Yang, A. Uemura, S.-i. Nishikawa, A. Moshiri, N. Tajima, H. Agren*, et al.* (2010). “TLX activates MASH1 for induction of neuronal lineage commitment of adult hippocampal neuroprogenitors.” Molecular and Cellular Neuroscience **45**(2): 121-131.

Emelyanov, A. and S. Parinov (2008). “Mifepristone-inducible LexPR system to drive and control gene expression in transgenic zebrafish.” Developmental Biology **320**(1): 113-121.

Estivill-Torrus, G., H. Pearson, V. van Heyningen, D.J. Price and P. Rashbass (2002). “Pax6 is required to regulate the cell cycle and the rate of progression from symmetrical to asymmetrical division in mammalian cortical progenitors.” Development **129**(2): 455-466.

Feil, R., J. Brocard, B. Mascrez, M. LeMeur, D. Metzger and P. Chambon (1996). “Ligand-activated site-specific recombination in mice.” Proceedings of the National Academy of Sciences of the United States of America **93**(20): 10887-10890.

Feil, R., J. Wagner, D. Metzger and P. Chambon (1997). “Regulation of Cre recombinase activity by mutated estrogen receptor ligand-binding domains.” Biochemical and biophysical research communications **237**(3): 752-757.

Fujimura, N., M.M. Taketo, M. Mori, V. Korinek and Z. Kozmik (2009). “Spatial and temporal regulation of Wnt/β-catenin signaling is essential for development of the retinal pigment epithelium.” Developmental Biology: 1-15.

Furutani-Seiki, M. and J. Wittbrodt (2004). “Medaka and zebrafish, an evolutionary twin study.” Mechanisms of development **121**(7-8): 629-637.

Gaj, T., C.A. Gersbach and I. Barbas, Carlos F (2013). “ZFN, TALEN, and CRISPR/Cas-based methods for genome engineering.” Trends in biotechnology **31**(7): 397-405.

Gehring, W.J. (1992). “The homeobox in perspective.” Trends in biochemical sciences **17**(8): 277-280.

Gehring, W.J. (1996). “The master control gene for morphogenesis and evolution of the eye.” Genes to cells : devoted to molecular & cellular mechanisms **1**(1): 11-15.

Gehring, W.J. and K. Ikeo (1999). “Pax 6: mastering eye morphogenesis and eye evolution.” Trends in genetics : TIG **15**(9): 371-377.

Gestri, G., M. Carl, I. Appolloni, S.W. Wilson, G. Barsacchi and M. Andreazzoli (2005). “Six3 functions in anterior neural plate specification by promoting cell proliferation and inhibiting Bmp4 expression.” Development (Cambridge, England) **132**(10): 2401-2413.

Geurts, A.M., G.J. Cost, Y. Freyvert, B. Zeitler, J.C. Miller, V.M. Choi, S.S. Jenkins, A. Wood, X. Cui, X. Meng*, et al.* (2009). “Knockout rats via embryo microinjection of zinc-finger nucleases.” Science (New York, NY) **325**(5939): 433.

Giangreco, A., E.N. Arwert, I.R. Rosewell, J. Snyder, F.M. Watt and B.R. Stripp (2009). “Stem cells are dispensable for lung homeostasis but restore airways after injury.” Proceedings of the National Academy of Sciences of the United States of America **106**(23): 9286-9291.

Gossler, A., A.L. Joyner, J. Rossant and W.C. Skarnes (1989). “Mouse embryonic stem cells and reporter constructs to detect developmentally regulated genes.” Science (New York, NY) **244**(4903): 463-465.

Grabher, C., T. Henrich, T. Sasado, A. Arenz, J. Wittbrodt and M. Furutani-Seiki (2003). “Transposon-mediated enhancer trapping in medaka.” Gene **322**: 57-66.

Graham, V., J. Khudyakov, P. Ellis and L. Pevny (2003). “SOX2 functions to maintain neural progenitor identity.” Neuron **39**(5): 749-765.

Grau, J., J. Boch and S. Posch (2013). “TALENoffer: genome-wide TALEN off-target prediction.” Bioinformatics (Oxford, England) **29**(22): 2931-2932.

Grindley, J.C., D.R. Davidson and R.E. Hill (1995). “The role of Pax-6 in eye and nasal development.” Development (Cambridge, England) **121**(5): 1433-1442.

Gurdon, J.B. (1962a). “Adult frogs derived from the nuclei of single somatic cells.” Developmental Biology **4**: 256-273.

Gurdon, J.B. (1962b). “The developmental capacity of nuclei taken from intestinal epithelium cells of feeding tadpoles.” Journal of embryology and experimental morphology **10**: 622-640.

Haffter, P., M. Granato, M. Brand, M.C. Mullins, M. Hammerschmidt, D.A. Kane, J. Odenthal, F.J. van Eeden, Y.J. Jiang, C.P. Heisenberg*, et al.* (1996). “The identification of genes with unique and essential functions in the development of the zebrafish, Danio rerio.” Development (Cambridge, England) **123**: 1-36.

Halder, G., P. Callaerts and W.J. Gehring (1995). “Induction of ectopic eyes by targeted expression of the eyeless gene in Drosophila.” Science (New York, NY) **267**(5205): 1788-1792.

Harris, W.A. and M. Perron (1998). “Molecular recapitulation: the growth of the vertebrate retina.” The International journal of developmental biology **42**(3): 299-304.

Harrison, D.A. and N. Perrimon (1993). “Simple and efficient generation of marked clones in Drosophila.” Current Biology **3**(7): 424-433.

He, J., G. Zhang, A.D. Almeida, M. Cayouette, B.D. Simons and W.A. Harris (2012). “How variable clones build an invariant retina.” Neuron **75**(5): 786-798.

Heasman, J. (2002). “Morpholino oligos: making sense of antisense?” Developmental Biology **243**(2): 209-214.

Heffron, D.S. and J.A. Golden (2000). “DM-GRASP is necessary for nonradial cell migration during chick diencephalic development.” The Journal of neuroscience : the official journal of the Society for Neuroscience **20**(6): 2287-2294.

Heisenberg, C.P., C. Houart, M. Take-Uchi, G.J. Rauch, N. Young, P. Coutinho, I. Masai, L. Caneparo, M.L. Concha, R. Geisler*, et al.* (2001). “A mutation in the Gsk3-binding domain of zebrafish Masterblind/Axin1 leads to a fate transformation of telencephalon and eyes to diencephalon.” Genes & Development **15**(11): 1427-1434.

Hinnen, A., J.B. Hicks and G.R. Fink (1978). “Transformation of yeast.” Proceedings of the National Academy of Sciences of the United States of America **75**(4): 1929-1933.

Hitotsumachi, S., D.A. Carpenter and W.L. Russell (1985). “Dose-repetition increases the mutagenic effectiveness of N-ethyl-N-nitrosourea in mouse spermatogonia.” Proceedings of the National Academy of Sciences of the United States of America **82**(19): 6619-6621.

Hockemeyer, D., H. Wang, S. Kiani, C.S. Lai, Q. Gao, J.P. Cassady, G.J. Cost, L. Zhang, Y. Santiago, J.C. Miller*, et al.* (2011). "Genetic engineering of human pluripotent cells using TALE nucleases." Nature Biotechnology **29**(8): 731-734.

Hollyfield, J.G. (1968). "Differential addition of cells to the retina in Rana pipiens tadpoles." Developmental Biology **18**(2): 163-179.

Holt, C.E., T.W. Bertsch, H.M. Ellis and W.A. Harris (1988). "Cellular determination in the Xenopus retina is independent of lineage and birth date." Neuron **1**(1): 15-26.

Horvath, P. and R. Barrangou (2010). "CRISPR/Cas, the immune system of bacteria and archaea." Science (New York, NY) **327**(5962): 167-170.

Howe, K., M.D. Clark, C.F. Torroja, J. Torrance, C. Berthelot, M. Muffato, J.E. Collins, S. Humphray, K. McLaren, L. Matthews*, et al.* (2013). "The zebrafish reference genome sequence and its relationship to the human genome." Nature: 1-6.

Hsu, P.D., D.A. Scott, J.A. Weinstein, F.A. Ran, S. Konermann, V. Agarwala, Y. Li, E.J. Fine, X. Wu, O. Shalem*, et al.* (2013). "DNA targeting specificity of RNA-guided Cas9 nucleases." Nature Biotechnology **31**(9): 827-832.

Huang, P., A. Xiao, M. Zhou, Z. Zhu, S. Lin and B. Zhang (2011). "Heritable gene targeting in zebrafish using customized TALENs." Nature Biotechnology **29**(8): 699-700.

Humke, E.W., K.V. Dorn, L. Milenkovic, M.P. Scott and R. Rohatgi (2010). "The output of Hedgehog signaling is controlled by the dynamic association between Suppressor of Fused and the Gli proteins." Genes & Development **24**(7): 670-682.

Hwang, W.Y., Y. Fu, D. Reyon, M.L. Maeder, P. Kaini, J.D. Sander, J.K. Joung, R.T. Peterson and J.-R.J. Yeh (2013). "Heritable and precise zebrafish genome editing using a CRISPR-Cas system." PLoS ONE **8**(7): e68708.

Inoue, D. and J. Wittbrodt (2011). "One for all--a highly efficient and versatile method for fluorescent immunostaining in fish embryos." PLoS ONE **6**(5): e19713.

Ishikawa, T., Y. Kamei, S. Otozai, J. Kim, A. Sato, Y. Kuwahara, M. Tanaka, T. Deguchi, H. Inohara, T. Tsujimura*, et al.* (2010). "High-resolution melting curve analysis for rapid detection of mutations in a Medaka TILLING library." BMC molecular biology **11**: 70.

Jablonski, M.M., J. Tombran-Tink, D.A. Mrazek and A. Iannaccone (2000). "Pigment epithelium-derived factor supports normal development of photoreceptor neurons and opsin expression after retinal pigment epithelium removal." The Journal of neuroscience : the official journal of the Society for Neuroscience **20**(19): 7149-7157.

Jablonski, M.M., J. Tombran-Tink, D.A. Mrazek and A. Iannaccone (2001). “Pigment epithelium-derived factor supports normal Müller cell development and glutamine synthetase expression after removal of the retinal pigment epithelium.” Glia **35**(1): 14-25.

Jao, L.-E., S.R. Wente and W. Chen (2013). “Efficient multiplex biallelic zebrafish genome editing using a CRISPR nuclease system.” Proceedings of the National Academy of Sciences of the United States of America **110**(34): 13904-13909.

Jiang, W., D. Bikard, D. Cox, F. Zhang and L.A. Marraffini (2013). “RNA-guided editing of bacterial genomes using CRISPR-Cas systems.” Nature Biotechnology **31**(3): 233-239.

Johns, P.R. (1977). “Growth of the adult goldfish eye. III. Source of the new retinal cells.” The Journal of Comparative Neurology **176**(3): 343-357.

Jordan, T., I. Hanson, D. Zaletayev, S. Hodgson, J. Prosser, A. Seawright, N. Hastie and V. van Heyningen (1992). “The human PAX6 gene is mutated in two patients with aniridia.” Nature genetics **1**(5): 328-332.

Joung, J.K. and J.D. Sander (2012). “TALENs: a widely applicable technology for targeted genome editing.” Nature reviews Molecular cell biology **14**(1): 49-55.

Kageyama, R., T. Ohtsuka and T. Kobayashi (2007). “The Hes gene family: repressors and oscillators that orchestrate embryogenesis.” Development (Cambridge, England) **134**(7): 1243-1251.

Kanekar, S., M. Perron, R. Dorsky, W.A. Harris, L.Y. Jan, Y.N. Jan and M.L. Vetter (1997). “Xath5 participates in a network of bHLH genes in the developing Xenopus retina.” Neuron **19**(5): 981-994.

Kasahara, M., K. Naruse, S. Sasaki, Y. Nakatani, W. Qu, B. Ahsan, T. Yamada, Y. Nagayasu, K. Doi, Y. Kasai*, et al.* (2007). “The medaka draft genome and insights into vertebrate genome evolution.” Nature **447**(7145): 714-719.

Kay, J.N., B.A. Link and H. Baier (2005). “Staggered cell-intrinsic timing of ath5 expression underlies the wave of ganglion cell neurogenesis in the zebrafish retina.” Development (Cambridge, England) **132**(11): 2573-2585.

Keller, P.J., A.D. Schmidt, J. Wittbrodt and E.H.K. Stelzer (2008). “Reconstruction of zebrafish early embryonic development by scanned light sheet microscopy.” Science (New York, NY) **322**(5904): 1065-1069.

Kennedy, B.N., G.W. Stearns, V.A. Smyth, V. Ramamurthy, F. van Eeden, I. Ankoudinova, D. Raible, J.B. Hurley and S.E. Brockerhoff (2004). “Zebrafish rx3 and mab21l2 are required during eye morphogenesis.” Developmental Biology **270**(2): 336-349.

Kenyon, K.L., N. Zaghloul and S.A. Moody (2001). “Transcription factors of the anterior neural plate alter cell movements of epidermal progenitors to specify a retinal fate.” Developmental Biology **240**(1): 77-91.

Kettleborough, R.N.W., E.M. Busch-Nentwich, S.A. Harvey, C.M. Dooley, E. de Bruijn, F. van Eeden, I. Sealy, R.J. White, C. Herd, I.J. Nijman*, et al.* (2013). “A systematic genome-wide analysis of zebrafish protein-coding gene function.” Nature: 1-6.

Kim, J.H., S.-R. Lee, L.-H. Li, H.-J. Park, J.-H. Park, K.Y. Lee, M.-K. Kim, B.A. Shin and S.-Y. Choi (2011). “High Cleavage Efficiency of a 2A Peptide Derived from Porcine Teschovirus-1 in Human Cell Lines, Zebrafish and Mice.” PLoS ONE **6**(4): e18556.

Kim, Y.G., J. Cha and S. Chandrasegaran (1996). “Hybrid restriction enzymes: zinc finger fusions to Fok I cleavage domain.” Proceedings of the National Academy of Sciences of the United States of America **93**(3): 1156-1160.

Kondoh, H. and Y. Kamachi (2010). “SOX-partner code for cell specification: Regulatory target selection and underlying molecular mechanisms.” The international journal of biochemistry & cell biology **42**(3): 391-399.

Koster, R., R. Stick, F. Loosli and J. Wittbrodt (1997). “Medaka spalt acts as a target gene of hedgehog signaling.” Development (Cambridge, England) **124**(16): 3147-3156.

Kubota, Y., A. Shimada and A. Shima (1995). “DNA alterations detected in the progeny of paternally irradiated Japanese medaka fish (Oryzias latipes).” Proceedings of the National Academy of Sciences of the United States of America **92**(1): 330-334.

Kuhn, H.G., H. Dickinson-Anson and F.H. Gage (1996). “Neurogenesis in the dentate gyrus of the adult rat: age-related decrease of neuronal progenitor proliferation.” The Journal of neuroscience : the official journal of the Society for Neuroscience **16**(6): 2027-2033.

Lekven, A.C., C.J. Thorpe, J.S. Waxman and R.T. Moon (2001). “Zebrafish wnt8 encodes two wnt8 proteins on a bicistronic transcript and is required for mesoderm and neurectoderm patterning.” Developmental Cell **1**(1): 103-114.

Li, J.J. and I. Herskowitz (1993). “Isolation of ORC6, a component of the yeast origin recognition complex by a one-hybrid system.” Science (New York, NY) **262**(5141): 1870-1874.

Lin, Y.-P., Y. Ouchi, S. Satoh and S. Watanabe (2009). “Sox2 plays a role in the induction of amacrine and Müller glial cells in mouse retinal progenitor cells.” Investigative Ophthalmology & Visual Science **50**(1): 68-74.

Liu, H.-K., Y. Wang, T. Belz, D. Bock, A. Takacs, B. Radlwimmer, S. Barbus, G. Reifenberger, P. Lichter and G. Schutz (2010). “The nuclear receptor tailless induces long-term neural stem cell expansion and brain tumor initiation.” Genes & Development **24**(7): 683-695.

Livesey, F.J. and C.L. Cepko (2001). “Vertebrate neural cell-fate determination: lessons from the retina.” Nature Reviews Neuroscience **2**(2): 109-118.

Livet, J., T.A. Weissman, H. Kang, R.W. Draft, J. Lu, R.A. Bennis, J.R. Sanes and J.W. Lichtman (2007). “Transgenic strategies for combinatorial expression of fluorescent proteins in the nervous system.” Nature **450**(7166): 56-62.

Locker, M., M. Agathocleous, M.A. Amato, K. Parain, W.A. Harris and M. Perron (2006). “Hedgehog signaling and the retina: insights into the mechanisms controlling the proliferative properties of neural precursors.” Genes & Development **20**(21): 3036-3048.

Lois, C. and A. Alvarez-Buylla (1993). “Proliferating subventricular zone cells in the adult mammalian forebrain can differentiate into neurons and glia.” Proceedings of the National Academy of Sciences of the United States of America **90**(5): 2074-2077.

Loosli, F., R.W. Köster, M. Carl, A. Krone and J. Wittbrodt (1998). “Six3, a medaka homologue of the Drosophila homeobox gene sine oculis is expressed in the anterior embryonic shield and the developing eye.” Mechanisms of development **74**(1-2): 159-164.

Loosli, F., R.W. Köster, M. Carl, R. Kühnlein, T. Henrich, M. Mücke, A. Krone and J. Wittbrodt (2000). “A genetic screen for mutations affecting embryonic development in medaka fish (Oryzias latipes).” Mechanisms of development **97**(1-2): 133-139.

Loosli, F., W. Staub, K.C. Finger-Baier, E.A. Ober, H. Verkade, J. Wittbrodt and H. Baier (2003). “Loss of eyes in zebrafish caused by mutation of chokh/rx3.” EMBO reports **4**(9): 894-899.

Loosli, F., S. Winkler, C. Burgtorf, E. Wurmbach, W. Ansorge, T. Henrich, C. Grabher, D. Arendt, M. Carl, A. Krone*, et al.* (2001). “Medaka eyeless is the key factor linking retinal determination and eye growth.” Development (Cambridge, England) **128**(20): 4035-4044.

Loosli, F., S. Winkler and J. Wittbrodt (1999). “Six3 overexpression initiates the formation of ectopic retina.” Genes & Development **13**(6): 649-654.

Lopez-Rios, J., D. Speziale, D. Robay, M. Scotti, M. Osterwalder, G. Nusspaumer, A. Galli, G.A. Holländer, M. Kmita and R. Zeller (2012). “GLI3 Constrains Digit Number by Controlling Both Progenitor Proliferation and BMP-Dependent Exit to Chondrogenesis.” Developmental Cell **22**(4): 837-848.

Lu, R., N.F. Neff, S.R. Quake and I.L. Weissman (2011). “Tracking single hematopoietic stem cells in vivo using high-throughput sequencing in conjunction with viral genetic barcoding.” Nature Biotechnology **29**(10): 928-933.

Macdonald, R., K.A. Barth, Q. Xu, N. Holder, I. Mikkola and S.W. Wilson (1995). “Midline signalling is required for Pax gene regulation and patterning of the eyes.” Development (Cambridge, England) **121**(10): 3267-3278.

Machon, O., J. Kreslova, J. Ruzickova, T. Vacik, L. Klimova, N. Fujimura, J. Lachova and Z. Kozmik (2010). “Lens morphogenesis is dependent on Pax6-mediated inhibition of the canonical Wnt/beta-catenin signaling in the lens surface ectoderm.” Genesis (New York, NY : 2000) **48**(2): 86-95.

Mali, P., J. Aach, P.B. Stranges, K.M. Esvelt, M. Moosburner, S. Kosuri, L. Yang and G.M. Church (2013a). “CAS9 transcriptional activators for target specificity screening and paired nickases for cooperative genome engineering.” Nature Biotechnology **31**(9): 833-838.

Mali, P., L. Yang, K.M. Esvelt, J. Aach, M. Guell, J.E. DiCarlo, J.E. Norville and G.M. Church (2013b). “RNA-guided human genome engineering via Cas9.” Science (New York, NY) **339**(6121): 823-826.

Marquardt, T., R. Ashery-Padan, N. Andrejewski, R. Scardigli, F. Guillemot and P. Gruss (2001). “Pax6 is required for the multipotent state of retinal progenitor cells.” CELL **105**(1): 43-55.

Marquardt, T. and P. Gruss (2002). “Generating neuronal diversity in the retina: one for nearly all.” Trends in Neurosciences **25**(1): 32-38.

Marraffini, L.A. and E.J. Sontheimer (2010). “CRISPR interference: RNA-directed adaptive immunity in bacteria and archaea.” Nature Reviews Genetics **11**(3): 181-190.

Martinez-De Luna, R.I., L.E. Kelly and H.M. El-Hodiri (2011). “The Retinal Homeobox (Rx) gene is necessary for retinal regeneration.” Developmental Biology **353**(1): 10-18.

Martinez-De Luna, R.I., H.E. Moose, L.E. Kelly, S. Nekkalapudi and H.M. El-Hodiri (2010). “Regulation of retinal homeobox gene transcription by cooperative activity among cis-elements.” Gene **467**(1-2): 13-24.

Martinez-Morales, J.R., M. Rembold, K. Greger, J.C. Simpson, K.E. Brown, R. Quiring, R. Pepperkok, M.D. Martin-Bermudo, H. Himmelbauer and J. Wittbrodt (2009). “ojoplano-mediated basal constriction is essential for optic cup morphogenesis.” Development (Cambridge, England) **136**(13): 2165-2175.

Martinez-Morales, J.R., M. Signore, D. Acampora, A. Simeone and P. Bovolenta (2001). “Otx genes are required for tissue specification in the developing eye.” Development (Cambridge, England) **128**(11): 2019-2030.

Mathers, P.H., A. Grinberg, K.A. Mahon and M. Jamrich (1997). “The Rx homeobox gene is essential for vertebrate eye development.” Nature **387**(6633): 603-607.

Matter-Sadzinski, L., J.M. Matter, M.T. Ong, J. Hernandez and M. Ballivet (2001). “Specification of neurotransmitter receptor identity in developing retina: the chick ATH5 promoter integrates the positive and negative effects of several bHLH proteins.” Development (Cambridge, England) **128**(2): 217-231.

McCallum, C.M., L. Comai, E.A. Greene and S. Henikoff (2000). “Targeting induced local lesions IN genomes (TILLING) for plant functional genomics.” Plant physiology **123**(2): 439-442.

McMahon, A., W. Supatto, S.E. Fraser and A. Stathopoulos (2008). “Dynamic analyses of Drosophila gastrulation provide insights into collective cell migration.” Science (New York, NY) **322**(5907): 1546-1550.

Meng, X., M.B. Noyes, L.J. Zhu, N.D. Lawson and S.A. Wolfe (2008). “Targeted gene inactivation in zebrafish using engineered zinc-finger nucleases.” Nature Biotechnology **26**(6): 695-701.

Metzger, D., S. Ali, J.M. Bornert and P. Chambon (1995a). “Characterization of the amino-terminal transcriptional activation function of the human estrogen receptor in animal and yeast cells.” The Journal of biological chemistry **270**(16): 9535-9542.

Metzger, D., J. Clifford, H. Chiba and P. Chambon (1995b). “Conditional site-specific recombination in mammalian cells using a ligand-dependent chimeric Cre recombinase.” Proceedings of the National Academy of Sciences of the United States of America **92**(15): 6991-6995.

Miller, J.C., M.C. Holmes, J. Wang, D.Y. Guschin, Y.-L. Lee, I. Rupniewski, C.M. Beausejour, A.J. Waite, N.S. Wang, K.A. Kim*, et al.* (2007). “An improved zinc-finger nuclease architecture for highly specific genome editing.” Nature Biotechnology **25**(7): 778-785.

Miller, J.C., S. Tan, G. Qiao, K.A. Barlow, J. Wang, D.F. Xia, X. Meng, D.E. Paschon, E. Leung, S.J. Hinkley*, et al.* (2011). “A TALE nuclease architecture for efficient genome editing.” Nature Biotechnology **29**(2): 143-148.

Moehle, E.A., E.A. Moehle, J.M. Rock, J.M. Rock, Y.-L. Lee, Y.L. Lee, Y. Jouvenot, Y. Jouvenot, R.C. DeKelver, R.C. Dekelver*, et al.* (2007). “Targeted gene addition into a specified location in the human genome using designed zinc finger nucleases.” Proceedings of the National Academy of Sciences of the United States of America **104**(9): 3055-3060.

Monaghan, A.P., E. Grau, D. Bock and G. Schütz (1995). “The mouse homolog of the orphan nuclear receptor tailless is expressed in the developing forebrain.” Development (Cambridge, England) **121**(3): 839-853.

Morrison, S.J. and J. Kimble (2006). “Asymmetric and symmetric stem-cell divisions in development and cancer.” Nature **441**(7097): 1068-1074.

Moscou, M.J. and A.J. Bogdanove (2009). “A simple cipher governs DNA recognition by TAL effectors.” Science (New York, NY) **326**(5959): 1501.

Muranishi, Y., K. Terada, T. Inoue, K. Katoh, T. Tsujii, R. Sanuki, D. Kurokawa, S. Aizawa, Y. Tamaki and T. Furukawa (2011). “An essential role for RAX homeoprotein and NOTCH-HES signaling in Otx2 expression in embryonic retinal photoreceptor cell fate determination.” The Journal of neuroscience : the official journal of the Society for Neuroscience **31**(46): 16792-16807.

Mussolino, C., R. Morbitzer, F. Lütge, N. Dannemann, T. Lahaye and T. Cathomen (2011). “A novel TALE nuclease scaffold enables high genome editing activity in combination with low toxicity.” Nucleic Acids Research **39**(21): 9283-9293.

Nakagawa, T., Y.-I. Nabeshima and S. Yoshida (2007). “Functional identification of the actual and potential stem cell compartments in mouse spermatogenesis.” Developmental Cell **12**(2): 195-206.

Nasevicius, A. and S.C. Ekker (2000). “Effective targeted gene 'knockdown' in zebrafish.” Nature genetics **26**(2): 216-220.

Negishi, K., W.K. Stell, T. Teranishi, A. Karkhanis, V. Owusu-Yaw and Y. Takasaki (1991). “Induction of proliferating cell nuclear antigen (PCNA)-immunoreactive cells in goldfish retina following intravitreal injection with 6-hydroxydopamine.” Cellular and molecular neurobiology **11**(6): 639-659.

Nelson, S.M., L. Park and D.L. Stenkamp (2009). “Retinal homeobox 1 is required for retinal neurogenesis and photoreceptor differentiation in embryonic zebrafish.” Developmental Biology **328**(1): 24-39.

Neumann, C.J. and C. Nuesslein-Volhard (2000). “Patterning of the zebrafish retina by a wave of sonic hedgehog activity.” Science (New York, NY) **289**(5487): 2137-2139.

Nishida, A., A. Furukawa, C. Koike, Y. Tano, S. Aizawa, I. Matsuo and T. Furukawa (2003). “Otx2 homeobox gene controls retinal photoreceptor cell fate and pineal gland development.” Nature neuroscience **6**(12): 1255-1263.

Nüsslein-Volhard, C. and E. Wieschaus (1980). “Mutations affecting segment number and polarity in Drosophila.” Nature **287**(5785): 795-801.

Obernier, K., I. Simeonova, T. Fila, C. Mandl, G. Hölzl-Wenig, P. Monaghan-Nichols and F. Ciccolini (2011). “Tlx is Expressed in Both Stem Cells and Transit Amplifying Progenitors Regulating Stem Cell Activation and Differentiation in the Neonatal Lateral Subependymal Zone.” STEM CELLS: N/A-N/A.

Ohnuma, S.-i., S. Hopper, K.C. Wang, A. Philpott and W.A. Harris (2002). “Co-ordinating retinal histogenesis: early cell cycle exit enhances early cell fate determination in the Xenopus retina.” Development (Cambridge, England) **129**(10): 2435-2446.

Oliver, G. and P. Gruss (1997). “Current views on eye development.” Trends in Neurosciences **20**(9): 415-421.

Orford, K.W. and D.T. Scadden (2008). “Deconstructing stem cell self-renewal: genetic insights into cell-cycle regulation.” Nature Reviews Genetics **9**(2): 115-128.

Orr-Weaver, T.L., J.W. Szostak and R.J. Rothstein (1981). “Yeast transformation: a model system for the study of recombination.” Proceedings of the National Academy of Sciences of the United States of America **78**(10): 6354-6358.

Pan, Y., R.I. Martinez-De Luna, C.-H. Lou, S. Nekkalapudi, L.E. Kelly, A.K. Sater and H.M. El-Hodiri (2010). “Regulation of photoreceptor gene expression by the retinal homeobox (Rx) gene product.” Developmental Biology **339**(2): 494-506.

Pan, Y.A., T. Freundlich, T.A. Weissman, D. Schoppik, X.C. Wang, S. Zimmerman, B. Ciruna, J.R. Sanes, J.W. Lichtman and A.F. Schier (2013). “Zebrabow: multispectral cell labeling for cell tracing and lineage analysis in zebrafish.” Development (Cambridge, England) **140**(13): 2835-2846.

Pang, Z.P., N. Yang, T. Vierbuchen, A. Ostermeier, D.R. Fuentes, T.Q. Yang, A. Citri, V. Sebastiano, S. Marro, T.C. Südhof*, et al.* (2011). “Induction of human neuronal cells by defined transcription factors.” Nature **476**(7359): 220-223.

Pattanayak, V., S. Lin, J.P. Guilinger, E. Ma, J.A. Doudna and D.R. Liu (2013). “High-throughput profiling of off-target DNA cleavage reveals RNA-programmed Cas9 nuclease specificity.” Nature Biotechnology **31**(9): 839-843.

Pera, E.M., O. Wessely, S.Y. Li and E.M. De Robertis (2001). “Neural and head induction by insulin-like growth factor signals.” Developmental Cell **1**(5): 655-665.

Perez, E.E., J. Wang, J.C. Miller, Y. Jouvenot, K.A. Kim, O. Liu, N. Wang, G. Lee, V.V. Bartsevich, Y.-L. Lee*, et al.* (2008). “Establishment of HIV-1 resistance in CD4+ T cells by genome editing using zinc-finger nucleases.” Nature Biotechnology **26**(7): 808-816.

Perron, M., S. Boy, M.A. Amato, A. Viczian, K. Koebernick, T. Pieler and W.A. Harris (2003). “A novel function for Hedgehog signalling in retinal pigment epithelium differentiation.” Development (Cambridge, England) **130**(8): 1565-1577.

Perron, M. and W.A. Harris (2000). “Retinal stem cells in vertebrates.” BioEssays **22**(8): 685-688.

Peterson, K.A., Y. Nishi, W. Ma, A. Vedenko, L. Shokri, X. Zhang, M. McFarlane, J.-M. Baizabal, J.P. Junker, A. van Oudenaarden*, et al.* (2012). “Neural-specific Sox2 input and differential Gli-binding affinity provide context and positional information in Shh-directed neural patterning.” Genes & Development **26**(24): 2802-2816.

Poggi, L., M. Vitorino, I. Masai and W.A. Harris (2005). “Influences on neural lineage and mode of division in the zebrafish retina in vivo.” The Journal of cell biology **171**(6): 991-999.

Qian, X., Q. Shen, S.K. Goderie, W. He, A. Capela, A.A. Davis and S. Temple (2000). “Timing of CNS cell generation: a programmed sequence of neuron and glial cell production from isolated murine cortical stem cells.” Neuron **28**(1): 69-80.

Ramialison, M., R. Reinhardt, T. Henrich, B. Wittbrodt, T. Kellner, C.M. Lowy and J. Wittbrodt (2012). "Cis-regulatory properties of medaka synexpression groups." Development (Cambridge, England) **139**(5): 917-928.

Ramirez, C.L., J.E. Foley, D.A. Wright, F. Müller-Lerch, S.H. Rahman, T.I. Cornu, R.J. Winfrey, J.D. Sander, F. Fu, J.A. Townsend*, et al.* (2008). "Unexpected failure rates for modular assembly of engineered zinc fingers." Nature Methods **5**(5): 374-375.

Raymond, P.A., L.K. Barthel, R.L. Bernardos and J.J. Perkowski (2006). "Molecular characterization of retinal stem cells and their niches in adult zebrafish." BMC developmental biology **6**: 36.

Rembold, M., F. Loosli, R.J. Adams and J. Wittbrodt (2006). "Individual cell migration serves as the driving force for optic vesicle evagination." Science (New York, NY) **313**(5790): 1130-1134.

Ring, K.L., L.M. Tong, M.E. Balestra, R. Javier, Y. Andrews-Zwilling, G. Li, D. Walker, W.R. Zhang, A.C. Kreitzer and Y. Huang (2012). "Direct Reprogramming of Mouse and Human Fibroblasts into Multipotent Neural Stem Cells with a Single Factor." Stem Cell: 1-10.

Rojas-Muñoz, A., R. Dahm and C. Nüsslein-Volhard (2005). "chokh/rx3 specifies the retinal pigment epithelium fate independently of eye morphogenesis." Developmental Biology **288**(2): 348-362.

Sambrook, J., E.F. Fritsch and T. Maniatis (1989). Molecular Cloning: A Laboratory Manual, Cold Spring Harbor, N.Y. : Cold Spring Harbor Laboratory Press.

Sander, J.D., L. Cade, C. Khayter, D. Reyon, R.T. Peterson, J.K. Joung and J.-R.J. Yeh (2011). "Targeted gene disruption in somatic zebrafish cells using engineered TALENs." Nature Biotechnology **29**(8): 697-698.

Sasaki, H., C. Hui, M. Nakafuku and H. Kondoh (1997). "A binding site for Gli proteins is essential for HNF-3beta floor plate enhancer activity in transgenics and can respond to Shh in vitro." Development (Cambridge, England) **124**(7): 1313-1322.

Schepers, A.G., H.J. Snippert, D.E. Stange, M. van den Born, J.H. van Es, M. van de Wetering and H. Clevers (2012). "Lineage Tracing Reveals Lgr5+ Stem Cell Activity in Mouse Intestinal Adenomas." Science (New York, NY) **337**(6095): 730-735.

Schneuwly, S., R. Klemenz and W.J. Gehring (1987). "Redesigning the body plan of Drosophila by ectopic expression of the homoeotic gene Antennapedia." Nature **325**(6107): 816-818.

Shen, B., J. Zhang, H. Wu, J. Wang, K. Ma, Z. Li, X. Zhang, P. Zhang and X. Huang (2013). "Generation of gene-modified mice via Cas9/RNA-mediated gene targeting." Cell research **23**(5): 720-723.

Shi, Y., D. Chichung Lie, P. Taupin, K. Nakashima, J. Ray, R.T. Yu, F.H. Gage and R.M. Evans (2004). "Expression and function of orphan nuclear receptor TLX in adult neural stem cells." Nature **427**(6969): 78-83.

Shimozaki, K., C.-L. Zhang, H. Suh, A.M. Denli, R.M. Evans and F.H. Gage (2012). “SRY-box-containing gene 2 regulation of nuclear receptor tailless (Tlx) transcription in adult neural stem cells.” The Journal of biological chemistry **287**(8): 5969-5978.

Snippert, H.J., A. Haegebarth, M. Kasper, V. Jaks, J.H. van Es, N. Barker, M. van de Wetering, M. van den Born, H. Begthel, R.G. Vries*, et al.* (2010a). “Lgr6 marks stem cells in the hair follicle that generate all cell lineages of the skin.” Science (New York, NY) **327**(5971): 1385-1389.

Snippert, H.J., L.G. van der Flier, T. Sato, J.H. van Es, M. van den Born, C. Kroon-Veenboer, N. Barker, A.M. Klein, J. van Rheenen, B.D. Simons*, et al.* (2010b). “Intestinal crypt homeostasis results from neutral competition between symmetrically dividing Lgr5 stem cells.” CELL **143**(1): 134-144.

Souren, M., J.R. Martinez-Morales, P. Makri, B. Wittbrodt and J. Wittbrodt (2009). “A global survey identifies novel upstream components of the Ath5 neurogenic network.” Genome biology **10**(9): R92.

Srinivas, S., T. Watanabe, C.S. Lin, C.M. William, Y. Tanabe, T.M. Jessell and F. Costantini (2001). “Cre reporter strains produced by targeted insertion of EYFP and ECFP into the ROSA26 locus.” BMC developmental biology **1**: 4.

Stenkamp, D.L., R.A. Frey, S.N. Prabhudesai and P.A. Raymond (2000). “Function for Hedgehog Genes in Zebrafish Retinal Development.” Developmental Biology **220**(2): 238-252.

Straznicky, K. and R.M. Gaze (1971). “The growth of the retina in Xenopus laevis: an autoradiographic study.” Journal of embryology and experimental morphology **26**(1): 67-79.

Suh, H., A. Consiglio, J. Ray, T. Sawai, K.A. D'Amour and F.H. Gage (2007). “In vivo fate analysis reveals the multipotent and self-renewal capacities of Sox2+ neural stem cells in the adult hippocampus.” Stem Cell **1**(5): 515-528.

Summerton, J. and D. Weller (1997). “Morpholino antisense oligomers: design, preparation, and properties.” Antisense & nucleic acid drug development **7**(3): 187-195.

Sun, G., R.T. Yu, R.M. Evans and Y. Shi (2007). “Orphan nuclear receptor TLX recruits histone deacetylases to repress transcription and regulate neural stem cell proliferation.” Proceedings of the National Academy of Sciences of the United States of America **104**(39): 15282-15287.

Swaroop, A., D. Kim and D. Forrest (2010). “Transcriptional regulation of photoreceptor development and homeostasis in the mammalian retina.” Nature Reviews Neuroscience **11**(8): 563-576.

Tada, M., T. Tada, L. Lefebvre, S.C. Barton and M.A. Surani (1997). “Embryonic germ cells induce epigenetic reprogramming of somatic nucleus in hybrid cells.” The EMBO Journal **16**(21): 6510-6520.

Tada, M., Y. Takahama, K. Abe, N. Nakatsuji and T. Tada (2001). “Nuclear reprogramming of somatic cells by in vitro hybridization with ES cells.” Current Biology **11**(19): 1553-1558.

Takahashi, K., K. Tanabe, M. Ohnuki, M. Narita, T. Ichisaka, K. Tomoda and S. Yamanaka (2007). “Induction of pluripotent stem cells from adult human fibroblasts by defined factors.” CELL **131**(5): 861-872.

Takahashi, K. and S. Yamanaka (2006). “Induction of pluripotent stem cells from mouse embryonic and adult fibroblast cultures by defined factors.” CELL **126**(4): 663-676.

Taranova, O.V., S.T. Magness, B.M. Fagan, Y. Wu, N. Surzenko, S.R. Hutton and L.H. Pevny (2006). “SOX2 is a dose-dependent regulator of retinal neural progenitor competence.” Genes & Development **20**(9): 1187-1202.

Tesson, L., C. Usal, S. Ménoret, E. Leung, B.J. Niles, S. Remy, Y. Santiago, A.I. Vincent, X. Meng, L. Zhang*, et al.* (2011). “Knockout rats generated by embryo microinjection of TALENs.” Nature Biotechnology **29**(8): 695-696.

Thermes, V., C. Grabher, F. Ristoratore, F. Bourrat, A. Choulika, J. Wittbrodt and J.-S. Joly (2002). “I-SceI meganuclease mediates highly efficient transgenesis in fish.” Mechanisms of development **118**(1-2): 91-98.

Thomas, K.R. and M.R. Capecchi (1987). “Site-directed mutagenesis by gene targeting in mouse embryo-derived stem cells.” CELL **51**(3): 503-512.

Thomas, K.R., K.R. Folger and M.R. Capecchi (1986). “High frequency targeting of genes to specific sites in the mammalian genome.” CELL **44**(3): 419-428.

Tropepe, V., B.L. Coles, B.J. Chiasson, D.J. Horsford, A.J. Elia, R.R. McInnes and D. van der Kooy (2000). “Retinal stem cells in the adult mammalian eye.” Science (New York, NY) **287**(5460): 2032-2036.

Tumbar, T., G. Guasch, V. Greco, C. Blanpain, W.E. Lowry, M. Rendl and E. Fuchs (2004). “Defining the epithelial stem cell niche in skin.” Science (New York, NY) **303**(5656): 359-363.

Turner, D.L. and C.L. Cepko (1987). “A common progenitor for neurons and glia persists in rat retina late in development.” Nature **328**(6126): 131-136.

Tyurina, O.V., B. Guner, E. Popova, J. Feng, A.F. Schier, J.D. Kohtz and R.O. Karlstrom (2005). “Zebrafish Gli3 functions as both an activator and a repressor in Hedgehog signaling.” Developmental Biology **277**(2): 537-556.

Urnov, F.D., E.J. Rebar, M.C. Holmes, H.S. Zhang and P.D. Gregory (2010). “Genome editing with engineered zinc finger nucleases.” Nature Reviews Genetics **11**(9): 636-646.

van de Water, S., M. van de Wetering, J. Joore, J. Esseling, R. Bink, H. Clevers and D. Zivkovic (2001). "Ectopic Wnt signal determines the eyeless phenotype of zebrafish masterblind mutant." Development (Cambridge, England) **128**(20): 3877-3888.

Van Raay, T.J., K.B. Moore, I. Iordanova, M. Steele, M. Jamrich, W.A. Harris and M.L. Vetter (2005). "Frizzled 5 signaling governs the neural potential of progenitors in the developing Xenopus retina." Neuron **46**(1): 23-36.

Vierbuchen, T., A. Ostermeier, Z.P. Pang, Y. Kokubu, T.C. Südhof and M. Wernig (2010). "Direct conversion of fibroblasts to functional neurons by defined factors." Nature **463**(7284): 1035-1041.

Vooijs, M., C.-T. Ong, B. Hadland, S. Huppert, Z. Liu, J. Korving, M. van den Born, T. Stappenbeck, Y. Wu, H. Clevers*, et al.* (2007). "Mapping the consequence of Notch1 proteolysis in vivo with NIP-CRE." Development (Cambridge, England) **134**(3): 535-544.

Voronina, V.A., E.A. Kozhemyakina, C.M. O'Kernick, N.D. Kahn, S.L. Wenger, J.V. Linberg, A.S. Schneider and P.H. Mathers (2004). "Mutations in the human RAX homeobox gene in a patient with anophthalmia and sclerocornea." Human molecular genetics **13**(3): 315-322.

Wakayama, T., A.C. Perry, M. Zuccotti, K.R. Johnson and R. Yanagimachi (1998). "Full-term development of mice from enucleated oocytes injected with cumulus cell nuclei." Nature **394**(6691): 369-374.

Wallace, V.A. (2008). "Proliferative and cell fate effects of Hedgehog signaling in the vertebrate retina." Brain research **1192**: 61-75.

Wang, H., H. Yang, C.S. Shivalila, M.M. Dawlaty, A.W. Cheng, F. Zhang and R. Jaenisch (2013). "One-Step Generation of Mice Carrying Mutations in Multiple Genes by CRISPR/Cas-Mediated Genome Engineering." CELL **153**(4): 910-918.

Wang, S.W., B.S. Kim, K. Ding, H. Wang, D. Sun, R.L. Johnson, W.H. Klein and L. Gan (2001). "Requirement for math5 in the development of retinal ganglion cells." Genes & Development **15**(1): 24-29.

Warren, N., D. Caric, T. Pratt, J.A. Clausen, P. Asavaritikrai, J.O. Mason, R.E. Hill and D.J. Price (1999). "The transcription factor, Pax6, is required for cell proliferation and differentiation in the developing cerebral cortex." Cerebral cortex (New York, NY : 1991) **9**(6): 627-635.

Watanabe, T. and M.C. Raff (1990). "Rod photoreceptor development in vitro: intrinsic properties of proliferating neuroepithelial cells change as development proceeds in the rat retina." Neuron **4**(3): 461-467.

Wetts, R. and S.E. Fraser (1988). "Multipotent precursors can give rise to all major cell types of the frog retina." Science (New York, NY) **239**(4844): 1142-1145.

Wienholds, E., S. Schulte-Merker, B. Walderich and R.H.A. Plasterk (2002). “Target-selected inactivation of the zebrafish rag1 gene.” Science (New York, NY) **297**(5578): 99-102.

Wilmut, I., A.E. Schnieke, J. McWhir, A.J. Kind and K.H. Campbell (1997). “Viable offspring derived from fetal and adult mammalian cells.” Nature **385**(6619): 810-813.

Winkler, S., F. Loosli, T. Henrich, Y. Wakamatsu and J. Wittbrodt (2000). “The conditional medaka mutation eyeless uncouples patterning and morphogenesis of the eye.” Development (Cambridge, England) **127**(9): 1911-1919.

Wong, L.L. and D.H. Rapaport (2009). “Defining retinal progenitor cell competence in Xenopus laevis by clonal analysis.” Development (Cambridge, England) **136**(10): 1707-1715.

Wu, H.-Y., M. Perron and T. Hollemann (2009). “The role of Xenopus Rx-L in photoreceptor cell determination.” Developmental Biology **327**(2): 352-365.

Yoshiura, S., T. Ohtsuka, Y. Takenaka, H. Nagahara, K. Yoshikawa and R. Kageyama (2007). “Ultradian oscillations of Stat, Smad, and Hes1 expression in response to serum.” Proceedings of the National Academy of Sciences of the United States of America **104**(27): 11292-11297.

Yu, R.T., M.Y. Chiang, T. Tanabe, M. Kobayashi, K. Yasuda, R.M. Evans and K. Umesono (2000). “The orphan nuclear receptor Tlx regulates Pax2 and is essential for vision.” Proceedings of the National Academy of Sciences of the United States of America **97**(6): 2621-2625.

Yu, R.T., M. McKeown, R.M. Evans and K. Umesono (1994). “Relationship between Drosophila gap gene tailless and a vertebrate nuclear receptor Tlx.” Nature **370**(6488): 375-379.

Zaghloul, N.A. and S.A. Moody (2007). “Alterations of rx1 and pax6 expression levels at neural plate stages differentially affect the production of retinal cell types and maintenance of retinal stem cell qualities.” Developmental Biology **306**(1): 222-240.

Zhang, L. (2003). “Targeted expression of the dominant-negative FGFR4a in the eye using Xrx1A regulatory sequences interferes with normal retinal development.” Development (Cambridge, England) **130**(17): 4177-4186.

Zhang, R., P. Han, H. Yang, K. Ouyang, D. Lee, Y.-F. Lin, K. Ocorr, G. Kang, J. Chen, D.Y.R. Stainier*, et al.* (2013). “In vivo cardiac reprogramming contributes to zebrafish heart regeneration.” Nature **498**(7455): 497-501.

Zhou, Q., J. Brown, A. Kanarek, J. Rajagopal and D.A. Melton (2008). “In vivo reprogramming of adult pancreatic exocrine cells to beta-cells.” Nature **455**(7213): 627-632.

Zuber, M.E., M. Perron, A. Philpott, A. Bang and W.A. Harris (1999). “Giant eyes in Xenopus laevis by overexpression of XOptx2.” CELL **98**(3): 341-352.

Acknowledgments

First of all, I would like to thank my supervisor Prof. Dr. Joachim Wittbrodt for giving me the opportunity to work in his lab and for providing me with an exciting thesis project. He supported me throughout my thesis with helpful scientific ideas.

I am grateful to my PhD advisory committee, Prof. Dr. Jan Lohmann and Dr. Stefano De Renzis, for their suggestions and the fruitful discussions during my thesis advisory committee meetings.

I would like to thank Dr. Juan Luis Mateo Cerdan and Dr. Mirana Ramialison for all the bioinformatic analyses they performed and the stimulating scientific discussions.

I would also like to thank Dr. Daigo Inoue and Dr. Juan Ramon Martinez Morales for providing the Rx2 antibody and Rx2 transgenic line, respectively.

Many thanks to my bay mates Beate, Lea and Tanja (a former bay mate) for supporting me, in particular when it came to doing molecular biology. Special credit belongs to Beate for the amount of work and time she put into genotyping and establishing the mutants.

APPENDIX

Abbreviations

AC	amacrine cell
Atoh7	atonal homolog 7
Bmp	Bone morphogenetic protein
BPC	bipolar cell
BrdU	bromodeoxyuridine
Cas	CRISPR-associated
cDNA	complementary DNA
CMV	cytomegalovirus
CMZ	ciliary marginal zone
CRE	*cis*-regulatory element
CRISPR	Clustered, regularly interspaced, short palindromic repeats
DAPI	4', 6-diamidino-2-phenylindole
DMSO	Dimethylsulfoxide
DNA	deoxyribonucleic acid
EMS	ethyl methanesulfonate
ENU	N-ethyl-N-nitrosourea
Fgf	fibroblast growth factor
GCL	ganglion cell layer
GFP	green fluorescent protein
H2A	histone 2A
H2B	histone 2B
HC	horizontal cell
Hh	hedgehog
IGF	insulin-like growth factor
INL	inner nuclear layer
IPL	inner plexiform layer
MGC	Muller glia cell
mRFP	monomeric red fluorescent protein
mRNA	messenger RNA
NHEJ	non-homologous end-joining
NR	neural retina

NSC	neural stem cell
O.l.	*Oryzias latipes*
o/n	overnight
ONL	outer nuclear layer
OPL	outer plexiform layer
Pax	Paired box
PBS	Phosphate Buffered Saline
PCR	polymerase chain reaction
PFA	paraformaldehyde
PTW	PBS with Tween20
Rax/Rx	Retinal homeobox
RGC	retinal ganglion cell
RNA	ribonucleic acid
RPC	retinal progenitor cell
RPE	retinal pigmented epithelium
RSC	retinal stem cell
RT	room temperature
SDS	sodium dodecyl sulfate
Shh	sonic hedgehog
Six	sine oculis homeobox homologue
Sox	Sex determining Y-box-related high-mobility group box
TALEN	Transcription activator-like effector nuclease
TF	transcription factor
TFBS	transcription factor binding site
TILLING	targeting induced local lesions in genomes
TRS	*trans*-regulation screen
WISH	whole mount in situ hybridization
Wnt	wingless and int-1
ZFN	zinc-finger nuclease

List of publications

ENCODE Project Consortium, B.E. Bernstein, E. Birney, I. Dunham, E.D. Green, C. Gunter *et al.* (2012). "An integrated encyclopedia of DNA elements in the human genome." Nature **489**(7414): 57-74.

Ramialison, M., R. Reinhardt, T. Henrich, B. Wittbrodt, T. Kellner, C.M. Lowy and J. Wittbrodt (2012). "Cis-regulatory properties of medaka synexpression groups." Development (Cambridge, England) **139**(5): 917-928.